National Library of Canada

Acquisitions and Bibliographic Services Branch

395 Wellington Street
Ottawa, Ontario
K1A 0N4

Bibliothèque nationale du Canada

Direction des acquisitions et des services bibliographiques

395, rue Wellington
Ottawa (Ontario)
K1A 0N4

Your file Votre référence

Our file Notre référence

NOTICE

The quality of this microform is heavily dependent upon the quality of the original thesis submitted for microfilming. Every effort has been made to ensure the highest quality of reproduction possible.

If pages are missing, contact the university which granted the degree.

Some pages may have indistinct print especially if the original pages were typed with a poor typewriter ribbon or if the university sent us an inferior photocopy.

AVIS

La qualité de cette microforme dépend grandement de la qualité de la thèse soumise au microfilmage. Nous avons tout fait pour assurer une qualité supérieure de reproduction.

S'il manque des pages, veuillez communiquer avec l'université qui a conféré le grade.

La qualité d'impression de certaines pages peut laisser à désirer, surtout si les pages originales ont été dactylographiées à l'aide d'un ruban usé ou si l'université nous a fait parvenir une photocopie de qualité inférieure.

Canada

CELLULOSE ACETATE METAL IMPREGNATED MEMBRANES FOR AIR SEPARATIONS

Wassim El-Taki

A THESIS

SUBMITTED TO THE SCHOOL OF GRADUATE STUDIES IN PARTIAL FULFILLMENT OF THE REQUIREMENTS FOR THE DEGREE OF MASTER OF APPLIED SCIENCE IN THE DEPARTMENT OF CHEMICAL ENGINEERING UNIVERSITY OF OTTAWA.

October 20th, 1995

ISBN 0-612-07846-9

Canada

UNIVERSITÉ D'OTTAWA
UNIVERSITY OF OTTAWA

Abstract

Polymeric membranes are widely used in the oxygen enrichment of air for medical purposes and in the preparation of nitrogen for use in blanketing applications. Membranes having both high selectivity and permeability are essential for these applications. In this work, several membranes were prepared by the phase inversion technique. Casting solutions containing cellulose acetate, EDTA and acetone were spread onto a backing material and gelled in iced water. The membranes were then subjected to several post-treatments such as annealing, silver impregnation and silver impregnation followed by reduction to silver metal. The effects of EDTA and film post-treatments were determined with respect to air permeability and oxygen concentration in the permeate. The porosity of the resulting membranes were determined using gas sorption techniques.

The presence of EDTA in the casting solution increased the entrapment of silver within the membrane. The air permeability of the membrane and oxygen concentration of the permeate were individually normalized. An objective function was defined as the product of the normalized air permeability and the normalized oxygen concentration in the permeate. The objective function exhibited an optimum at the solubility limit of 2% EDTA in water. However, the excessive presence of EDTA reduced both membrane air permeability and oxygen separation. The presence of silver in the membrane caused the blockage of pores in the 30-100 Å diameter range. The pore size distributions of the membranes, measured using gas sorption techniques, provided a good explanation for the observed air permeability and oxygen separation of the membranes.

Acknowledgments

I am extremely grateful to Dr. A.Y. Tremblay for his guidance, direction, encouragement and supervision during the course of this work.

I would like to thank Mr. L. Tremblay and Mr. F. Ziroldo for their help with the set-up of the experiment.

Nomenclature

A	Membrane area (cm^2)
b	Hole affinity constant (bar^{-1})
C	Total concentration of a gas in glassy polymer ($cm^3(STP)/cm^2$, mol/m^3)
C_o	Concentration at the upstream side of the membrane ($cm^3(STP)/cm^2$, mol/m^3)
C_l	Concentration at the downstream side of the membrane ($cm^3(STP)/cm^2$, mol/m^3)
C_D	Concentration of gas molecules dissolved according to Henry's law ($cm^3(STP)/cm^2$, mol/m^3)
C_H	Concentration of gas molecules absorbed in microcavities "frozen" into the polymer matrix ($cm^3(STP)/cm^2$, mol/m^3)
C'_H	Hole saturation constant (cm^3 (STP)/cm^2.bar, mol/m^2.Pa)
D	Diffusivity coefficient (cm^2/s, m^2/s)
$Davg_I$	Average pore diameter incremented at I^{th} data point (Å)
Dp_I	Pore diameter incremented at I^{th} data point (Å)
Dp_{I+1}	Pore diameter incremented at I^{th+1} data point (Å)
E_d	Lennard-Jones Potential (Å)
l	Effective membrane thickness (cm, m)
Lp_I	Length of pore incremented at I^{th} data point (cm^2/g)
M	Molecular weight of the gas (Kg/mol, g/mol)
J	Flux of diffusion of a single gas ($cm^3(STP)/cm^2.s$, $mol/m^2.s$)
K_D	Solubility constant (cm^3 (STP)/cm^2.bar, mol/m^2.Pa)
K_{MY}	Formation constant for EDTA-complex (dim)

p	Partial pressure (bar, Pa)
p_o	Partial pressure at the upstream side of the membrane (bar, Pa)
p_l	Partial pressure at the downstream side of the membrane (bar, Pa)
p^o	Saturated vapor pressure of the system (mmHg)
P	Membrane air permeability (cm^3(STP).cm /cm^2.psi.sec, mol.m/m^2.s.Pa)
$\underline{P}$	Absolute pressure (bar, Pa, psi)
Δp_A	Total pressure difference across the membrane (bar, Pa, psi)
r	Pore radius (m,nm, Å)
r_o	Characteristic radius of the molecule (m,nm, Å)
r_p	Effective or hydrodynamic membrane pore radius (m, nm, Å)
r_k	Kelvin radius of cylindrical capillary (m, nm, Å)
R	Universal gas constant (J/mol. ^oK)
S	Solubility coefficient (cm^3(STP)/ cm^3-bar, mol/m^3.Pa)
SA_I	Incremental surface area (m^2/g)
t	Thickness of the adsorbed layer of vapor in the pores (m, nm,Å)
T	Temperature (°K)
T_c	Critical constant of the gas (°K)
T_b	Boiling point of the gas (°K)
T_R	Room temperature (°K)
V	Air flow rate (cm^3/s)
V_L	Molar volume of the adsorbate in liquid form (m^3)
x	Distance (m)

x Normalized air permeability = $[P/l/(500x10^{-7} - 0)]$

y Normalized oxygen concentration in the permeate = [$\%O_2$ in permeate/(40-21.55)]

Greek Letters

λ Mean free path of gases (m, Å)

γ Surface tension of the adsorbate in liquid form (N/m)

η Coefficient of viscosity of gases (Pa.s)

σ Characteristic diameter of the molecule (Å)

θ' Angle of contact between the liquid and the walls of the pore (degree)

θ Objective function = [x · y]

ε/k Lennard-Jones potential force constant (°K)

Membrane Identification

A Annealed

NA Non-annealed

0-16 % EDTA in the nonsolvent mixture

SN Silver nitrate impregnation

SM Silver metal impregnation

1-3 Coupon number

Abbreviation

ASAP 2000 Accelerated surface area and porosimetry system

BJH Barret, Joyner and Halenda

Table of Contents

List of Tables

List of Figures

Chapter 1

Introduction

The search for better separation and purification methods has focused attention on membrane technologies as a new, energy efficient separation method which has grown from a simple laboratory tool to an industrial process with considerable technical and commercial impact (Strathmann, 1981). Membrane technologies have been used industrially for many years in the concentration of dissolved solids from liquid streams. Applications such as reverse osmosis (RO), ultrafiltration (UF), microfiltration (MF), are common unit operations in several industries. The advancement of membrane technologies in these areas has also led to the development of membranes suitable for gas separations. Gas separations by membranes are widely used in many industrial processes such as the recovery of hydrogen in refinery streams, petrochemical applications, natural gas processing, helium recovery, enrichment of oxygen and inert gas generations from air, and pollution control (Henis and Tripodi, 1983).

Traditionally, separations of mixtures of light gases, such as oxygen and nitrogen in air, were performed using cryogenic distillation. Separations based on membrane permeation and pressure swing adsorption (PSA) have become increasingly competitive (Ruthven, 1989). In order to achieve these separations, factors such as differences in equilibrium adsorption capacities, adsorption/desorption kinetics and micropore

diffusivities are very important. Micropores of a size comparable to the molecular diameter of the sorbate (a few angstroms for light gases) are required in order to achieve the kinetic selectivity of a gas. In addition to size, the difference in solubilities of the gases within the membrane are also important in the separation process (Ruthven, 1989). Therefore factors which control kinetic selectivity and gas solubility within a membrane should be considered and methods should be developed to control these factors in order to incorporate suitable modifications in the membrane.

1.1 State of the Technology

Gas separation technologies utilizing membranes are rapidly attaining the technical maturity of other membrane based processes used in the separation of liquids, such as; Dialysis, RO, UF, MF, Electrodyalisis (ED), and Controlled Release (CR) technologies. This is clearly seen in the development status of membrane processes shown in Figure 1.1 (Zhu and Liu, 1988). The state of development of this technology, gives gas separations a considerable industrial growth potential. Gas separation by membranes is classified as a successful new unit operation which can be integrated industrially and can compete on the basis of overall economics and convenience with other processes such us cryogenics and adsorption/absorption processes (Spillman, 1989).

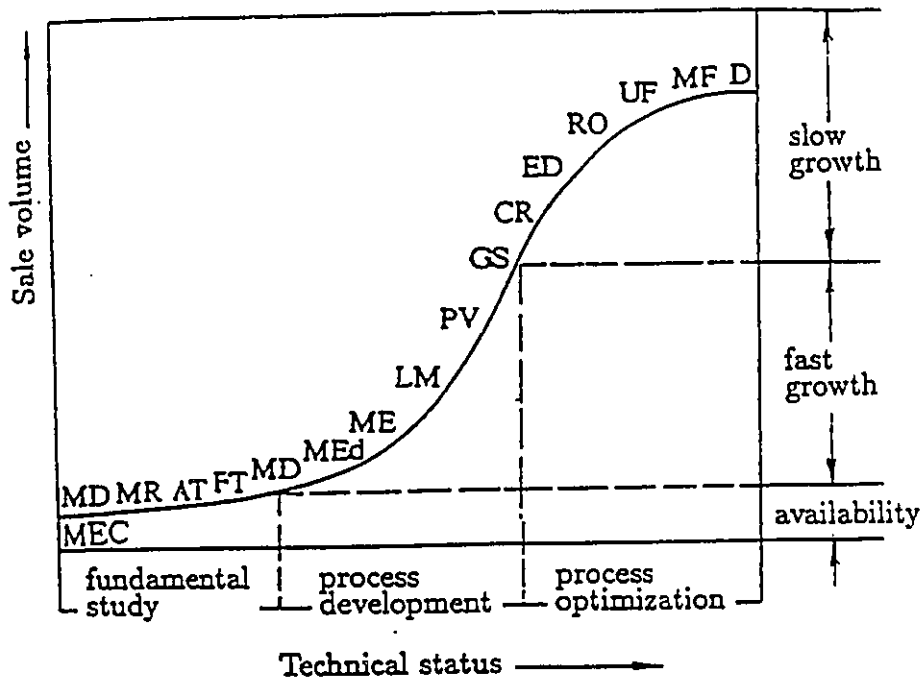

Figure 1.1: The development status of membrane processes. D-dialysis, MF-microfiltration, UF-ultrafiltration, RO-reverse osmosis, ED-electrodialysis, CR-controlled release, GS-gas separation, PV-pervaporation, LM-liquid membrane, ME-membrane electrodes, MEd-membrane electrolyzers, MD-membrane medical devices, FT-facilitated transport, AT-active membranes, MR-membrane reactor, MEC-membrane energy conversion system (Zhu and Liu, 1988).

1.2 Objectives

The objective of this work is to prepare several metal impregnated composite cellulose acetate membranes. The approach is to capture silver ions within the nanoporous structure of the membrane, then reduce the ion to silver metal and anneal the membrane to entrap the silver within the polymer matrix of the membrane. The addition of an additive (EDTA) followed by silver impregnation should, reduce the porosity of the membrane, and increase the affinity of the membrane material for oxygen. The effects of the fabrication parameters such as the EDTA levels in the casting solution and the effect of membrane post-treatments such as heat treatment, metal impregnation and metal impregnation followed by the reduction of the metal are to be studied. The separation of oxygen from air was used and the membrane characterized with respect to air permeability and oxygen separation. The permeability of the membranes was measured with a gas permeation device and the permeate composition determined by gas chromatography. The porosity of the resulting membranes were measured by gas sorption techniques.

Chapter 2

Background and Literature Review

2.1 Historical Overview

Although the demonstration of gas separations by membranes using natural rubber was reported as early as 1830, this technology is relatively new having developed to commercial maturity only in the past two decades. In 1866, Thomas Graham realized that different gases possessed different permeation velocities through a membrane and demonstrated that natural rubber could cause the oxygen enrichment of air (Stanley, 1986).

In the early 1960's, Loeb and Sourirajan discovered an asymmetrically skinned cellulose acetate membrane suitable for reverse osmosis (Loeb and Sourirajan, 1962). In 1968, the Loeb-Sourirajan cellulose acetate membrane was dried using quick freezing and vacuum sublimation techniques giving a membrane with high flux for helium when compared to nitrogen (Gantzel and Merten, 1970). This technique turned out to be uneconomical for industrial use (Minhas et al., 1986). In the 1970's this membrane was finally used for gas separations by adding surfactants to dry the membranes. This treatment improved the performance of the membranes without compromising the

permeable selective skin or its porous support (Gantzel and Merten, 1970; Vos and Burris, 1969).

The air dried Loeb-Sourirajan type cellulose acetate membranes cannot be used directly for gas separations because they tend to lose their permeselective properties due to the collapse of the support layer on drying (Young et al., 1989). These membranes must be dried using a solvent exchange technique to be suitable for gas separation. This method has successfully been used to dry cellulose acetate membranes in order to preserve the membrane structure (MacDonald and Pan, 1978, Minhas et al., 1984). The method consists in replacing the water in the membrane with a volatile solvent having a lower surface tension than that of water. Typically isopropyl alcohol, is used followed by hexane, the membrane is then air dried (Fouda et al., 1987). Manos, (1978) and Stern et al., (1974) helped in developing the solvent exchange method industrially together with Schell (Schell, 1975).

In the mid 1970's, Union Carbide developed a dense walled membrane using a water flotation method. This technique produced homogeneous ultrathin membranes with high permeability silicone rubber or silicone rubber polycarbonate copolymers (Koros and Fleming, 1993). In addition, Du Pont developed and tested a gas separation membrane for industrial applications but it was commercially unsuccessful (Gardner et al., 1977). In 1973, the first gas selective polymeric membranes designed specifically for gas separations were prepared from various polymers (Bouchilloux et al., 1973; Kimura, 1973).

Subsequently, a composite membrane with both high permeation and selectivity was developed. This membrane was made by preparing an asymmetric membrane from a

specific polymer and then coating it with a rubbery polymer to eliminate the defects and the pores resulting from the asymmetric case. These composite membranes are considered the most economical for gas separations (Henis and Tripodi, 1980).

During the 1970's, Monsanto developed a hollow fiber gas separation membrane (PRISM). This product was used commercially in a variety of hydrogen separation processes particularly for purge gas recycling in ammonia plants. With the introduction of the PRISM membrane, gas separation technologies based on membrane systems became commercially viable and more widely used.

Gregor et al., (1978) and Haggin, (1988) reported on some of the membranes which were available commercially. Kim et al., (1988) have reviewed the manufacturing of new polymeric materials and the development of asymmetric membranes with a thin gas selective skin on a porous support (Henis and Tripodi, 1983). In the late 1980's, high flux flat membranes with a skin less than 0.2 μm were prepared using solvent evaporation (Pinnau and Koros, 1990).

Since the membrane produced in this work is an organic-inorganic hybrid, a short history of inorganic membranes follows. In 1940, the industrial use of inorganic membranes in the enrichment of Uranium 235 from approximately 0.71% to 3% by weight was reported. However, this process became unsuccessful in the face of competition from alternative processes (Werner, 1986).

Inorganic membranes have been studied since the late 1950's, they can be divided into three types based on the mechanism of separation (Govind et al., 1991); porous membranes such as vycor glass, ceramic, dense membranes produced from metals, and

composite membranes with a porous structure for support and a thin dense layer for separation.

Porous membranes are characterized by high permeabilities but low selectivities based on Knudsen diffusion. Dense membranes have low permeabilities but very high selectivities based on the solution diffusion model (Lewis, 1967). Composite membranes, consisting of a porous material which serves as a support and a thin metal layer, offer high permeability and high selectivity.

2.2 Applications of Synthetic Membranes in Gas Separations

In chemical industries, unreacted hydrogen can be recovered and recycled from waste gas streams, i.e., from shale, tar sands and coal conversion processes (Henis and Tripodi, 1983). Valuable nonrenewable resources such as helium can be recovered and recycled. Carbon dioxide and hydrogen sulfide can be removed from low grade natural gases. Their removal purifies the treated stream and reduces a pollution problem. Further more, carbon dioxide could be reused in tertiary oil recovery, in the recovery of methane from mines, landfills, and in the recovery of certain exhaust gases. Air can also be separated into oxygen and nitrogen by techniques other than membranes (Henis and Tripodi, 1983).

Applications of membranes for hydrogen recovery from various gas streams concentrates on purging ammonia and methanol gases, on syngas ratio adjustment and on the recovery from shale, tar sands and coal conversion processes (Laverty and O'Hair,

1986, MacLean, 1980). Another important application related to sour gas processing is the recovery and reuse of carbon dioxide in enhanced oil recovery (EOR) (Schendel, 1986), natural gas sweeting (Mazur and Chan, 1982) and landfill gas upgrading (Ruf and Egli, 1988). Membranes can also be used in the dehydration of process gases, acid gas treatment and the recovery of helium from natural gas and deep-sea diving atmospheres (Pan and Habgood, 1978b; Stern, 1986).

Separating organic vapors from contaminated air is another interesting application (Strathmann et al., 1986). In addition membrane systems are presently used for gasoline vapor recovery (Kokan, 1987). Membrane technology is also used in removing radioactive rare elements from the waste gases emitted from nuclear plants. Membrane technology is considered to be the safest method for the treatment of radioactive waste gases. Membrane processes are capable of functioning easily at normal temperature with ease of operation when compared to other methods previously used such as cryogenic adsorption, cryogenic distillation and solvent absorption (Ohno et al., 1977).

Metalized polymer membranes are already widely used in space technology for thermal blanketing (Stoever, 1986), as superinsulating materials in winter clothing and emergency blankets, for winding to form capacitors, for decorative purposes (Chapman and Anderson, 1974) and in the food packaging field. The majority of these metalized membranes are available commercially and are made of aluminum, zinc or gold deposited on base of polyesters, polypropylene or polyimide.

Dense inorganic membranes with the exception of palladium membranes, utilized in Russia (Gryaznov, 1986), have not been widely used in the industry. Some dense metal

membranes such as those made of palladium and its alloys have been used industrially in Russia for separating hydrogen from other gaseous or liquid components. Dense zirconia membranes have been used on a limited scale in oxygen sensors (Gryaznov, 1986).

Currently commercial porous inorganic membranes are produced from alumina, glass, silver, stainless steel and zirconia. Most of the industrial applications of inorganic membranes are for the separation of liquids. Porous ceramic membranes of alumina and zirconia have been used earlier in separating uranium isotopes in the nuclear industry, but porous inorganic membranes have not been used commercially in the field of gas separations, though there are a few studies involving their possible applications (Hsieh, 1988).

Metal and inorganic metal composite membranes are used in the field of gas separations at ambient and elevated temperatures in the areas of;

- nitrogen and oxygen separation from air,
- hydrogen recovery from refinery gas streams,
- recovery of tritium from liquid lithium and lithium-lead alloys in liquid metal tritium breeders (Oxidative permeation palladium membranes have been used successfully to remove tritium from liquid sodium and hydrogen from zirconium),
- separation of hydrogen from coal gasifiers,
- increasing the effectiveness of fuel cells by using hydrogen permeable electrodes,
- production of ultrapure hydrogen for semiconductor industry applications,
- hydrogen sensor applications,
- separation of sulfur dioxide and nitrogen oxides from stack gases,

- purification of methane.

Considerable research has also been devoted to the use of inorganic membranes as catalytic reactors in view of their thermal and mechanical stability, selective permeabilities, catalyst impregnation, membrane reaction considerations, reactor configuration, and reaction coupling.

Metal membranes have been used for the following reactor applications (Hsieh, 1988):

- hydrocarbon oxidation, such as methane to methanol, ethylene to ethylene oxide,
- steam reforming of natural gas,
- dehydrogenation reactions, such as cyclohexane to benzene, ethylbenzene to styrene, i-butene to butadiene,
- hydrations reactions, such as ethylene to ethanol using acid catalysts,
- separation of intermediates, such as gasoline without aromatics from methanol,
- hydrogenation reactions, such as synthesis gas to methanol,
- hydroformylation reactions with homogeneous catalysts,
- olefin metathesis reactions.

Metal porous substrate composite membranes can exhibit high permeation rates and high selectivities for gases at elevated temperatures (Hsieh, 1988).

Air separation is potentially the most important application for membrane gas separations because of its tremendous market size. In 1989, nitrogen was the second and oxygen was the third largest commodity chemical produced in the United States with a total market value of approximately 2.3 billion dollars (Anonymous, 1990). However, as

of 1991, only nitrogen production from air was economical using membranes compared to other competing processes due to the limited selectivity of existing polymeric material for oxygen.

Oxygen concentrations up to 40% and nitrogen concentration up to 98% can be achieved in a single stage membrane system. Such systems operate under lower energy requirements with favorable capital and operating costs when compared to pressure swing adsorption (PSA) or other technology. The best oxygen selective membrane made of silicone rubber produces no more than 35% oxygen in a single stage pass (Ward et al., 1976; Asakawa, 1985). An improvement for oxygen permeselectivity have been made by adding a small amount of surface-active polydimethylsiloxane graft copolymer to polystyrene and poly(methyl methacrylate) films where small domains have been observed acting as highly soluble regions for oxygen (Kawakami et al., 1986). The selective transport of molecular oxygen in a polymer containing a cobalt prophyrin complex was reported to improve oxygen permeselectivity (Nishide et al., 1986). It was found that the addition of substances (i.e. thiourea, lithium chloride and cesium chloride) alters significantly the oxygen permeselectivity (Zhang et al., 1987).

The use of oxygen enriched air is common in many commercial and medical applications such as; industrial burner combustion and efficiency improvement, fermentation cell growth improvement, pulp bleaching, and inhalation therapy (Gollan and Kleper, 1988). A stream with oxygen, free of particulate is useful in the biomedical field. For example systems using silicone rubber membranes produce oxygen enriched air for home use by people having lung diseases and asthma (Baker and Blume, 1986). Oxygen-

enriched air is also used in the liquification and gasification of coal to produce suitable process gas (Laverty and O'Hair, 1986).

Nitrogen production via membranes is useful for many applications requiring inert gas blanketing for the storage and shipment of flammable liquids, and fresh fruits and vegetables providing a non toxic, non residual protection (Spillman, 1989). Nitrogen is also used in enhanced oil recovery applications in the same way as carbon dioxide. The use of nitrogen in offshore oil production has been reported (Laverty and O'Hair, 1986). Nitrogen has been used in drying, moisture exclusion, purging, oxygen exclusion, inflation, chilling, biological decontamination and dust exclusion (Bhat and Beaver, 1988).

Commercially, membranes must compete with gas cylinders, delivered liquids, on-site pressure swing adsorption and on site cryogenic production. The separation of oxygen from nitrogen using membranes is favored and more attractive for the lower volume and lower purity applications (Bhat and Beaver, 1988).

Gas separation by membranes compete with cryogenics and many adsorption-absorption processes like amine treatment, pressure swing adsorption. Membranes systems are characterized by ease of operation, low capital investment, low energy consumption, cost effectiveness at lower gas volumes, good weight and a space efficiency (Spillman, 1989), ease of fabrication, good to high permselectivity (Anderson et al., 1988). Compactness, flexibility and simplicity are the three strongest points that characterize membrane technologies (MacLean, 1986).

2.3 Integration with Other Technologies

Integration of other technologies such as adsorption, catalytic and cryogenic with membranes provides high purity gas at low energy cost, something presently impossible with membrane technology alone (Bhat and Beaver, 1988, MacLean, 1986). The combination of membrane based air separation with other technologies in hybrid systems is often advantageous. Such combinations are useful in gas generations systems for aircraft (Beaver et al., 1988). Membranes can be also combined with cryogenics in both large scale and small scale systems, improving efficiency and economy (Agrawal and Auvil, 1986).

Membranes can be used in conjunction with catalytic oxygen removal providing an initial separation ahead of the polishing unit and reducing the oxygen content to around 0.5% (Beaver et al., 1988). Characteristics of integrated systems with membranes can be seen in Table 2.1 (Beaver et al., 1988).

Table 2.1 : Characteristics of integrated systems.

Process	Portability	Purity	Scale	Surge Capacity
Adsorption+ membrane	good	two streams good	medium	limited
Catalytic+ membrane	fair	one stream good	medium	limited
Cryogenic+ membrane	fair	one stream good	small to medium	excellent

2.4 Membranes and Materials

Polymers which are mainly glassy (cellulose acetates, polyamides, polysulfones polyimides) are widely used in the field of membranes based gas separations because these membranes have a high permeselectivity for smaller molecules compared to larger ones.

A number of companies such as Dow, Separex, Envirogenic are using hollow fiber or spiral wound cellulose acetate membranes (Zhu and Liu, 1988). Polymers which are rubbery such as silicone rubber and nitrile rubber have successfully been utilized as coating materials to plug the defects in skinned polysulfone membranes eliminating the flow of unseparated gases through these defects (Henis and Tripodi, 1980).

Glassy polymers are characterized by a low intrasegmental mobility and long relaxation times, whereas rubbery polymers exhibit the opposite characteristics (Stern, 1994).

An ideal asymmetric membrane should meet the following requirements according to Koros and Chern (1987); the skin layer should be defect free, the skin layer should be as thin as possible to maximize membrane productivity and to reduce flow resistance. The substructure should have sufficient mechanical strength to support the delicate skin layer during high pressure operations. The composite structure should resist fluid dynamic shear, wear, handling and cleaning.

Unfortunately, the combination of an ultrathin and defect free skin layer is very difficult to obtain (Henis and Tripodi, 1981, Murphy et al., 1989). The key membrane performance variables are selectivity, permeability and durability. However in practice,

in practice, there are tradeoffs between selectivity and permeability (Maclean, 1986): highly selective membranes have low permeabilities and vice versa. These limitations imply that higher selectivities increase product losses and increase area requirements while lower selectivities decrease permeate partial pressure and in turn reduce membrane area with a small increase in gas loss (Spillman, 1989).

Therefore, to be commercially viable, a membrane must satisfy a number of requirements, including: high permeability, high selectivity, high membrane area per unit volume (membrane area density in the support module), high stability (good chemical, mechanical, and thermal properties), and ease of fabrication. The intrinsic permeability and selectivity are mostly determined by the membrane material; the membrane area density is controlled by the engineering approach to membrane making, while the stability is affected by both permeability and selectivity. In the field of gas separation by membranes, there is always a constant search for membrane materials with favorable properties, and the techniques of fabricating a thinner effective membrane and module with large membrane area densities. Several methods have been used to enhance selectivity such as the continuous membrane column (Hwang and Thorman, 1990), the dual membrane permeator (Perrin and Stern, 1985; Sirkar, 1980), permeators with a sweep stream (Pan and Habgood, 1978a), plasma polymerization (Lonsdale, 1984), and facilitated transport membranes (Gottschlich et al., 1988).

Cellulosic esters are widely used in the production of gas separation membranes. Cellulose acetate (CA) used in this study is not considered to be the best polymer in the field of air separation due to its lower selectivity regarding oxygen. However, it is easily

soluble in an acetone/water mixed solvent which is less toxic compared to other solvents commonly used in membrane preparation. The presence of water in the solvent mixture used to produce reverse osmosis (RO) membrane permits the incorporation of a water soluble ligand into the casting solution. Despite its lower oxygen selectivity, cellulose acetate (CA) was used in this study since we are not searching for the best possible polymer but we are interested in studying the performance of metal impregnated membranes.

2.5 Ion Exchangers and Polyectrolytes

Ion exchangers are defined as insoluble solid materials carrying exchangeable cations or anions. These ions can be interchanged with an equivalent amount of ions of the same charge, when the ion exchanger comes into contact with an electrolyte solution. Ion exchangers having exchangeable cations are termed cations exchangers while those having exchangeable anions, are termed anions exchangers (Helfferich, 1962).

Synthetic organic ion exchanger resin are classified as the most important group of ion exchangers. They are produced and widely employed. They could be described as gels and visualized as an elastic three dimensional network of hydrocarbon chain which consist of a framework or matrix. These matrices carry ionic groups such as;

$$-SO_3^- \ , \quad -COO^- \ , \quad -PO_3^{2-} \ , \quad -AsO_3^{2-} \ ,$$

in cations exchangers, and;

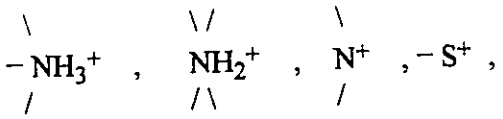

in anions exchangers (Helfferich, 1962).

Ion-exchange resins are often referred to as cross linked polyelectrolytes. The most important hydrocarbon network developed to this moment is the one manufactured by the copolymerization of styrene and divinylbenzene (DVB). This structure has excellent properties such as maximum resistance to breakage, oxidation, mechanical wear and oxidation and is insoluble in common solvents. The polymerization of styrene gives a linear or two dimensional polymer where the copolymerization of this polymer with a crosslinking agent called divinylbenzene gives rise to an insoluble three dimensional polymer.

The amount of cross linking agent (DVB), determines the permeability of the ion exchange resin, and the particle size, is controlled during the preparation of these three dimensional structures. The framework of the matrix is hydrophobic but hydrophilic ionic groups such as $-SO_3^-H^+$, are introduced into the matrix. In general the incorporation of such groups into linear hydrocarbon macromolecule makes it soluble in water, but crosslinking makes the ion exchange resins insoluble because various hydrocarbon chains are interconnected.

The ion exchange resin particle can be considered as one single macromolecule and its dissociation would require rupture of carbon-carbon bonds. This implies that the resins are insoluble in all solvents by which they are not destroyed. However, the matrix is elastic and can be expanded. The resins have the ability to swell by taking up solvent. A schematic representation of the framework of the resins can be visualized (Figure 2.1) as a flexible random network where the mesh width is not uniform, a fact that is referred to as "heteroporosity" or "heterodictiality" (Helfferich, 1962).

Therefore the chemical, thermal, and mechanical stability and the ion-exchange behavior of the resins will be governed by the structure and the degree of cross linking of the matrix and on the nature and number of the fixed ionic groups. The degree of crosslinking determines the mobility of counterions in the resin as well as the mesh width of the matrix and the swelling ability of the resin. The mobility of counterions in the resins will determine the rate of ion exchange and other processes and the electric conductivity of the resin. The mesh width of a very weakly cross linked and fully swollen resins may exceed 100 Å while it is in the order of only a few angstrom units for a highly crosslinked resins. The latter are much harder and are more resistant to mechanical breakdown and attrition (Helfferich, 1962).

Furthermore, the ion-exchange behavior of the resins is greatly determined by chemical nature of the group that affects the ion-exchange equilibrium. The number of fixed ionic groups will also affect behavior by determining the ion-exchange capacity of the resin. A very important factor that must be considered in selecting an ion exchange resin is the acid or base strength of ionic groups.

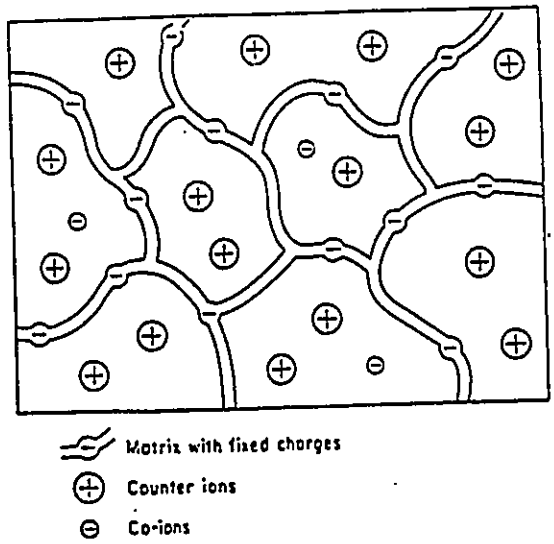

Figure 2.1: Structure of a polyelectrolyte (Helfferich, 1962).

2.6 EDTA as a Ligand

Ethylenediaminetetraacetic acid (EDTA), is the most commonly used polyaminocarboxylic acid. It is used as a water softener (complexation of calcium and magnesium), as a textile dyeing assistant (complexation of heavy metals), as a masking reagent to prevent interference and to increase the selectivity of analytical chemistry tests (Cheng, 1963), as a chromogenic agent in spectrophometric procedures, in polarography and ion exchange procedures (Flaschka, 1964). In addition EDTA is frequently used in analytical applications such as titrant reagent (Welcher, 1958).

EDTA is a weak acid, where the first two protons are lost more readily than the remaining two. In addition to the four acidic hydrogens of the COOH groups, the two nitrogens have an unshared pair of electrons each. There are thus six potential bonding sites for complexing with metal ions and it is therefore considered a sexadante ligand (Skoog and West, 1974). The structure of EDTA is shown in Figure 2.2.

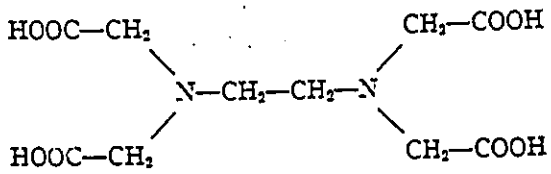

Figure 2.2: Structure of EDTA (Skoog and West, 1974).

EDTA can combine with metal ions in a 1:1 ratio for any cationic charge. It can form complexes with nearly all polyvalent metal ions and with many monovalent cations, including alkali metals (Flaschka, 1964). The complexed metal ions are held firmly in place and are fairly stable. The structure and stability of this complex can be illustrated by the tentacle like embrace in which the cations are held by the six potential sites, all of which participate in the complexing reaction. The abbreviations H_4Y, H_3Y^-, H_2Y^{2-}, HY^{3-} and Y^{4-} are often used to refer to EDTA and its ions.

At a pH higher than 10 (i.e. in strongly alkaline solution), EDTA will be present as Y^{4-} , while it is presented in its protonated forms H_4Y, H_3Y^-, H_2Y^{2-}, HY^{3-} at lower pH. The presence of EDTA in the membrane polymer matrix is expected to help in holding

metal ions in the membrane through metal-EDTA chelate formation as shown in Figure 2.3 (Skoog and West, 1974).

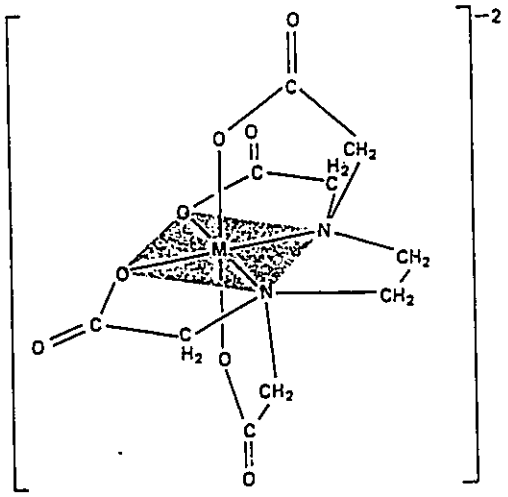

Figure 2.3: Structure of a metal -EDTA chelate (Skoog and West, 1974).

The formation constant (K_{MY}) values for many EDTA complexes are reported in the literature (Schwarzenbach, 1957). This constant refers to the equilibrium involving the fully ionized anion of EDTA (Y^{4-}) (unprotonated ligand) that forms complexes with the metal ion M^{n+} ,That is;

$$M^{n+} + Y^{4-} \Leftrightarrow MY^{(n-4)+} \qquad (1)$$

The equilibrium constant for this reaction is given by;

$$K_{MY} = \frac{\left[MY^{(n-4)+}\right]}{\left[M^{n+}\right]\left[Y^{4-}\right]} \qquad (2)$$

Metal ions having an affinity for a particular gaseous species can be incorporated into the porous structure of the membrane. The selective adsorption and subsequent transport of these gaseous species will be enhanced when EDTA is available to capture the metal within the membrane. The formation constant K_{MY} for EDTA complex with silver metal Ag^+ is reported to be equal to 2.1×10^7 (Schwarzenbach, 1957), which is much greater than 1 indicating that binding of Ag^+ with EDTA is highly favorable.

2.7 Swelling of Membranes

Ion-exchange membranes swell and imbibe water and ions when they are immersed in an aqueous solution. This water is important because in their absence the conductance of the membranes will be too low to be used for practical purposes in elecrodialysis (ED) or other applications utilizing ion-exchange membranes. Water is needed to dissociate the ions and plasticize the polymeric network.

Water penetration into the membrane is due to four important factors (Meares, 1968):

1. Absorption of solvent by the polymers where the polymers tend always to absorb water in order to increase their total configuration entropy, and the amount of

water absorbed is determined by the hydrophobic-hydrophilic balance of the polymeric material to which the fixed ions are attached.

2. The fixed charges and counterions will bind water of hydration to a degree that will depend on the charge, size and the polarizability of the ions concerned.
3. The counterions and fixed charges become dissociated and this result in an osmotic pressure which causes more water to flow into the membrane because of the higher molality within the membrane side compared to that of the surrounding solution.
4. As in the case of polyelectrolytes, the network will extend and expand because of the electrostatic repulsion between the chains, the counterions and the fixed charges.

The degree of swelling is chiefly limited by the elastic tension which are found in the chain segments between fixed points. Swelling is favored by the following (Helfferich, 1962):

1. Polar solvents: Because of the strong interactions that exists in the resin between the ions and the polar groups, polar solvents are therefore much better swelling agents than the non polar ones.
2. Low degree of cross linking of the resin: The greater number of links present in the membrane, the greater the swelling reduction because the matrix is more rigid.

3. High capacity of the resin: The existence of higher concentrations of charged groups, enhances the ability to dilute the liquid within membrane pores. The swelling behavior will be more pronounced compared to the low capacity resins.
4. Strong solvation tendency of the fixed ionic groups.
5. Large and strongly solvated counter ions.
6. Low valence of the counter ions.
7. Complete dissociation in the resin: The formation of complexes reduces the swelling when there is an association between counter ions and fixed groups. The position of the counterions reduces the free energy of mixing in molecular models while it will reduce the osmotic activity and the ability to create solvation shells according to macroscopic models.
8. Low concentration of the external solution: A lower solution concentration increases the swelling, but a higher concentration will reduce the solvent uptake and this in turn will reduce the free mixing energy in the molecular model or the difference in the osmotic pressure in the interior of the resin.

2.8 The Development of Polymer-Metal Impregnated Composite Membranes

Few papers have been published on polymer-metal composite membranes. Papers by Springer and Brite, (1979), and Sakai et al., (1985), both deal with the preparation of a metal composite membrane based on the perfluorosulfonic acid membrane Nafion^{TM} as the bulk polymer. The concept in fabricating both membranes was to incorporate a charged

metal into a polymer matrix of opposite charge and then dry the membrane. The presence of the metal improves the selectivity of the membrane at a given permeability by affecting the sorption characteristics of a specific gas in a mixture and by blocking larger pores which reduce the selectivity of the membrane (Mercea et al., 1985).

Silver has a higher affinity for oxygen than nitrogen (Johnson and Larose, 1924, Shumilova and Zhutaeva, 1978). Several silver alloys have been incorporated into membranes and their ability to separate oxygen from air determined (Union Carbide Corp., 1967, General American Transportation Corp., 1970). Cobalt (II) complexes were also incorporated into polystyrene membranes and their affinity for oxygen was reported to cause the enrichment of oxygen in compressed air (Drago and Balkus, 1986, Balkus et al., 1988). It was reported that ruthenium and rhodium complexes could be easily incorporated into an ion exchange resin or neutral cellulose acetate with reactivity toward small gaseous molecules such as hydrogen, carbon monoxide, oxygen and ethene (Park and Shim, 1991, Shim and Risen, 1988).

Generally speaking, metal membranes offer good thermal stabilities at high temperature, chemical resistance, high thermal conductivity for heat flow, high selectivities for specific gases, and catalytic properties for certain reactions. The major disadvantages are lower permeation rates by a factor of 100 (Ilias and Govind, 1989), poisoning from contaminants, high thermal expansion, and in some cases the ability to catalyze unwanted side reactions (Govind et al., 1991).

2.9 The Production of Gas Separation Membranes

Membrane making is an important parameter that influences membrane performance and transport properties. Two methods are widely used to prepare an asymmetric non-porous membrane. The first method is phase inversion (Kesting, 1985), while the second method is the deposition of a very thin polymer film on a microporous substructure (Strathmann, 1986). Many commercial gas separation membranes and supports for film coating are produced by the phase inversion technique.

Kesting (1985) reported phase inversion as a process where a polymer, solubilized in a liquid phase, is precipitated into a solid state. Phase inversion covers a range of different techniques such as; precipitation by solvent evaporation, precipitation from the vapor phase, precipitation by controlled evaporation, thermal precipitation and immersion precipitation (Wijmans and Smolders, 1986).

Phase inversion by immersion precipitation is widely used commercially and was used to prepare all membranes in this study. In this method, a casting a solution consisting of a polymer, solvent, and nonsolvent is spread onto a support, and immersed into a gelation bath containing a gelling agent, usually water. The gelling agent then penetrates the casting solution and the solvent leaves the casting solution, as shown in Figure 2.4. In this Figure J1 represents the flux of the gelling agent into the cast film and J2 represents the flux of the solvent into the coagulation bath.

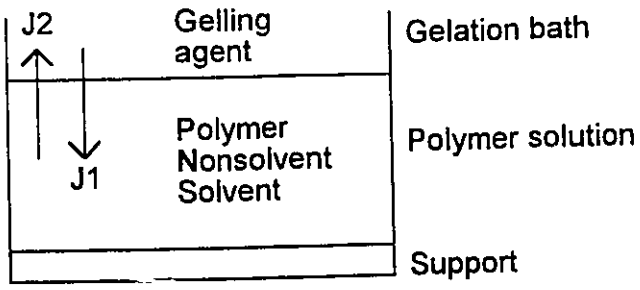

Figure 2.4: Phase inversion immersion precipitation (Mulder, 1991).

The exchange of solvent and gelling agent eventually causes the solution to be thermodynamically unstable so that de-mixing takes place until a solid film starts to form resulting in an asymmetric structure which consist of a very thin dense top layer or skin with a thickness of 0.1 to 0.5 μm and it is supported by a porous sub layer about 50 to 150 μm (Mulder, 1991).

Several parameters influence the structure and properties of phase inversion membranes including (Strathmann, 1986): (1) the polymer and its concentration in the casting solution, (2) the solvent or solvent system, (3) the precipitant or precipitant system, (4) the form of the precipitant (vapor or liquid), (5) the temperature of precipitation, (6) the pre- and post-precipitation procedures, such as an evaporation step or an annealing step, which have some effect on membrane properties. Certain membrane structures can always be correlated with the rate of precipitation during the membrane structure formation stage. High precipitation rates lead to a finger structure, while slow precipitation leads to asymmetric membranes with a sponge structure (Strathmann, 1985).

The role of the nonsolvent additive in the casting solution is that of a swelling agent, it is neither a total solvent nor a total precipitant with respect to the polymer. Kesting (1965), reported that the role of inorganic salts in aqueous solution, as additives in casting cellulosic materials, is related to the capacity of the component ions to swell the cellulosic substrates. In addition, many additives can form a complex with the polymer which forces additional water to enter the polymer network on gelation (Vinit et al., 1974).

Chapter 3

Theory

3.1 Transport Mechanisms

In general, most gas separation membranes are of the glassy-amorphous polymeric type. According to Graham (1866), the transport of gases through polymeric films occurs by the sorption on the high pressure side of the membrane, followed by diffusion through the film and desorption on the low pressure side of the membrane. Graham also reported that permeation is based on gas diffusion and on the concentration difference of the gas across the membrane.

The transport and sorption of gases in glassy polymers can be described by the dual-mode sorption theory. In this model, two populations of gas molecules exhibiting different types of adsorption are said to exist within the polymer matrix, namely:

1) The first population consists of molecules which yield ideal and linear sorption isotherms described by Henry's law where the solubility inside the polymer is proportional to the applied partial pressure and independent of gas concentration. This is shown by the following equation (Stannett et al., 1979);

$$C_D = K_D\ p \tag{3}$$

2) The second population of molecules follows Langmuir type adsorption in the microcavities "frozen" into the polymer matrix where there is a relationship between the concentration of the gas molecules and the applied pressure, as follows;

$$C_H = \frac{C_H' \, bp}{1+bp} \tag{4}$$

where C_H' and b are two constants representing "the hole saturation" and "the ratio of rate constants of gas adsorption and desorption in the microcavities or the affinity constant", respectively.

Therefore, in combining both isotherms, we can calculate the total concentration for any gas in any glassy polymers. This can be represented by the following equation;

$$C = C_D + C_H = K_D \; p + \frac{C_H' \, bp}{1+bp} \tag{5}$$

Meares (1968), reported that a different theory called the solution-diffusion model could also be used to describe the transport of simple gases across polymeric membranes. It postulates that membrane "molecular brownian motion" is the main factor that controls the slow transport of gas through the membrane. In addition to that, the polymer and gas within the membrane first behave homogeneously and are thermodynamically stable, but

when transport across the membrane takes place, diffusion as a result of a concentration gradient is caused by the random motion of the polymer chains and the gas molecules.

This diffusion-phenomena can be expressed by Fick's-law where flux J, through the membrane is a function of the diffusion coefficient D and the concentration gradient across the membrane, dc/dx as follows (Crank, 1975);

$$J = -D\frac{dc}{dx} \tag{6}$$

At steady-state, the above equation can be integrated to give the following equation when applying boundary conditions ($c = Co$, at x = 0 and $c = C_l$, at x = l);

$$J = \frac{D(Co - C_l)}{l} \tag{7}$$

Where, C_o and C_l represents the value of the concentration at the upstream side and the downstream side of the membrane, while l represents the thickness of the membrane.

According to Henry's law, a linear-relationship exists between the concentration inside the membrane and the partial pressure of gas outside the membrane, setting $K_D = S$ in Equation (3);

$$C = S \cdot p \tag{8}$$

where S denotes the solubility coefficient.

The flux of a gas having C_o and C_l as an inlet and outlet concentrations can be calculated by combining the two equations written above assuming that the solubility S and the diffusivity D are constants at constant temperature, and which yields the following equation;

$$J = \frac{DS(p_o - p_l)}{l} = \frac{P(p_o - p_l)}{l} \tag{9}$$

where, the product of the solubility and the diffusivity inside and outside the polymer matrix gives the permeability P ($P = DS$).

The solubilities of gases in polymers are very low (<0.2% by volume), and the diffusion coefficient will depend on the sizes of the molecules, the amount of excess or free volume, and subtle polymer motions.

3.2 Method of Data Analysis

Much has been published on polymer permeability (Crank and Park, 1968, Crank, 1975). In addition several references exist on the specific subject of gas separation through polymeric membranes (Hwang et al., 1974, Koros et al., 1988). The membrane permeation process can be described by Equation (9) above, derived from Henry's and Fick's law.

The precise thickness of an asymmetric membrane is often unknown and also hard to obtain. Therefore, membrane permeability is expressed as the thickness normalized air permeability, (P/l), which can be determined from experimental measurements. From an engineering point of view, (P/l) is more relevant than P alone as this value reflects the performance of the entire membrane. In this work, air permeabilities expressed as P/l have been calculated by measuring the volume of the permeate leaving the test cell, corrected for the room temperature using the relation;

$$\frac{P}{l} = \frac{V}{A}\frac{1}{\Delta p_A}\left(\frac{273.15}{T_R + 273.15}\right) \qquad (10)$$

Where Δp_A is the air or feed pressure drop. All permeabilities in this work were based on the total pressure difference across the membrane (85.33 psi = 5.89×10^5 Pa).

The objective in membrane design is to produce membranes having both high selectivity and permeability. A design can only be considered beneficial if it increases both permeability and selectivity. An objective function (θ), was used to determine the benefits of a particular casting formulation or post-treatment. This function was the product of the normalized air permeability (x), and normalized oxygen concentration in the permeate (y) ($\theta = x \cdot y$). Such a function follows the same general behavior as most data on membrane permeation and separation. The air permeability data were normalized between 0 and 500×10^{-7} (cm^3(STP)/cm^2.psi.sec), and the oxygen concentration data normalized between the oxygen concentration recorded in the feed (21.55 mole %) and a concentration of

40 mole % which is slightly greater than the maximum concentration recorded in the permeate.

3.3 Membrane Characterization

Various methods have been used to characterize the porous structure (pore size, pore size distribution, pore volume) including X-ray scattering, bubble point determination, mercury intrusion and fluid permeation measurements (Kesting, 1971). As previously discussed, asymmetric membranes consist of a very thin dense top layer (skin) and a porous structure. The skin layer is responsible for the permeation and selectivity of the membrane. Therefore, the most important characteristics of the skin layer are the thickness of the top layer and the pore structure (pore size and pore size distribution). In this work, gas sorption was used to characterize membranes. Both the skin and support layers of the skin were characterized using this method. It is assumed here that, for cellulose acetate membranes, the fine pores of the support layer less than 100 Å diameter are representative of those found in the skin layer, this will be further substantiated in Chapter 5.

3.3.1 BJH Desorption Pore Area Distributions Calculations

The ASAP 2000 (Accelerated surface area and porosimetry system) uses the BJH method to calculate porosity. The BJH method is named after its developers Barret, Joyner, and Halenda (Barret et al., 1951). A brief explanation of the steps used in

calculating the pore area will be given here. The exacts details of this technique are included in Barret et al. (1951).

When a pore is filled with condensed liquid nitrogen, it consists of three zones: The core, the adsorbed layer, and the wall of the cylindrical pore itself. A schematic representation of these zones are shown below in Figure 3.1.

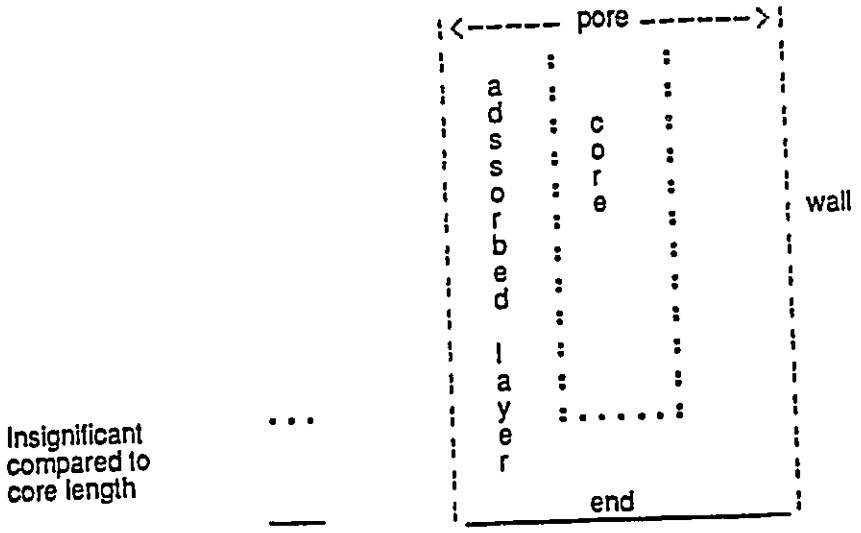

Figure 3.1: The zones in a pore filled with condensable liquid nitrogen (Micromeritics, 1989).

Before using gas adsorption/desorption techniques, the membrane must be air dried without damaging the pore structure (Lloyd, 1985). The determination of pore size and pore size distribution from gas adsorption/desorption involves the study of the hysteresis loop between the adsorption and the desorption curve of a full isotherm. In these experiments a nitrogen adsorption curve is produced where the volume of nitrogen

absorbed in the polymer is plotted against the relative pressure which is the ratio between the applied nitrogen pressure and the saturation pressure.

The desorption branch of an isotherm is used to relate the amount of adsorbate lost in a desorption step to the average sizes of the pores emptied in the step. When a pore loses its condensed liquid adsorbate, it is defined as the core of the pore at a particular relative pressure related to the core radius by the Kelvin equation given by (Kelvin, 1871);

$$RT \ln \frac{p}{p^o} = \frac{-2\gamma V_L}{r_K} \cos \theta' \tag{11}$$

Assuming that the pores are cylindrical in shape and the contact angle is zero, the Kelvin radius is simplified for the case of nitrogen adsorption/desorption as follows;

$$r_k = \frac{-4.1}{\log(p/p^o)} \tag{12}$$

The pore radius (r_p) can be calculated by;

$$r_p = r_k + t \tag{13}$$

After the core is evaporated, a layer of adsorbate remains on the wall of the cores. The thickness of this layer, t in Å is calculated for a particular relative pressure from the Harkins/Jura thickness equation, given by (Harkins and Jura, 1943);

$$t = \left(\frac{13.99}{0.0340 - \log(p / p^{o})} \right)^{1/2} \qquad (14)$$

With successive decreases in pressure this layer becomes thinner, therefore the measured quantities of gas desorbed in a step is equal to the quantities of liquid evaporated in that step plus the quantities desorbed from the pore walls of pores whose cores have been evaporated in that and the previous steps.

The desorption isotherm is divided into intervals which lie between consecutive partial pressure and adsorbed volume measurements as follows.

a) The thickness of the adsorbed layer at the end of an interval is computed using equation (14): The volume desorbed from walls of previously opened pores is equal to zero for the first pressure interval: The change in the thickness of the wall layer from the desorption of the previous opened pores is computed. The annular cross-sectional area of the wall layer desorbed is computed for all previously opened pores. The total volume of the gas desorbed from walls of previously-opened pores is computed for all pores previously opened.

b) The nature of the physical process occurring during the pressure interval is determined;

i) If the volume desorbed from the walls of previously opened pores is greater than the volume desorbed from the walls in the step, desorption from the walls only is occurring, and the total surface of walls exposed thus far is then computed for all previously opened pores. In addition, a new layer thickness is defined and computed to make up for the actual volume desorbed in this interval. Since no cores are evaporated

during this pressure interval, therefore no new pores are calculated, and Kelvin radius and average pore diameter are not computed.

ii) If the volume desorbed from the walls of previously opened pores is less than the volume desorbed from the wall in the step, the core evaporation takes place due to the new pores available: The volume desorbed due to the new opened pores is computed in this interval: The Kelvin radius at the end of this interval is computed: The weighted average pore diameter is computed for all new pores opened in this interval and the relative pressure for this average is computed: The thickness of the adsorbed layer at this pressure is computed from equation (14): The decrease in the thickness of the wall layer due to desorption from the walls of the new pores is computed in this interval: The cross-sectional area and the length of the new opened pores is computed.

c) The pore diameters and the radius are adjusted due to the change in the thickness of the adsorbed wall layer in this interval: The average diameter is adjusted during the second portion of the desorption interval: The layer thickness change is added to the diameters of previously opened pores: The layer thickness change during the whole interval is added to the radius corresponding to the ends of the pressure interval is computed.

All steps from a to c are repeated for each pressure interval. After all these calculations, the diameters corresponding to the ends of intervals are computed. The pore area distribution calculation dA/dD (m^2/g-Å) is calculated only for the average diameter of this interval that lies between a specified minimum and maximum diameter.

Therefore, the pore area frequency for the I^{th} data point is given by;

$$\frac{dA}{dD_I} = \frac{SA_I}{(Dp_I - Dp_{I+1})} \tag{15}$$

Where;

$$SA_I = (3.1416)(Lp_I)(10^{-2}\ \text{m/cm})(Davg_I)(10^{-10}\ \text{m/Å}) \tag{16}$$

Chapter 4

Experimental

This chapter deals with the type of materials, the equipment and the experimental methodology followed in this work. Preliminary tests performed using ion exchange resins (Dowex-50w) and tests to determine the solubility of EDTA in water-acetone mixtures are also discussed in this section.

4.1 Materials

The polymer used to produce all membranes was cellulose acetate E398-6 supplied by Eastman Chemicals (Kingsport, Tennessee). The solvent used in all membrane casting solutions was acetone (BDH Chemicals, Toronto) with a purity of 99.5%. The water used in all test was reverse osmosis water produced on site from tap water.

The resin used in the early experimental work was Dowex-50w (Dow Chemical) which is a strongly acidic cation exchanger. The 50w grade of Dowex has the following properties; ionic form: hydrogen, cross linkage : 2%, drymesh: 200-400, moisture content: 80%, maximum operating temperature: 150°C, total exchange capacity: 0.6 meq/ml or 4.8 meq/g. In addition, in early experimental work, formamide (purity 98%, BDH Chemicals) was used in the resin casting solution formulation.

The additive used during most of this study was the tetrasodium salt of ethylenediaminetetraacetic acid, (EDTA). It was supplied as Versene 220-chelating agent from (Dow Chemical). EDTA is a white, crystalline powder, odorless and with an acid taste, not poisonous, insoluble in acids and common organic solvents, soluble in caustic and ammonium solution and sparingly soluble in water with a solubility limit of 0.02 g in 100 g of water (Flaschka, 1964).

For the preparation of metal impregnated membranes, silver nitrate (purity 99.8%) and sodium borohydride (purity 95%), (BDH Chemicals, Toronto) were used. For membrane drying, isopropyl alcohol (purity 99.5%) and hexane (purity 99.8%), also from BDH Chemicals were utilized. The backing material used was Hollytex, a spunbond polyester produced by Ahlstrom Filtration (Pennsylvania). Chromatographic grade helium (purity of 99.99%) was used as the carrier gas in the gas chromatograph and was obtained from Air Products.

Compressed air (zero grade) was obtained from Air Products and had the following specifications listed in Table 4.1.

Table 4.1: Compressed air zero grade gas specifications.

Analysis	Guarantee	Typical
Oxygen	19.5-23.5 %	21 %
Carbon Dioxide	< 0.5 ppm	< 0.5 ppm
Carbon monoxide	< 1 ppm	< 1 ppm
Acetylene	< 0.05 ppm	< 0.05 ppm
Nitrous Oxide	< 0.1 ppm	< 0.1 ppm
Total Hydrocarbons	< 1 ppm	< 0.1 ppm
Dew point (H_2O)	89°F	125°F

4.2 Equipment

4.2.1 Experimental Setup

A schematic representation of the permeation cell used in this work is shown in Figure 4.1. The cell consisted of two detachable stainless steel cylinders. The membrane was placed between these two parts with the selective layer facing the feed gas. The membrane was placed on two sheets of filter paper to eliminate membrane cracking under pressure. The high pressure side of the membrane was sealed with a flat 1 mm thick rubber gasket placed on top of the membrane. The two parts of the cell were pressed together by an overhead compression bolt. The schematic representation of the test cell is shown in Figure 4.1.

The test cell was incorporated into the system shown in Figure 4.2. The feed inlet to the cell was connected to an air cylinder, the residue was connected to a valve and 200 cc/min (STP) of air were vented to the atmosphere. This gas flow rate ensured a constant feed composition within the cell. The air feed was controlled by a Matheson pressure regulator. The test cell was enclosed in a box and the temperature was measured and recorded using a platinum resistance thermal detector (RTD) and a microcomputer. The atmospheric pressure was also recorded using a pressure transducer (MKS Instruments, Burlington) whose output was also recorded throughout the run using a microcomputer. The permeate stream was connected to an 8 port GC injection valve. The outlet from this valve was connected to a bubble flowmeter used to determine permeate flux, and vented to atmosphere.

A Hewlett-Packard model 5700A gas chromatograph (GC) fitted with a thermal conductivity detector was used to analyze the compositions of the permeate and feed. The thermal conductivity response from the gas chromatograph (GC) was integrated with a Hewlett-Packard model HP 3393A integrator and the results sent to a microcomputer. A molecular sieve column (Alltech) was linked to the injection port of the gas chromatograph (GC). The column had the following specifications: 6 ft length with 1/8 inch outlet diameter stainless steel with a 5Å molecular sieve (Mesh 80/100). Chromatographic grade helium (purity of 99.99%) was used as the carrier gas in the gas chromatograph and was obtained from Air Products. The helium flow rate through the column was 30 ml/min.

A total of fifteen injections were performed and recorded automatically. After ten injections, the composition of the permeate stabilized. But to ensure that the permeate compartment of the test cell was purged of air at atmospheric composition, only the last four injections of the fifteen, were retained to determine permeate compositions.

Dietz (1967), reported that in order to obtain quantitative results from gas chromatography, it is necessary to use correction factors to account for the different responses of gases to the thermal conductivity detector. The area under the peak from the gas chromatograph (GC) divided by the thermal response value gives a corrected response value which is representative of the molar quantities present under the peak. The thermal response values for oxygen and nitrogen are equal to 40 and 42 , respectively (Dietz, 1967). The volume % of oxygen and nitrogen were then calculated based on these corrected response values and used throughout this work.

4.2.2 Permeability Measurements

The permeate side was open to the atmosphere, and the permeability rate of pure air was measured as P/l using a bubble flow meter having 1/10 ml demarcations. The value of P/l was calculated from Equation 10. In Equation 10, V is the volumetric permeation of air measured by a bubble flow meter, cm^3/min, A is the cross sectional area of the test cell available for gas permeation, 9.62 cm^2, Δp_A is the pressure drop across the membrane, (100 - 14.67) = 85.3 psi, T_R is the room temperature recorded as 23°C.

The experimental raw data for the volumetric permeation of air for different post-treatment conditions, using the bubble flow meter, are listed in Appendix A.

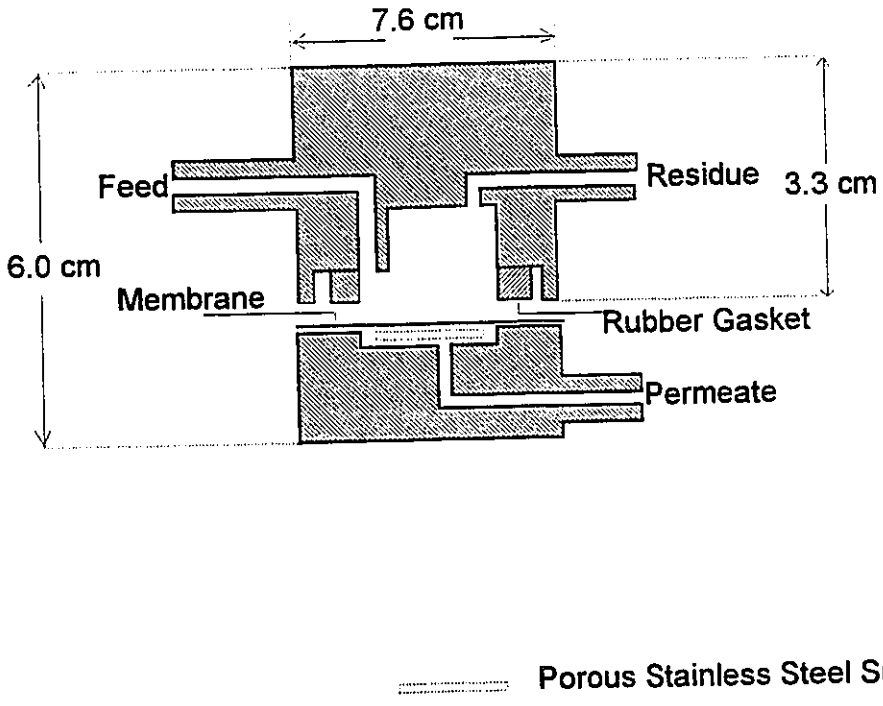

Figure 4.1: Schematic diagram of the test cell.

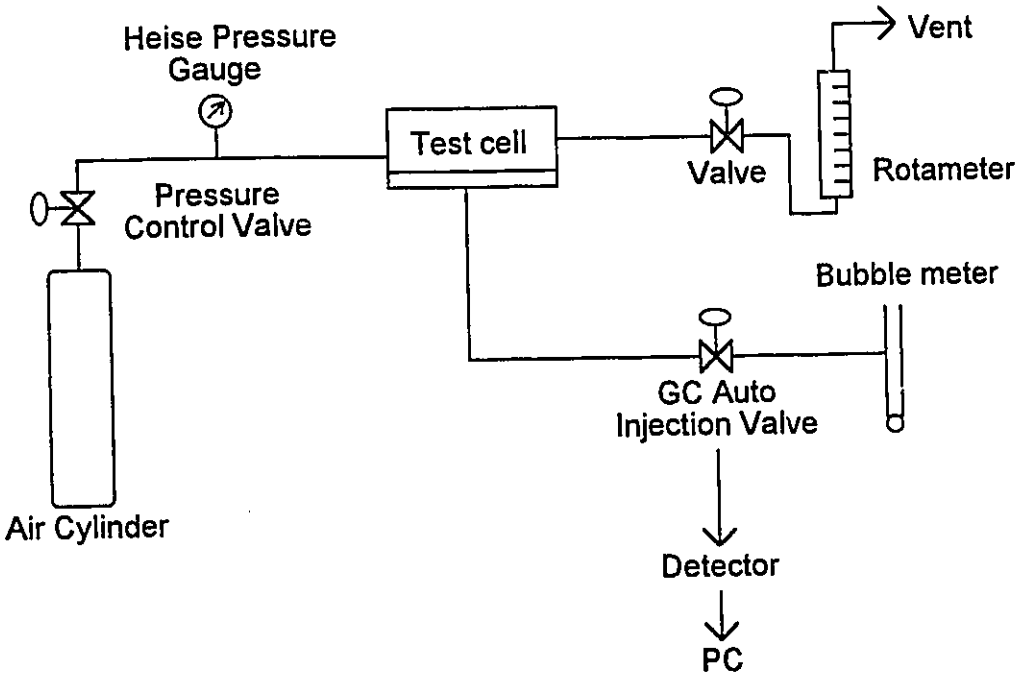

Figure 4.2: Schematic diagram of the experimental setup.

4.3 Pore Size Analyzes

The pore size distribution of a membrane was measured using an ASAP 2000 "Accelerated surface area and porosimetry system". The ASAP 2000 manufactured by Micromeritics (Norcross, U.S.A) consists of an automated gas sorption instrument with two degassing and one analysis ports connected to a control module which in turn is connected to an IBM PC and a printer. A sketch representing this apparatus is shown in Figure 4.3.

The membrane polymer was scraped from the backing using a sharp blade before testing for porosity. The membranes were degassed at 30°C under vacuum to remove any moisture or solvents present within or on its surface. After weighing the sample, it was inserted into a glass tube and connected to the degassing port where the degassing step started. Degassing the sample took 24 hours. The sample was then weighed again after degassing and the exact weight calculated.

The sample tube was connected to the analysis port of the ASAP 2000. The samples were analyzed over a 6 to 24 hour period. An isotherm, of the volume of nitrogen adsorbed and desorbed versus the relative nitrogen pressure in the sample tube was obtained. The isotherm was then analyzed using the BJH (Barret, Joyner and Halenda, 1951) method and a BJH desorption pore area distribution reported. The BJH desorption pore area results for all membranes are listed in Appendix B.

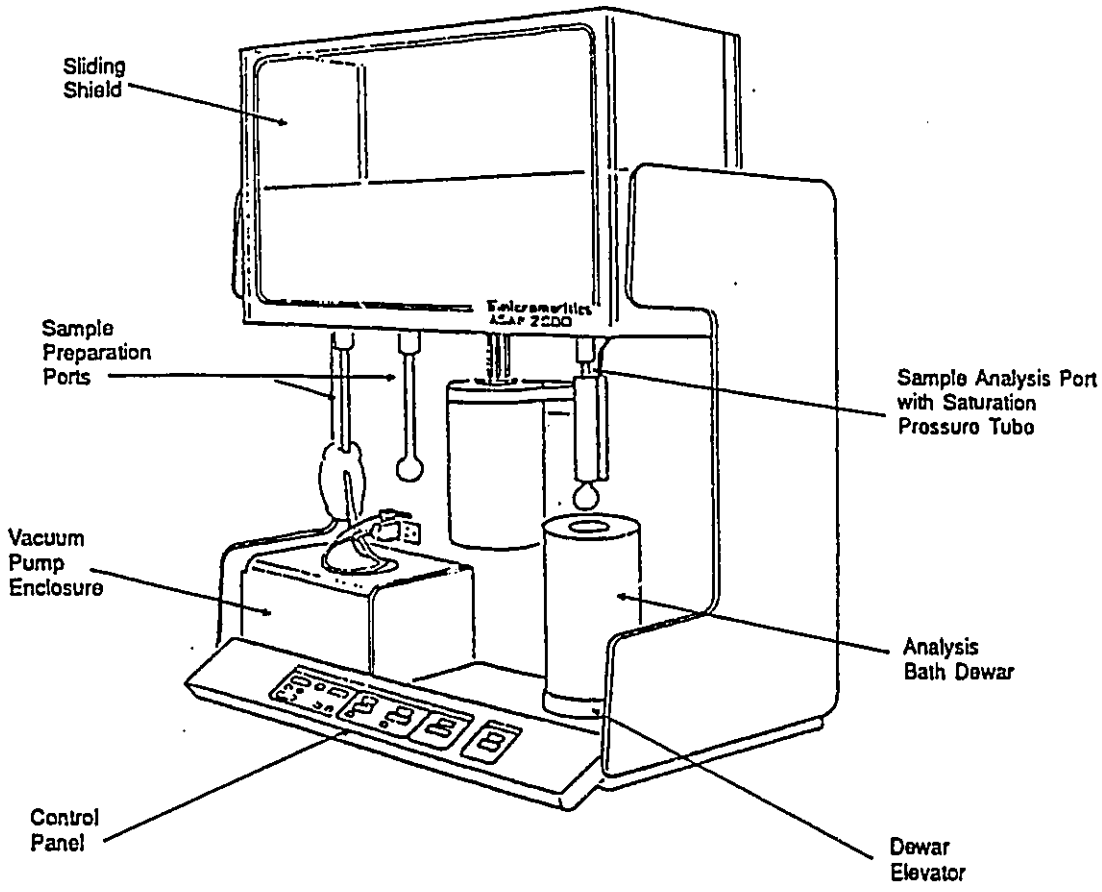

Figure 4.3: Illustration of the ASAP 2000 (Micromeritics, 1989).

4.4 Methodology

4.4.1 Casting Solution Containing Dowex-50w as the Ion Exchange Resin

In early experimental studies, a casting solution was prepared based on Manjikian's formulation (Manjikian, 1967): Cellulose acetate, 25 wt %; acetone, 45 wt %; formamide, 30 wt %. Different amounts of ion exchange resin (Dowex-50w) were incorporated into this solution, varying the compositions of cellulose acetate and acetone at each time. But the method of incorporating charged groups within the membrane was not very successful since the resin did not readily dissolve in the casting solution.

The ion exchange resin (Dowex-50w) was slightly dissolved and swollen in NMP (1-Methy-2-pyrrolidinone), a strong solvent commonly used in membrane fabrication. The resin was still incorporated into casting solutions and membranes were produced. The skin layer of these membranes was not integral and the separation of these membranes was non existent. Although the resin had an extremely low degree of cross-linking, 2%, the results obtained with the ion exchange resin were largely unsuccessful due to the difficulty in solubilizing the resin and incorporating it into the membrane.

4.4.2 Casting Solution Containing EDTA as a Nonsolvent

4.4.2.1 Solubility Tests for a Solution Containing Acetone, Water and EDTA

The solubility of EDTA was determined in an acetone-water system. The standard casting solution composition for a Loeb-Sourirajan membrane was used (cellulose acetate, 17 wt %; acetone, 69.2 wt %; water H_2O, 12.3 wt %; magnesium perchlorate $Mg(ClO_4)_2$;1.5 wt %). The total amount of nonsolvent in the liquid phase of this mixture was determined by dividing the total compositions of the magnesium perchlorate-H_2O mixture (13.8 wt %) over the sum of the total composition of magnesium perchlorate-H_2O (13.8 wt %) and the acetone composition in the casting solutions (69.2 wt %), which gives a total of 16.6 wt % nonsolvent mixture in the liquid phase of the casting solution.

In this work, the amount of nonsolvent mixture was varied from 8% to 16.6%. Concentrations of EDTA within the nonsolvent mixture ranged from 2% to 8%. A solubility test was performed to determine the solubility limit of EDTA in water-acetone. The results of this test are included in Table 4.2.

Table 4.2: Solubility test for the acetone-water-EDTA system.

Total nonsolvent [wt %]	EDTA conc. in nonsolvent mixture [wt %]	Observations
16.6	8	Cloudy, 2 liquid phases
16.6	6	Cloudy, 2 liquid phases
16.6	4	Clear, 1 liquid phase
16.6	2	Clear, 1 liquid phase
14	8	Cloudy, Bott. ppt.
14	6	Cloudy, Bott. ppt.
14	4	NonCloudy, Bott. ppt.
14	2	Cloudy, Bott. ppt.
12	8	NonCloudy, Bott. ppt.
12	6	Cloudy, Bott. ppt.
12	4	NonCloudy, Bott. ppt.
12	2	NonCloudy, Bott. ppt.
10	8	Cloudy, Bott. ppt.
10	6	Cloudy, Bott. ppt.
10	4	Cloudy, Bott. ppt.
10	2	Cloudy, Bott. ppt.
8	8	Cloudy, Slight Bott. ppt.
8	6	Cloudy, Bott. ppt.
8	4	NonCloudy, Bott. ppt.
8	2	NonCloudy, Bott, ppt.

It is seen from Table 4.2 that lower amounts of water in the acetone-water-EDTA system leads to the precipitation of EDTA. In order to assure that most formulations would dissolve EDTA, it was decided to use a total concentration of at least 16% nonsolvent mixture (acetone + water) in all casting solution formulations.

4.5 Preparation of Membranes

Casting solutions were produced by dissolving a certain amount of EDTA in water, then combining the EDTA-water nonsolvent mixture with acetone and cellulose acetate. The casting solution was then mixed by rolling it in a bottle at room temperature for about 24 hours to form a homogeneous solution. The casting solution was then spread uniformly over a polyester backing material taped onto a 7 by 12 in (18x30 cm) glass plate. The solution was spread using a casting knife having a 0.2 cm wide x 500 μm height gap.

The membrane was then quenched in iced water (4°C), for a period of two hours, then transferred to a room temperature bath for at least 24 hours before any post-treatments were made. The temperature of the casting solution and the environment were both maintained at 23°C and the relative humidity of the air was less than 60%. The evaporation time was set at 5 sec.

The original sheet was cut into four equal pieces each being subjected to a different post-treatment. Before use for gas separation experiments, all membranes were carefully dried to avoid damaging their structure. A solvent exchange technique was used to remove water from the wet membranes (MacDonald and Pan, 1974). In this technique, the water in the wet membrane was displaced by isopropyl alcohol over a period of 24 hours. This solvent was then displaced by hexane for another 24 hours, after which the membrane was air dried.

After performing the solubility test (Table 4.2), the maximum concentration of EDTA in the non solvent mixture was chosen to be 16.4%. The components and their composition for the casting solution are found in Table 4.3.

Table 4.3: Casting solution compositions.

EDTA conc. in the nonsolvent mixture [wt %]	EDTA [g]	H_2O [g]	Acetone [g]	Cellulose Acetate [g]
0	0.0	16.4	83.6	20.48
1	0.164	16.236	83.6	20.48
2	0.328	16.072	83.6	20.48
3	0.492	15.908	83.6	20.48
4	0.656	15.744	83.6	20.48
8	1.312	15.088	83.6	20.48
12	1.968	14.432	83.6	20.48
14	2.296	14.104	83.6	20.48
16	2.624	13.776	83.6	20.48

4.5.1 Non-annealed Membranes

In the first set of experiments, the gelled cellulose acetate membranes were dried using solvent exchange technique and tested for air permeability and oxygen separation.

4.5.2 Annealed Membranes

The gelled cellulose acetate membranes were annealed before drying. This was done by immersing them in a hot water bath at a temperature of 80°C for 10 minutes then solvent exchanged, dried and tested for air permeability and oxygen separation.

4.5.3 Membranes Impregnated with Silver Nitrate, Non-annealed

The gelled membranes were soaked in a 0.01M silver nitrate solution for a period of two hours, then washed with water, solvent exchanged, dried and tested for air permeability and oxygen separation.

4.5.4 Membranes Impregnated with Silver Nitrate followed by Reduction to Silver Metal, Non-annealed

In this step, the silver ions deposited in the membrane were reduced to silver metal with a solution of sodium borohydride. Gelled membranes were soaked in a 0.01M silver nitrate solution, for a period of two hours, washed with water then soaked in a 0.025M sodium borohydride solution, $NaBH_4$ for a period of 30 minutes. The membranes were then transferred to a water bath for three hours before solvent exchanging, drying and testing.

4.5.5 Membranes Impregnated with Silver Nitrate, Annealed

Gelled membranes were soaked in a 0.01M silver nitrate solution for a period of two hours, then washed with water, annealed in a water bath at 80°C for 10 minutes, soaked in room temperature water for 24 hours, solvent exchanged, dried and tested for air permeability and oxygen separation.

4.5.6 Membranes Impregnated with Silver Nitrate followed by Reduction to Silver Metal, Annealed

Gelled membranes were soaked in a 0.01M silver nitrate solution for a period of two hours, washed with water then soaked in a 0.025M sodium borohydride solution, $NaBH_4$ for a period of 30 minutes, then transferred to a room temperature water bath for three hours. The membranes were then annealed in a water bath at 80°C for 10 minutes. The membranes were then transferred to water bath for three hours before solvent exchange, drying and testing.

Chapter 5

Results and Discussion

The focus of this work, was to prepare composite metal impregnated membranes and study their air permeability, oxygen separation, and porosity. As stated in the objectives the approach was to capture silver within the nanoporous structure of a phase inversion membrane then shrink the membrane by annealing followed by reduction of silver nitrate to silver. A slightly crosslinked ion exchange resin (Dowex-50w) and a low molecular weight ligand (EDTA) were both incorporated in casting solutions to facilitate the introduction of silver into the membrane.

As described in section 4.4.1, the results obtained with the ion exchange resin (Dowex-50w) were largely unsuccessful. Although the resin had an extremely low degree of cross-linking, 2%, it was slightly dissolved and swollen by NMP (1-Methyl-2-pyrrolidinone) a strong solvent commonly used in membrane fabrication, and even less in the cellulose acetate-acetone-formamide formulation. As previously mentioned in section 4.4.1, the solubility was also limited in the acetone-formamide solvent system. The resin was still incorporated into casting solutions and membranes were produced. The skin layer of these membranes was not integral and the oxygen separation of these membranes was rather poor. For this reason trials using ion exchange resins were not pursued and efforts were concentrated on the addition of a low molecular weight ligand, EDTA to the

casting solution. In this section, the results obtained using EDTA as an additive in the casting solution are presented and discussed.

5.1 Effect of EDTA

All membranes were tested without any film post-treatments. Results for the composition of the permeate, its air permeability and the values of the objective function (θ) for different EDTA concentrations in the nonsolvent mixture are listed in Table 5.1. The compositions of the permeate (mole % oxygen) and air permeabilities vs. the concentration of EDTA in the nonsolvent mixture used in the casting solution are shown in Figures 5.1 and 5.2. For all casting solution formulations, a plot of the composition of the permeate (mole % oxygen) vs. the air permeability of the membrane is shown in Figure 5.3. Values of the objective function (θ) vs. the concentration of EDTA in the nonsolvent mixture are shown in Figure 5.4.

The behavior shown in Figure 5.3 is typical, where membranes with the lowest air permeability have high oxygen separation and those with the highest air permeability have low oxygen separation. From Figures 5.1 and 5.2, it can be seen that membranes cast without EDTA gave the highest oxygen separation but a very low air permeability. However, a maximum in the air permeability of the membrane is obtained at a 2% EDTA concentration. Air permeability then decreases sharply as EDTA is added and remains relatively constant for concentrations greater than 2%. This optimum is reflected in the value of the objective function (θ) in Figure 5.4, which displays a slight peak at the 2%

level. However as seen in Figure 5.1 this slight increase is due to the very large air permeability exhibited at this EDTA concentration and not due to a shift in performance towards the goals of high oxygen separation and air permeability.

According to Kesting (1965), the role of inorganic salts in aqueous solutions as additives, is related to the capacity of the constituent ions to swell the cellulosic substrate. Swelling is effected by the formation of metastable complexes involving the highly hydrated cationic fraction of the salt and both the hydroxyl and acetate groups in the cellulose acetate polymer. Since the cellulose acetate material swells, it is assumed that the hydrated salt ions are capable of association (complex formation) with certain sites on the polymer with the eventual result that polar cross-linking sites are ruptured and additional water is incorporated in the polymer network. The inclusion of such salts in a casting solution containing polymer and water results in salt-polymer interactions and the formation of more open networks than those which would have formed in the absence of such salts.

As gelation proceeds, the amount and rate of salt leaving the film decreases, therefore the salt within the cast film has to diffuse through the gelled polymer layer at the interface between polymer and the gelation medium. The gelled polymer layer acts as a barrier to salt leaching, and the rate of salt leaching gives some information regarding the thickness and the porosity of the gelled polymer layer which is mainly responsible for the selective air permeability of a membrane. Therefore the EDTA content in the casting solution is a very important parameter in the control of membrane performance.

This optimum in the air permeability of the membrane at the 2% EDTA level can easily be explained considering the maximum solubility of EDTA in water which is 2% by weight at 25°C (Flaschka, 1964). According to the above discussion, further addition of EDTA should lead to increased air permeability due to imperfections in the skin layer of the membrane, however this is not the case. This leads us to conclude that further addition of EDTA beyond the solubility limit of EDTA in the nonsolvent water, causes pore blocking since EDTA cannot leach out of the skin layer, thereby reducing the air permeability of the membrane.

Table 5.1: Objective function (θ) for various EDTA concentrations in the nonsolvent mixture for non-annealed membranes. Raw data is contained in Appendix A, Tables A7, A8.

Membrane Ident.	EDTA [wt %]	% O_2 Average Corrected	*P/l* *1E7[a] Average	x[b]	y[c]	θ = x · y
NA0-1	0	35.2	15.2	0.03	0.74	0.02
NA0-2	0	39.6	11.6	0.02	0.98	0.02
NA0-3	0	29.8	106	0.18	0.45	0.08
NA1-1	1	25.9	78.5	0.13	0.24	0.03
NA2-1	2	23.0	1523	2.60	0.08	0.21
NA2-2	2	22.1	1734	2.96	0.03	0.08
NA3-1	3	23.3	515	0.88	0.10	0.09
NA4-1	4	26.9	152	0.26	0.29	0.08
NA4-2	4	27.7	105	0.18	0.33	0.06
NA8-1	8	25.9	77.7	0.13	0.24	0.03
NA8-2	8	26.3	117	0.20	0.26	0.05
NA12-1	12	23.9	328	0.56	0.13	0.07
NA12-2	12	30.6	38.7	0.07	0.49	0.03
NA14-1	14	23.9	115	0.20	0.13	0.03
NA14-2	14	23.16	281	0.48	0.09	0.04
NA16-1	16	24.1	76.4	0.22	0.14	0.03

[a]Air permeability *P/l* [cm^3(STP)/cm^2.psi.sec]
[b]Normalized air permeability x = (*P/l* /(500x10^{-7} -0))
[c]Normalized oxygen concentration in the permeate y = (% O_2 in permeate/(40-21.55))

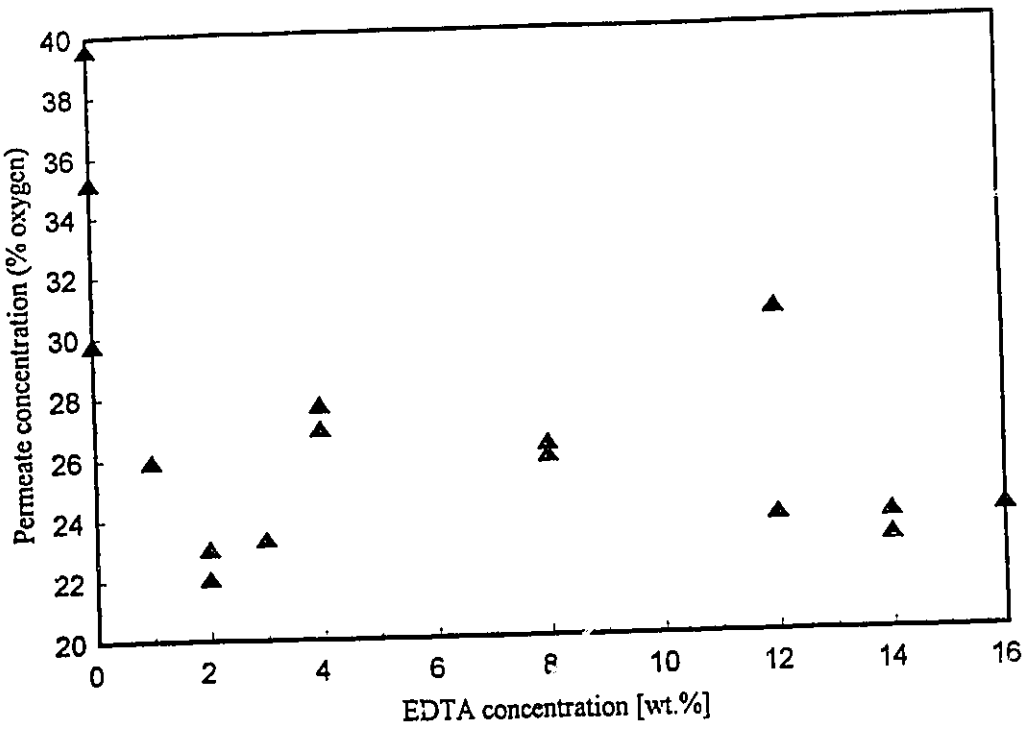

Figure 5.1: Composition of the permeate (mole % oxygen) for non-annealed membranes at various EDTA conc. in the nonsolvent mixture.

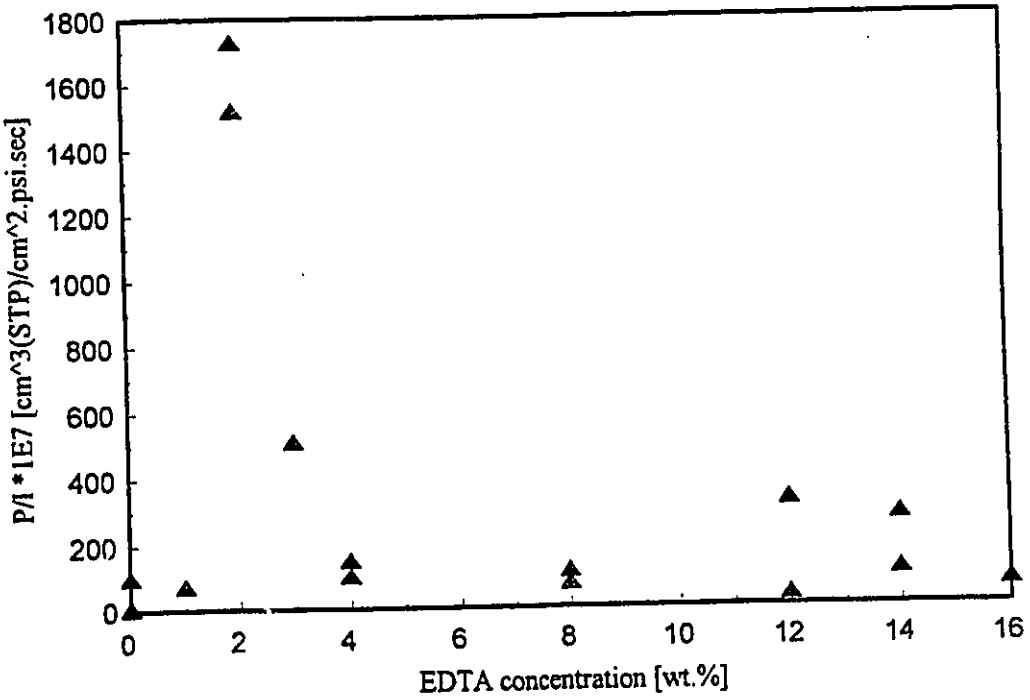

Figure 5.2: Air permeability (*P/l*) for non-annealed membranes at various EDTA conc. in the nonsolvent mixture.

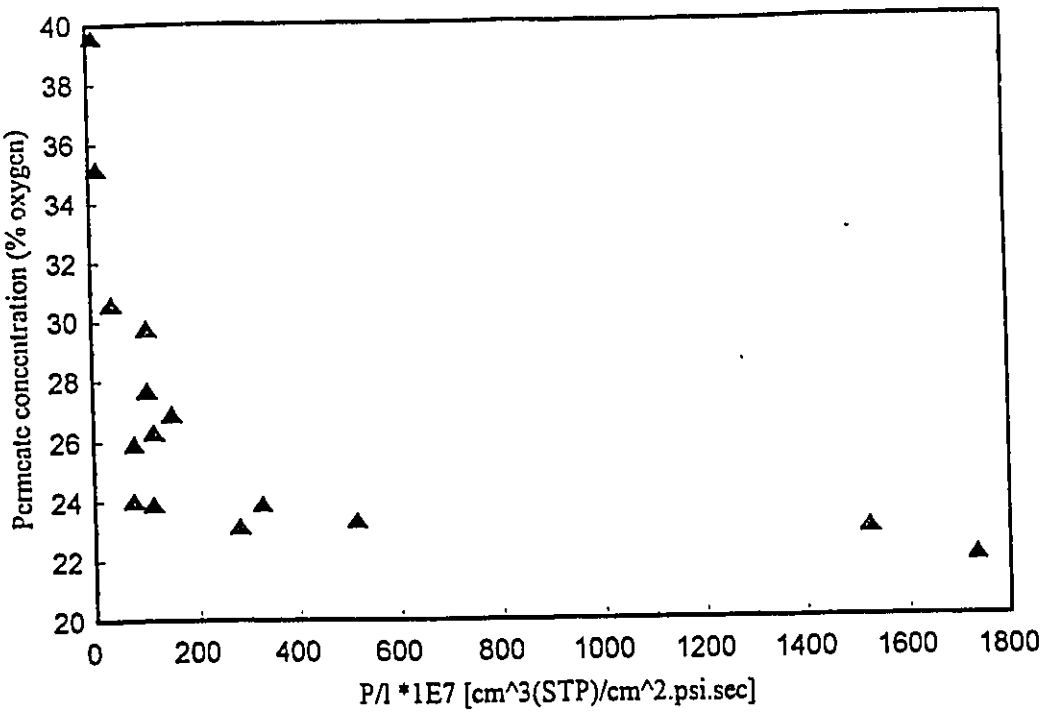

Figure 5.3: Composition of the permeate (mole % oxygen) vs. the air permeability for non-annealed membranes at various EDTA conc. in the nonsolvent mixture.

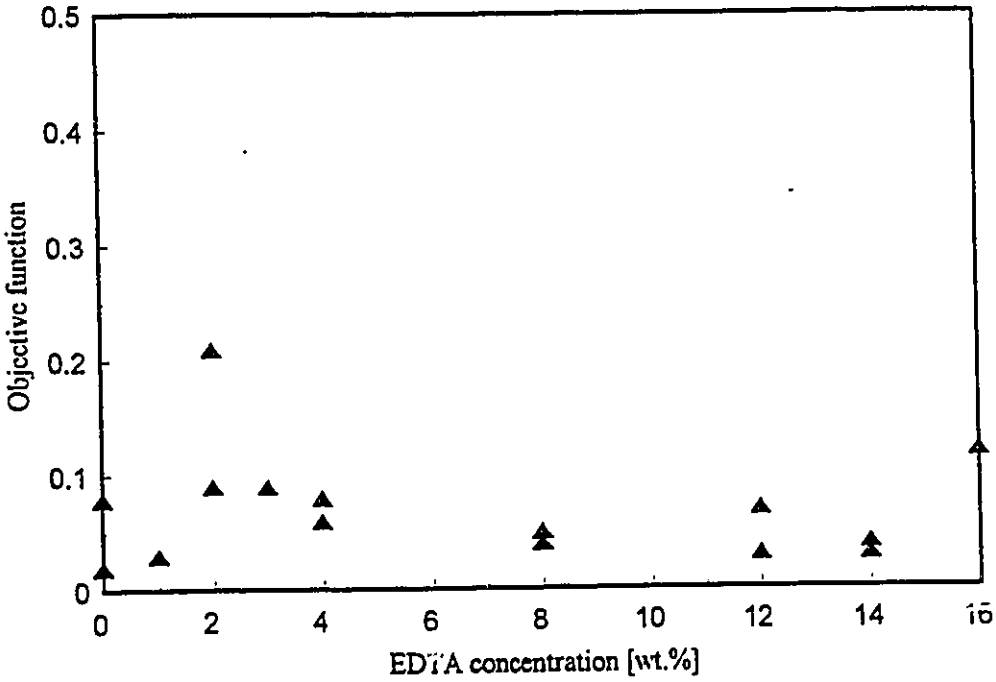

Figure 5.4: Objective function (θ) vs. the EDTA conc. in the nonsolvent mixture for non-annealed membranes.

5.2 Effect of Annealing

In the second set of experiments, following the gelation step in the film making process, the membranes were annealed by immersing them in hot water at 80°C for 10 minutes. The membrane were then transferred to water at ambient temperature. The film was then dried using the solvent exchange method before testing.

The results for the composition of the permeate, its air permeability and the values of the objective function (θ) for different EDTA concentrations in the nonsolvent mixture are listed in Table 5.2. The compositions of the permeate (mole % oxygen) and air permeabilities vs. the concentration of EDTA in the nonsolvent mixture used in the casting solution are shown in Figures 5.5 and 5.6. For all casting solution formulations, a plot of the composition of the permeate (mole % oxygen) vs. the air permeability of the membrane is shown in Figure 5.7. Values of the objective function (θ) vs. the concentration of EDTA in the nonsolvent mixture is shown in Figure 5.8.

The optimum in air permeability at 2% EDTA remains but with a much higher value (Figure 5.6). From Table 5.2 we can see that annealing the membrane lowers the oxygen separation and increases the air permeability especially at 2% EDTA level which is the opposite of what would have been expected. These results indicate that annealing, may have helped to remove some of the excess additive, reducing pore blockage, since the air permeabilities are higher than those obtained in the non-annealed case shown in Table 5.1.

Table 5.2: Objective function (θ) for various EDTA concentrations in the nonsolvent mixture for annealed membranes. Raw data is contained in Appendix A, Tables A9, A10.

Membrane Ident.	EDTA [wt %]	% O_2 Average Corrected	*P/l* *1E7[a] Average	x[b]	y[c]	θ = x · y
A0-1	0	35.3	20.1	0.03	0.75	0.03
A0-2	0	38.5	15.3	0.03	0.92	0.02
A1-1	1	25.2	121	0.21	0.20	0.04
A2-1	2	22.7	7875	13.44	0.06	0.86
A2-2	2	22.3	8086	13.80	0.04	0.55
A3-1	3	23.5	32.6	0.06	0.11	0.01
A4-1	4	26.1	328	0.56	0.24	0.14
A4-2	4	24.9	285	0.49	0.18	0.09
A8-1	8	28.9	90.9	0.16	0.39	0.06
A8-2	8	25.0	86.0	0.15	0.19	0.03
A12-1	12	25.4	55.4	0.09	0.21	0.02
A12-2	12	23.8	164	0.28	0.12	0.03
A14-1	14	23.1	288	0.49	0.08	0.04
A14-2	14	22.5	566	0.97	0.05	0.05
A16-1	16	23.9	94.1	0.16	0.13	0.02

[a]Air permeability *P/l* [cm^3(STP)/cm^2.psi.sec]
[b]Normalized air permeability x = (*P/l* /(500x10^{-7} -0))
[c]Normalized oxygen concentration in the permeate y = (% O_2 in permeate/(40-21.55))

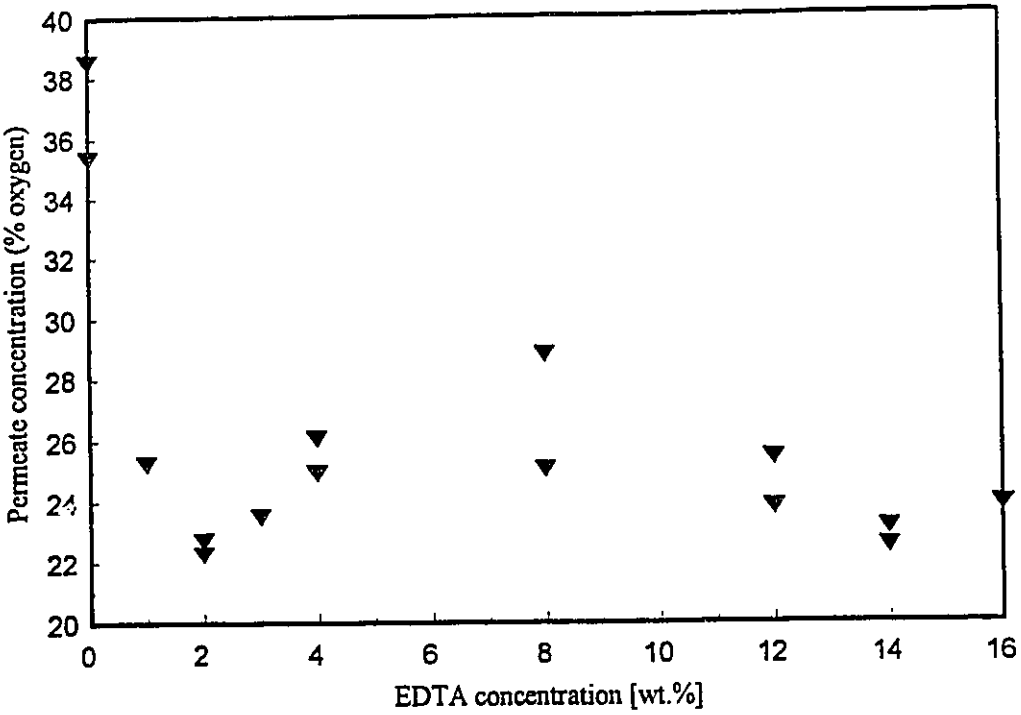

Figure 5.5: Composition of the permeate (mole % oxygen) for annealed membranes at various EDTA conc. in the nonsolvent mixture.

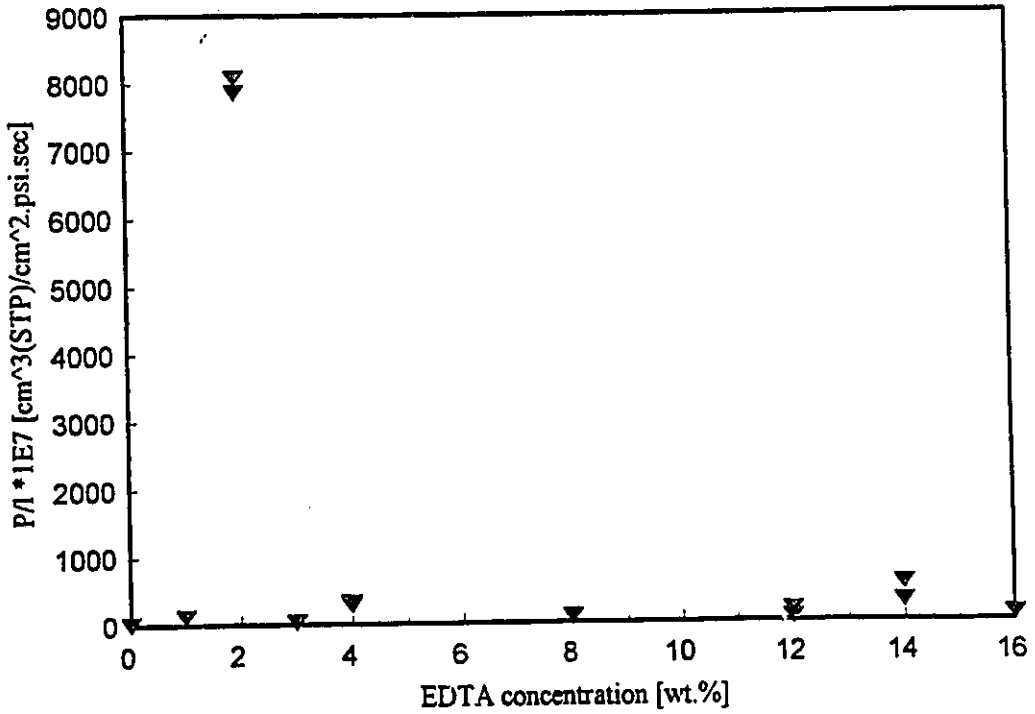

Figure 5.6: Air permeability (*P/l*) for annealed membranes at various EDTA conc. in the nonsolvent mixture.

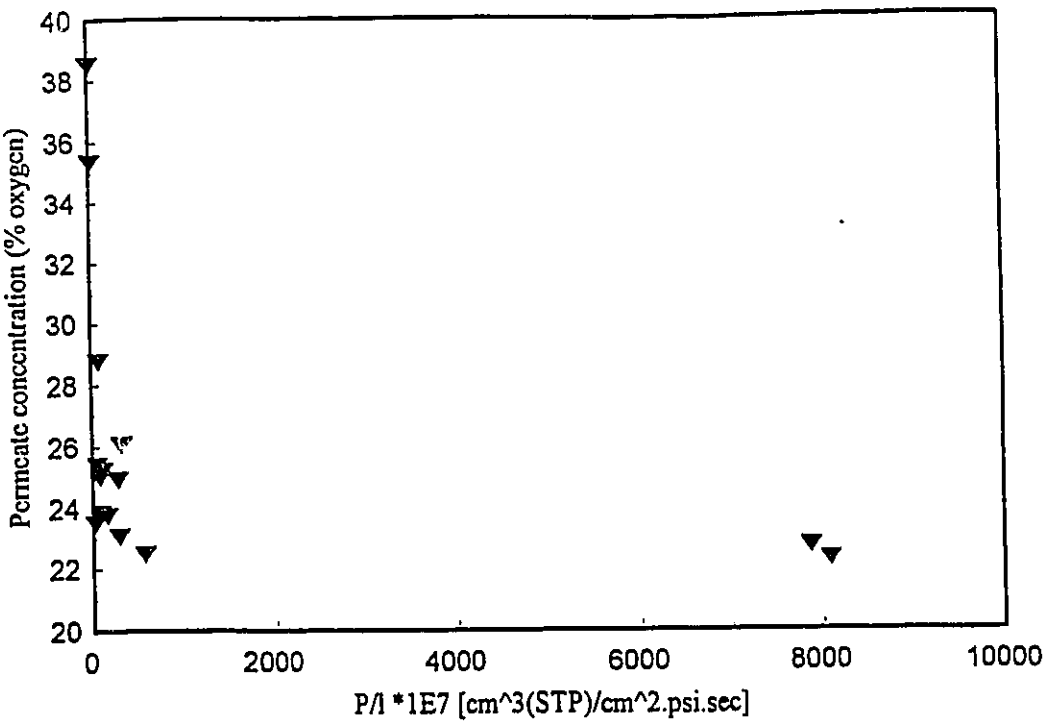

Figure 5.7: Composition of the permeate (mole % oxygen) vs. the air permeability for annealed membranes at various EDTA conc. in the nonsolvent mixture.

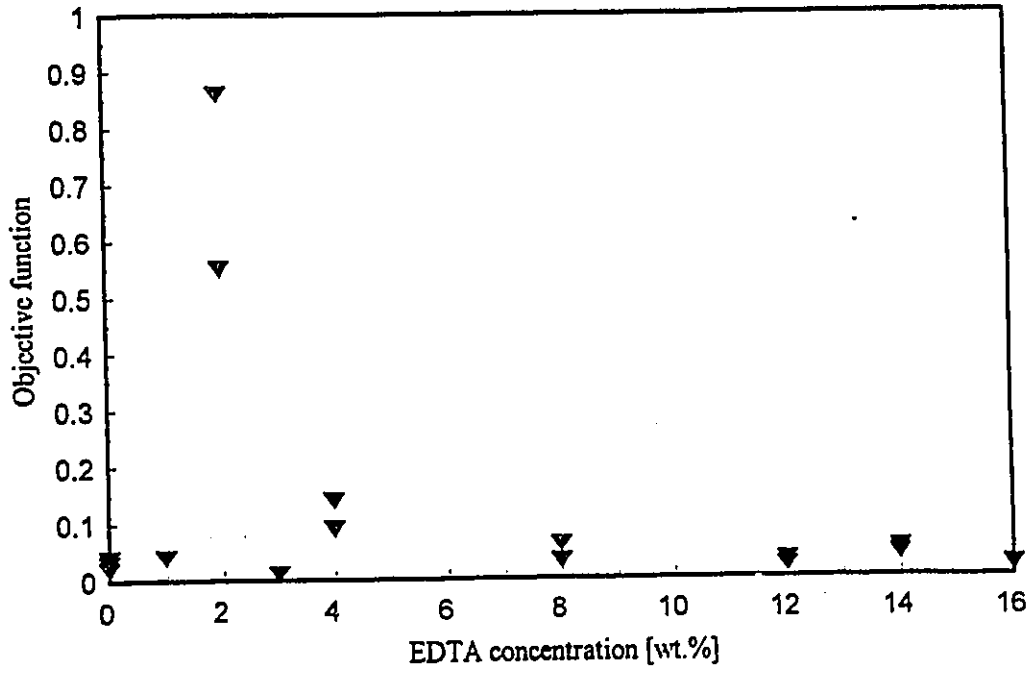

Figure 5.8: Objective function (θ) vs. the EDTA conc. in the nonsolvent mixture for annealed membranes.

5.3 Effect of Silver Nitrate Impregnation for Non-annealed Membranes

In a third set of experiments, following the gelation step in the film making process, the cast cellulose acetate membranes were soaked in a silver nitrate solution for a period of three hours, then washed with de-ionized water, solvent exchanged and dried as described earlier before testing.

The results for the composition of the permeate, its air permeability and the values of the objective function (θ) for different EDTA concentrations in the nonsolvent mixture are listed in Table 5.3. The compositions of the permeate (mole % oxygen) and air permeabilities vs. the concentration of EDTA in the nonsolvent mixture used in the casting solution are shown in Figures 5.9 and 5.10. For all casting solution formulations, a plot of the composition of the permeate (mole % oxygen) vs. the air permeability of the membrane is shown in Figure 5.11. Values of the objective function (θ) vs. the concentration of EDTA in the nonsolvent mixture is shown in Figure 5.12.

As seen in Figure 5.10, the large permeability value at 2% EDTA, observed in sections 5.1 and 5.2 are no longer present. The value of the objective function at EDTA levels around 2% is more than for membranes without silver nitrate treatment. Treatment with silver nitrate appears to decrease the overall air permeability of the membranes but improves oxygen separation, thereby causing a net enhancement in the value of the objective function as seen in Figure 5.12.

Table 5.3: Objective function (θ) for various EDTA concentrations in the nonsolvent mixture, for non-annealed membranes impregnated with silver nitrate. Raw data is contained in Appendix A, Tables A11, A12.

Membrane Ident.	EDTA [wt %]	% O_2 Average Corrected	*P/l* *1E7[a] Average	x[b]	y[c]	θ = x · y
NA0SN-1	0	30.1	2.24	0.00	0.46	0.00
NA1SN-1	1	25.5	226	0.39	0.22	0.08
NA1SN-1	1	24.6	150	0.26	0.17	0.04
NA2SN-1	2	32.9	326	0.56	0.62	0.34
NA2SN-2	2	30.7	500	0.85	0.50	0.43
NA2SN-3	2	32.9	397	0.68	0.61	0.42
NA3SN-1	3	23.2	236	0.40	0.09	0.04
NA3SN-2	3	23.8	235	0.40	0.12	0.05
NA4SN-1	4	25.3	80.5	0.14	0.20	0.03
NA8SN-1	8	23.7	148	0.25	0.12	0.03
NA12SN-1	12	24.1	103	0.18	0.14	0.02
NA14SN-1	14	23.1	306	0.52	0.09	0.05
NA16SN-1	16	26.8	25.1	0.04	0.29	0.01

[a]Air permeability *P/l* [cm^3(STP)/cm^2.psi.sec]
[b]Normalized air permeability x = (*P/l* /(500x10^{-7}-0))
[c]Normalized oxygen concentration in the permeate y = (% O_2 in permeate/(40-21.55))

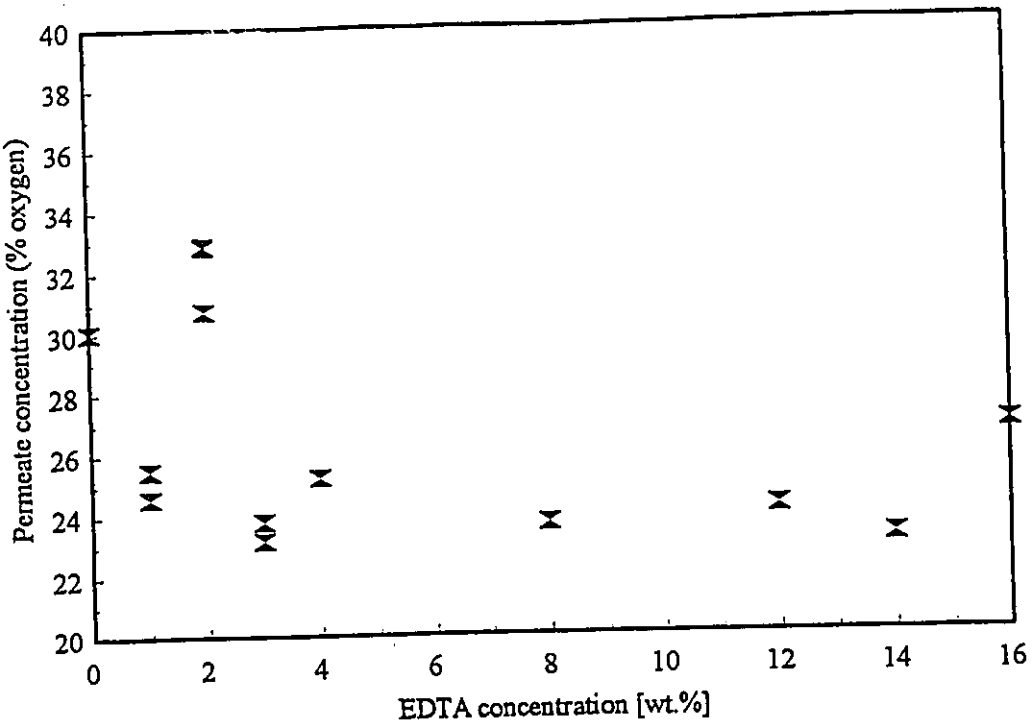

Figure 5.9: Composition of the permeate for non-annealed membranes after silver nitrate impregnation at various EDTA conc. in the nonsolvent mixture.

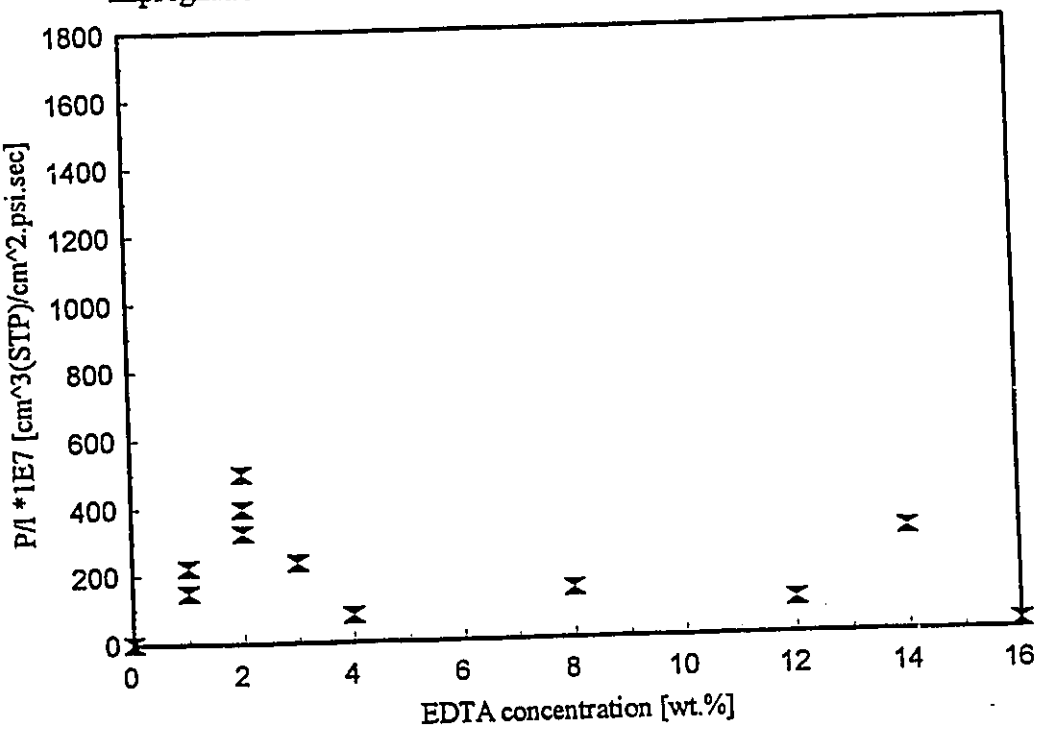

Figure 5.10: Air permeability for non-annealed membranes after silver nitrate impregnation at various EDTA conc. in the nonsolvent mixture.

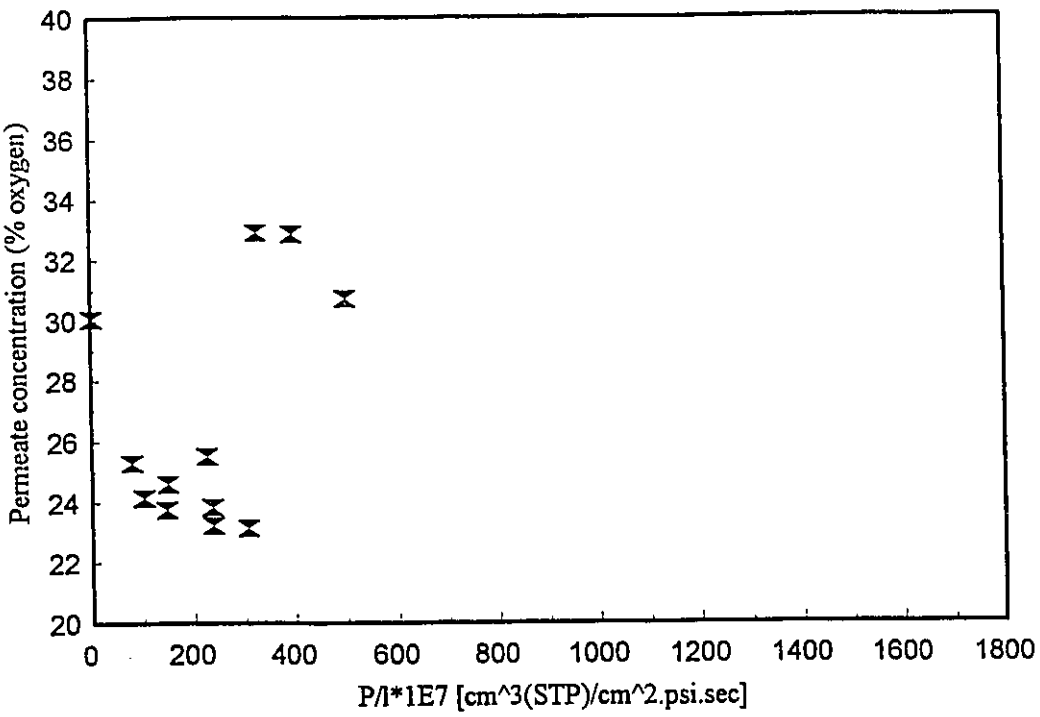

Figure 5.11: Composition of the permeate (mole % oxygen) vs. the air permeability for non-annealed membranes after silver nitrate impregnation at various EDTA conc. in the nonsolvent mixture.

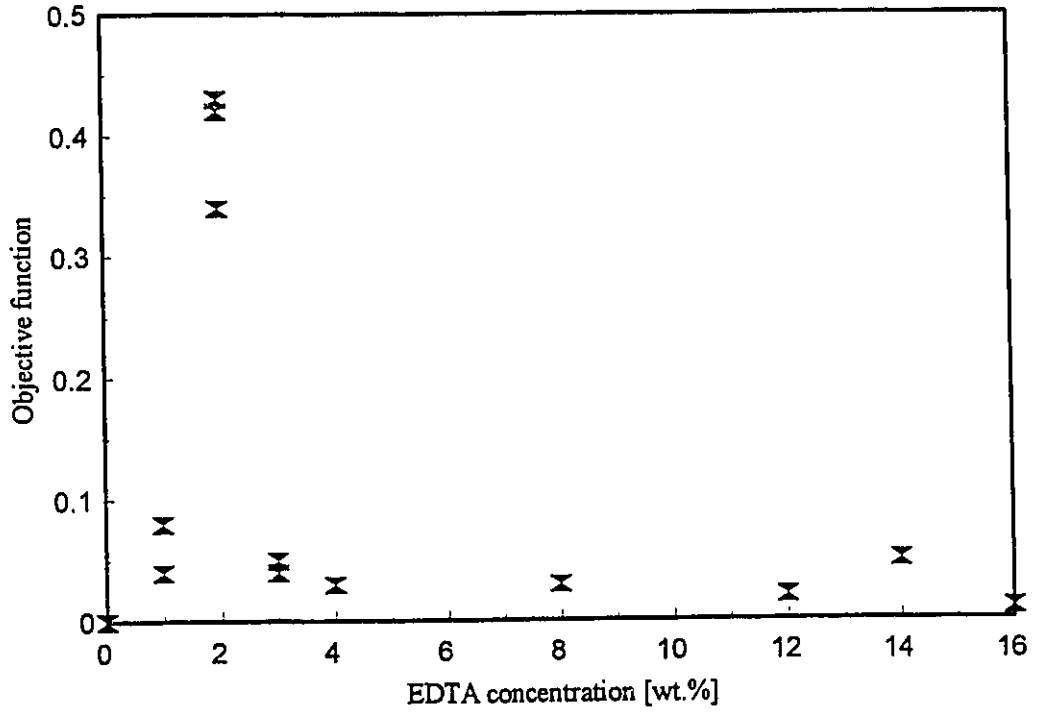

Figure 5.12: Objective function (θ) vs. the EDTA conc. in the nonsolvent mixture for non-annealed membranes after silver nitrate impregnation.

5.4 Effect of Silver Nitrate Impregnation and Reduction to Silver Metal for Non-annealed Membranes

In the fourth set of experiments, following gelation, each cast membrane was placed in a silver nitrate solution for three hours, washed with de-ionized water then placed in a sodium borohydride solution for half-an hour, then transferred to a room temperature water bath for three hours in order to remove excess sodium borohydride from the membrane, then solvent exchanged, dried and tested.

The result of this procedure was to reduce the silver in the membrane to silver metal. This was observed in the resulting dark-brown to black color of the membrane after silver reduction. Silver uptake increased as the concentration of EDTA in the nonsolvent mixture increased evidenced by a shift from light brown to a dark brown nearly black color of the membranes obtained on increasing EDTA. Sraping the membrane showed a substantial amount of silver uptake throughout the membrane.

The results for the composition of the permeate, its air permeability and the values of the objective function (θ) for different EDTA concentrations in the nonsolvent mixture are listed in Table 5.4. The compositions of the permeate (mole % oxygen) and air permeabilities vs. the concentration of EDTA in the nonsolvent mixture used in the casting solution are shown in Figures 5.13 and 5.14. For all casting solution formulations, a plot of the composition of the permeate (mole % oxygen) vs. the air permeability of the membrane is shown in Figure 5.15. Values of the objective function (θ) vs. the concentration of EDTA in the nonsolvent mixture is shown in Figure 5.16.

Again, the same peak at a 2% EDTA addition level is observed for the objective function. The air permeabilities of these silver membranes were a lot less than those for pure cellulose acetate membranes. This is attributed to the binding of silver with EDTA, which causes pore blockage and increase oxygen separation. The value of the objective function decreases with increasing levels of EDTA.

Table 5.4: Objective function (θ) for various EDTA concentrations in the nonsolvent mixture, for non-annealed membranes impregnated with silver nitrate and reduced to silver metal. Raw data is contained in Appendix A, Tables A13, A14.

Membrane Ident.	EDTA [wt %]	% O_2 Average Corrected	*P/l* *1E7[a] Average	x[b]	y[c]	θ = x · y
NA0SM-1	0	28.1	5.61	0.01	0.36	0.00
NA1SM-1	1	24.8	145	0.25	0.18	0.04
NA2SM-1	2	30.9	407	0.70	0.51	0.35
NA2SM-2	2	29.9	482	0.82	0.46	0.38
NA2SM-3	2	29.3	454	0.78	0.42	0.33
NA3SM-1	3	24.6	102	0.17	0.17	0.03
NA3SM-2	3	24.7	104	0.18	0.17	0.03
NA4SM-1	4	25.1	148	0.25	0.19	0.05
NA8SM-1	8	24.1	112	0.19	0.14	0.03
NA12SM-1	12	24.0	97.7	0.17	0.13	0.02
NA14SM-1	14	25.6	61.4	0.10	0.22	0.02
NA16SM-1	16	24.4	35.9	0.06	0.15	0.01

[a]Air permeability *P/l* [cm^3(STP)/cm^2.psi.sec]
[b]Normalized air permeability x = (*P/l* /(500x10^{-7}-0))
[c]Normalized oxygen concentration in the permeate y = (% O_2 in permeate/(40-21.55))

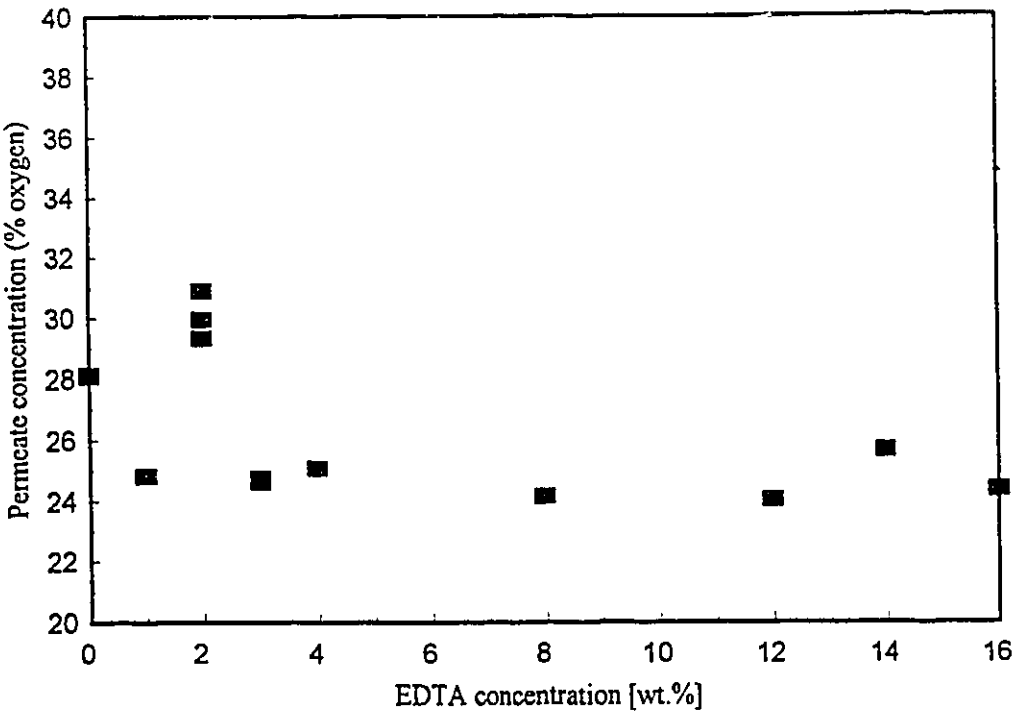

Figure 5.13: Composition of the permeate (mole % oxygen) for non-annealed membranes after silver nitrate impregnation and reduction at various EDTA conc. in the nonsolvent mixture.

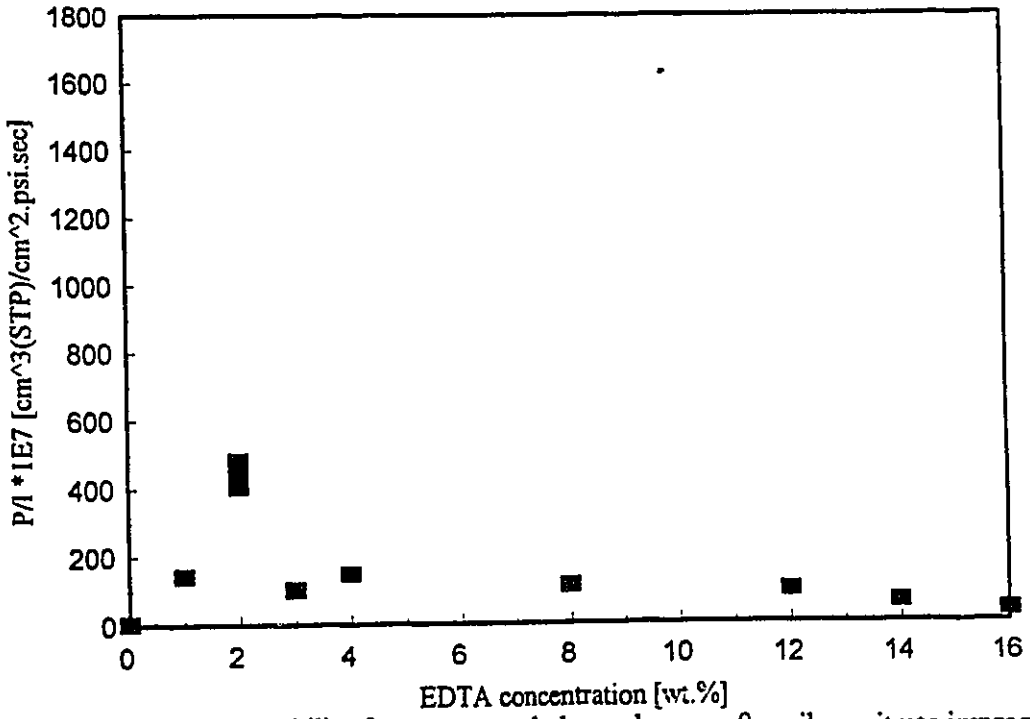

Figure 5.14: Air permeability for non-annealed membranes after silver nitrate impregnation and reduction at various EDTA conc. in the nonsolvent mixture.

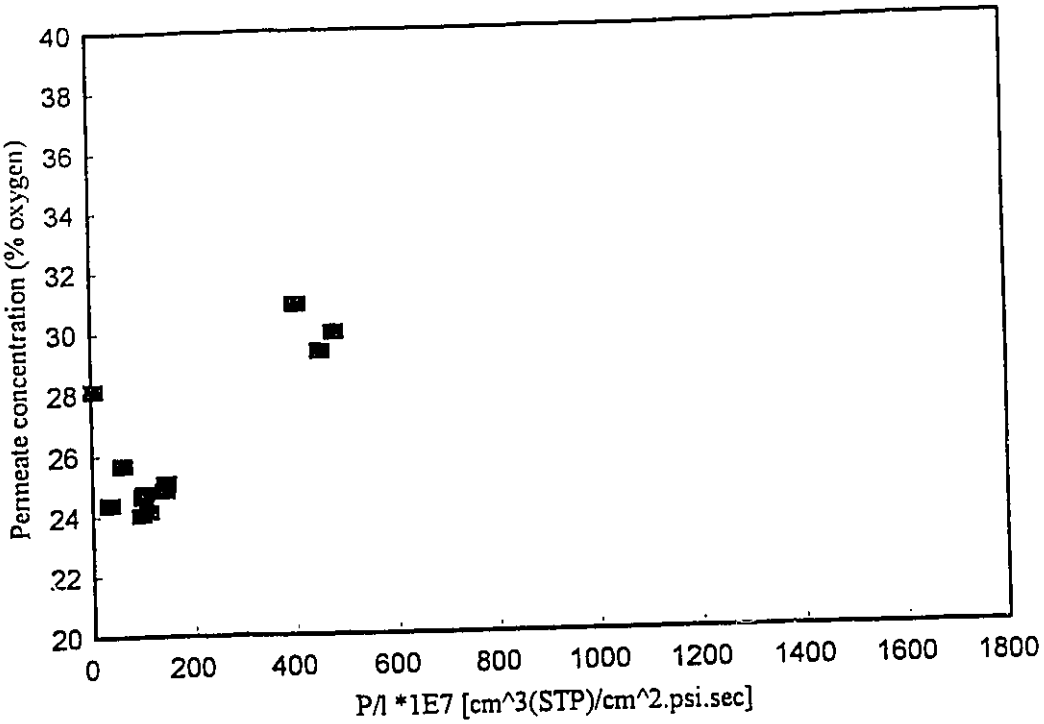

Figure 5.15: Composition of the permeate (mole % oxygen) vs. the air permeability for non-annealed membranes after silver nitrate impregnation and reduction at various EDTA conc. in the nonsolvent mixture.

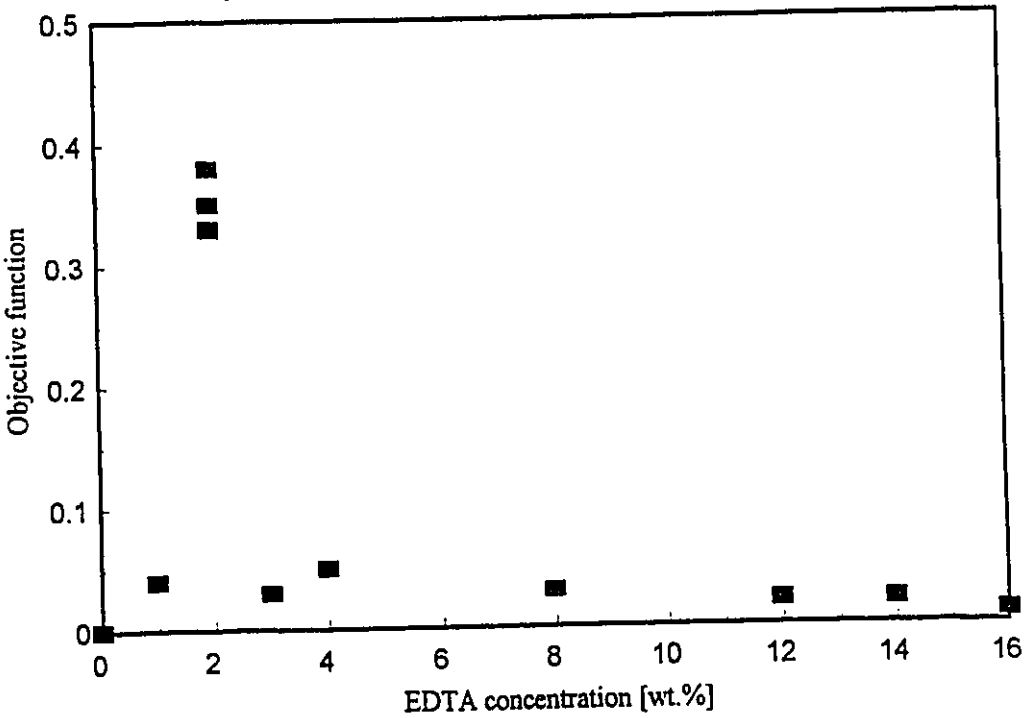

Figure 5.16: Objective function (θ) vs. the EDTA conc. in the nonsolvent mixture for non-annealed membranes after silver nitrate impregnation and reduction.

5.5 Effect of Silver Nitrate Impregnation for Annealed Membranes

In the fifth set of experiments, membranes impregnated with silver nitrate were prepared as previously described, then heat treated, dried and tested. The results for the composition of the permeate, its air permeability and the values of the objective function (θ) for different EDTA concentrations in the nonsolvent mixture are listed in Table 5.5. The compositions of the permeate (mole % oxygen) and air permeabilities vs. the concentration of EDTA in the nonsolvent mixture used in the casting solution are shown in Figures 5.17 and 5.18. For all casting solution formulations, a plot of the composition of the permeate (mole % oxygen) vs. the air permeability of the membrane is shown in Figure 5.19. Values of the objective function (θ) vs. the concentration of EDTA in the nonsolvent mixture is shown in Figure 5.20.

From Figure 5.17, it can be seen that there is a slight increase in the oxygen separation up to an addition level of 8% and from Figure 5.18 a decrease in the air permeabilities values for addition levels above 2%. The resulting objective function values are much smaller as compared to those for the annealed membrane without silver nitrate impregnation. The membrane color became darker with increasing EDTA levels due to a greater uptake of silver.

Table 5.5: Objective function (θ) for various EDTA concentrations in the nonsolvent mixture, for annealed membranes impregnated with silver nitrate. Raw data is contained in Appendix A, Tables A15, A16.

Membrane Ident.	EDTA [wt %]	% O_2 Average Corrected	P/l *1E7[a] Average	x[b]	y[c]	θ = x · y
A0SN-1	0	36.1	14.6	0.03	0.79	0.02
A0SN-2	0	33.5	15.0	0.03	0.65	0.02
A0SN-3	0	29.4	39.3	0.07	0.43	0.03
A2SN-1	2	22.3	191	0.33	0.04	0.01
A2SN-2	2	22.3	470	0.80	0.04	0.03
A4SN-1	4	26.3	25.4	0.04	0.26	0.01
A4SN-2	4	25.2	178	0.30	0.20	0.06
A8SN-1	8	28.3	60.2	0.10	0.37	0.04
A8SN-2	8	25.7	92.1	0.16	0.23	0.04
A12SN-1	12	22.9	298	0.51	0.08	0.04
A12SN-2	12	28.6	30.2	0.05	0.38	0.02
A14SN-1	14	25.1	52.7	0.09	0.19	0.02
A14SN-2	14	23.0	281	0.48	0.08	0.04
A16SN-1	16	24.6	36.3	0.06	0.16	0.01

[a]Air permeability P/l [cm^3/cm^2.psi.sec]
[b]Normalized air permeability x = (P/l /(500x10^{-7}-0))
[c]Normalized oxygen concentration in the permeate y = (% O_2 in permeate/(40-21.55))

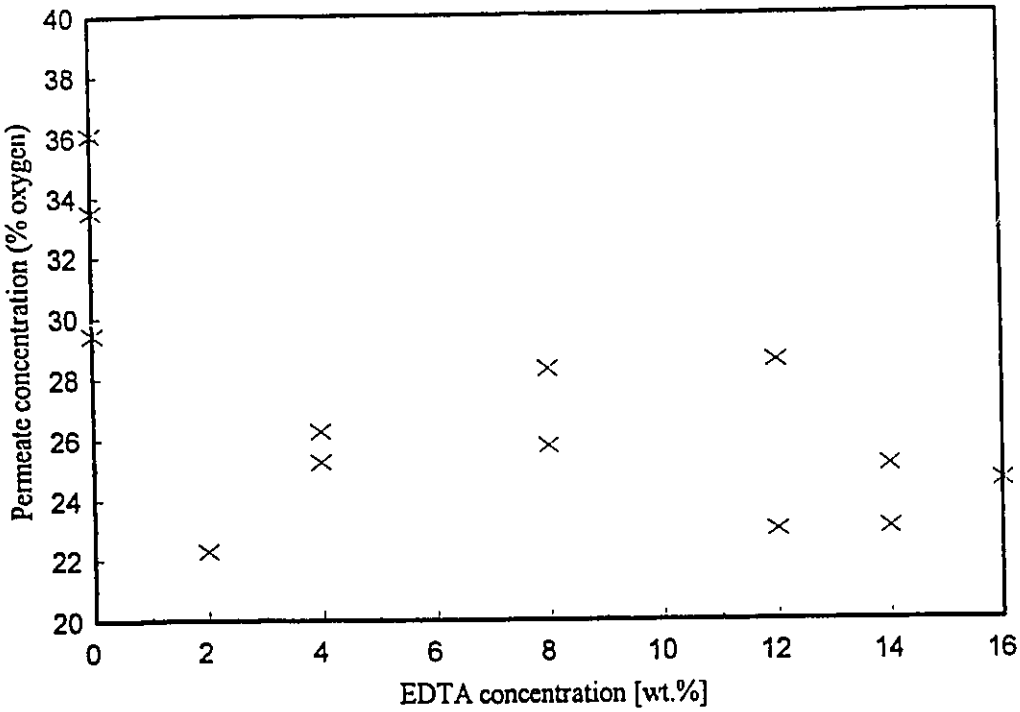

Figure 5.17: Composition of the permeate (mole % oxygen) vs. the air permeability for anncaled membranes after silver nitrate impregnation at various EDTA conc. in the nonsolvent mixture.

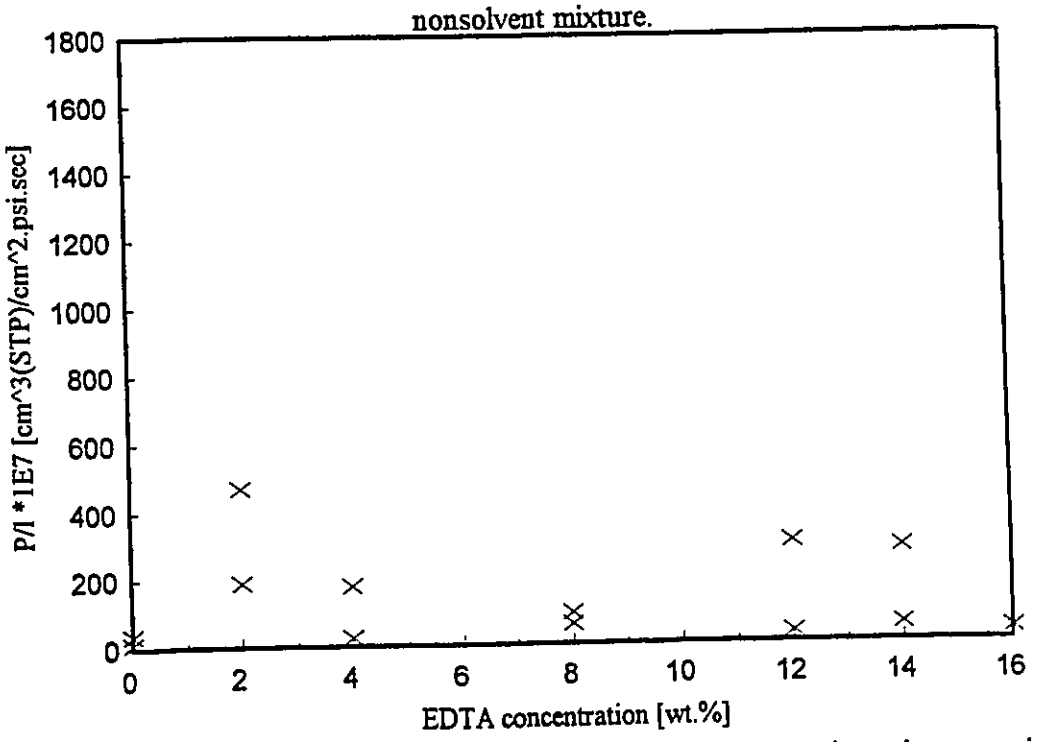

Figure 5.18: Air permeability for annealed membranes after silver nitrate impregnation at various EDTA conc. in the nonsolvent mixture.

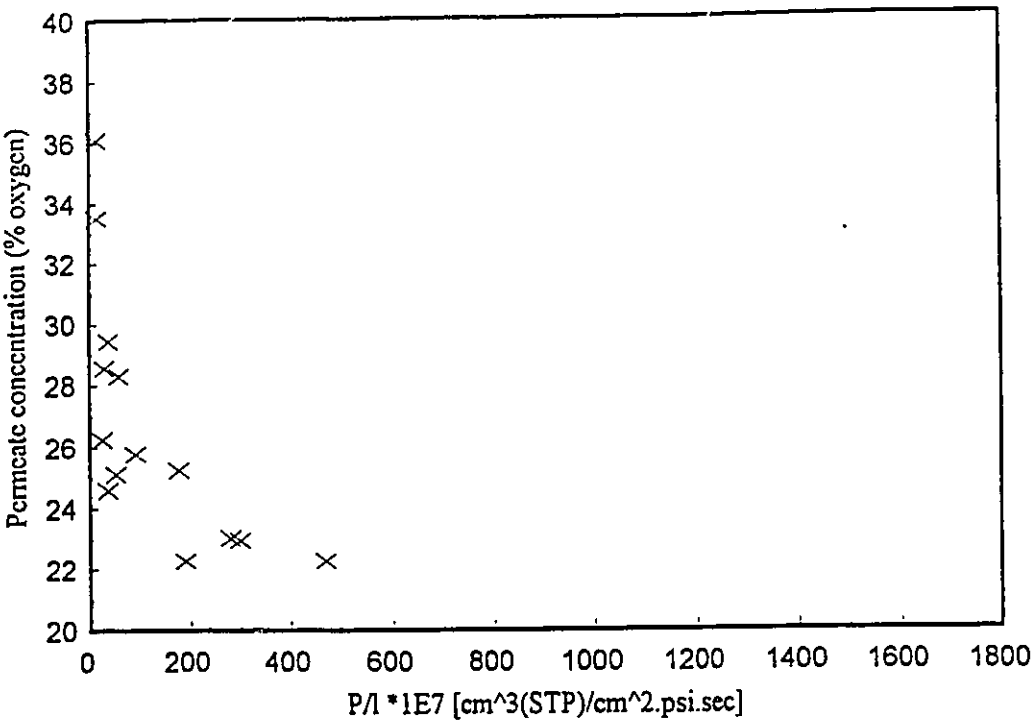

Figure 5.19: Composition of the permeate (mole % oxygen) vs. the air permeability for annealed membranes after silver nitrate impregnation at various EDTA conc. in the nonsolvent mixture.

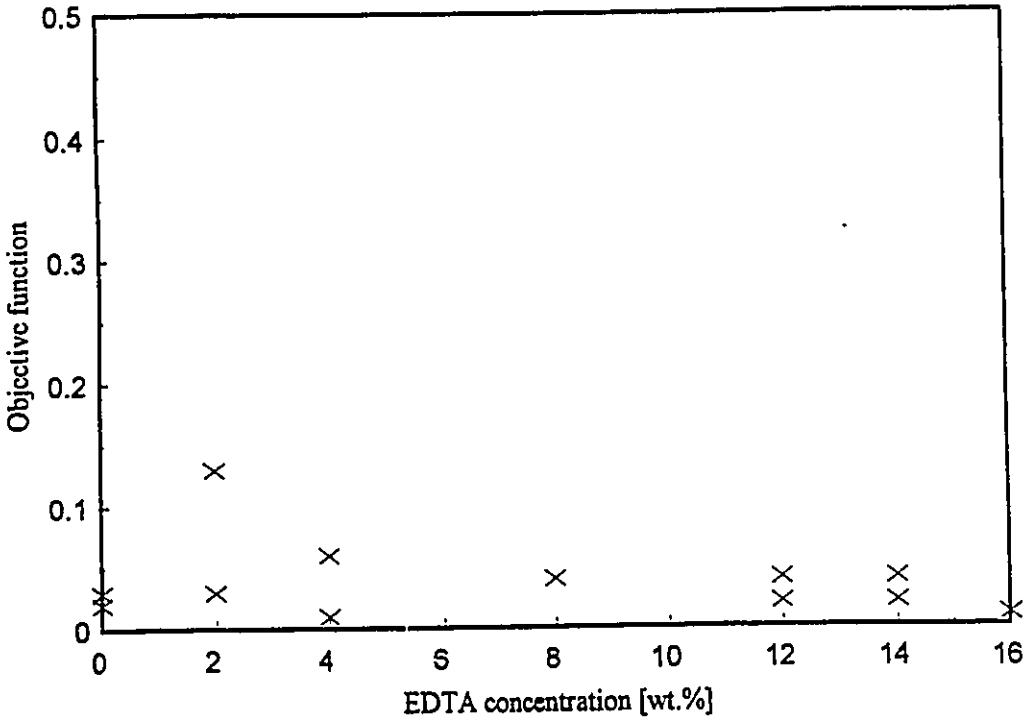

Figure 5.20: Objective function (θ) vs. the EDTA conc. in the nonsolvent mixture for annealed membranes after silver nitrate impregnation.

5.6 Effect of Silver Nitrate Impregnation and Reduction to Silver Metal for Annealed Membranes

In a final set of experiments, the membranes treated with silver nitrate were subsequently soaked in a sodium borohydride solution, then annealed, solvent exchanged, dried and tested. The results for the composition of the permeate, its air permeability and the values of the objective function (θ) for different EDTA concentrations in the nonsolvent mixture are listed in Table 5.6. The compositions of the permeate (mole % oxygen) and air permeabilities vs. the concentration of EDTA in the nonsolvent mixture used in the casting solution are shown in Figures 5.21 and 5.22. For all casting solution formulations, a plot of the composition of the permeate (mole % oxygen) vs. the air permeability of the membrane is shown in Figure 5.23. Values of the objective function (θ) vs. the concentration of EDTA in the nonsolvent mixture is shown in Figure 5.24.

From Figure 5.21, we can see that a higher percentage of oxygen is obtained without EDTA addition. From Figure 5.22, large variation were found above 4% EDTA levels in the casting solutions which could be due to imperfections or cracks in the membrane skin.

From Table 5.6, we can see that without EDTA, we have a higher percentage of oxygen permeated but a lower air permeability yielding a lower objective function. From Figure 5.24, we can see a slight increase in the objective function up to a maxima at 4%, almost the same behavior as before. Further addition of EDTA decreases the values of the objective function. In general, the decrease in air permeability of annealed membranes could be due to the introduction of thermal energy which causes translational motion of

the various elements which form the borders of the pores in the various separation regimes (Kesting and Fritzche, 1993). In time, polymer chain segments on the same and/or neighboring macromolecules approach one another closely enough to forms virtual crosslinks. These tend to decrease chain mobility and, in a non solvent medium, are irreversible because of the inability of the nonsolvent to solvate and therefore lessen the polymer-polymer interaction forces.

Table 5.6: Objective function (θ) for various EDTA concentrations in the nonsolvent mixture, for annealed membranes impregnated with silver nitrate, reduced to silver metal. Raw data is contained in Appendix A, Tables A17, A18.

Membrane Ident.	EDTA [wt %]	% O_2 Average Corrected	*P/l* *1E7[a] Average	x[b]	y[c]	θ = x • y
A0SM-1	0	32.6	26.2	0.04	0.60	0.03
A0SM-2	0	34.9	7.49	0.01	0.73	0.01
A0SM-3	0	33.4	24.61	0.04	0.64	0.03
A2SM-1	2	23.2	536	0.91	0.09	0.08
A2SM-2	2	23.0	962	1.64	0.08	0.13
A4SM-1	4	29.9	153	0.26	0.46	0.12
A8SM-1	8	22.4	1629	2.78	0.05	0.13
A8SM-2	8	23.9	161	0.28	0.13	0.03
A12SM-1	12	22.4	932	1.59	0.05	0.08
A14SM-1	14	28.4	21.8	0.04	0.03	0.00
A14SM-2	14	23.4	140	0.24	0.10	0.02
A16SM-1	16	24.1	29.2	0.05	0.14	0.01

[a]Air permeability *P/l* [cm^3(STP)/cm^2.psi.sec]
[b]Normalized air permeability x = (*P/l* /(500x10^{-7} -0))
[c]Normalized oxygen concentration in the permeate y = (% O_2 in permeate/(40-21.55))

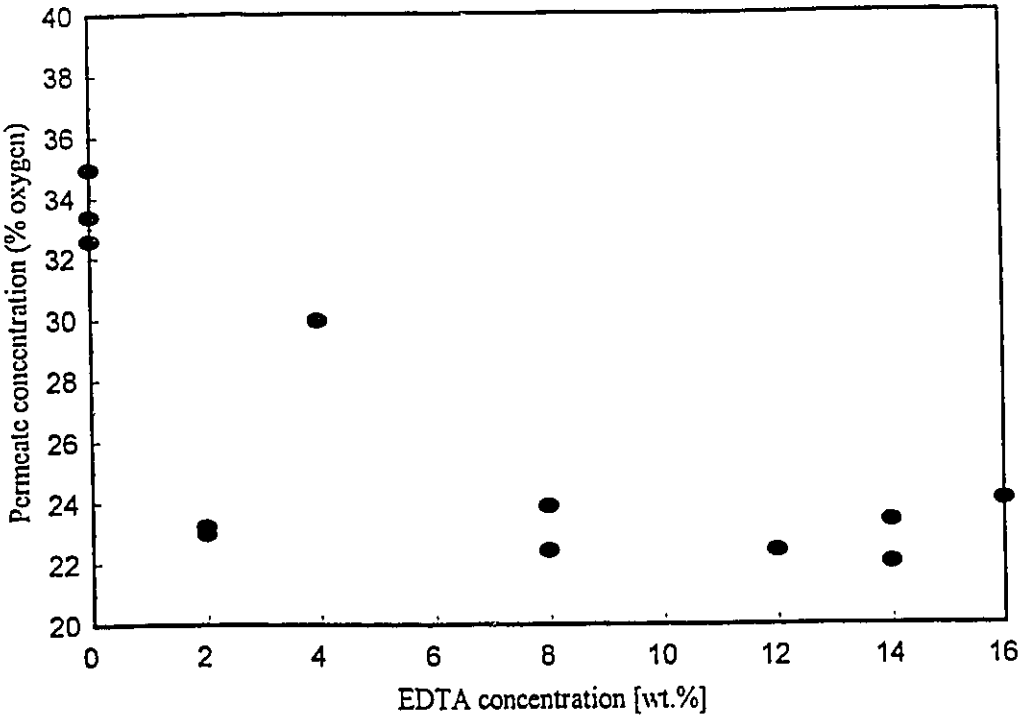

Figure 5.21: Composition of the permeate (mole % oxygen) for annealed membranes after silver nitrate impregnation and reduction at various EDTA conc. in the nonsolvent mixture.

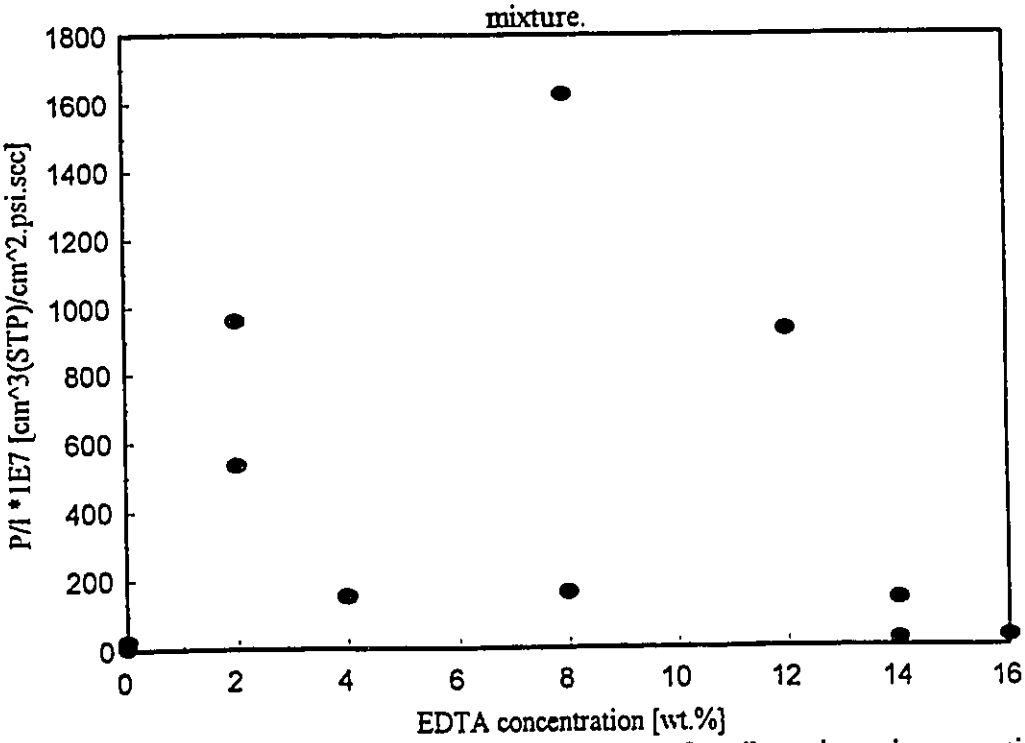

Figure 5.22: Air permeability for annealed membranes after silver nitrate impregnation and reduction at various EDTA conc. in the nonsolvent mixture.

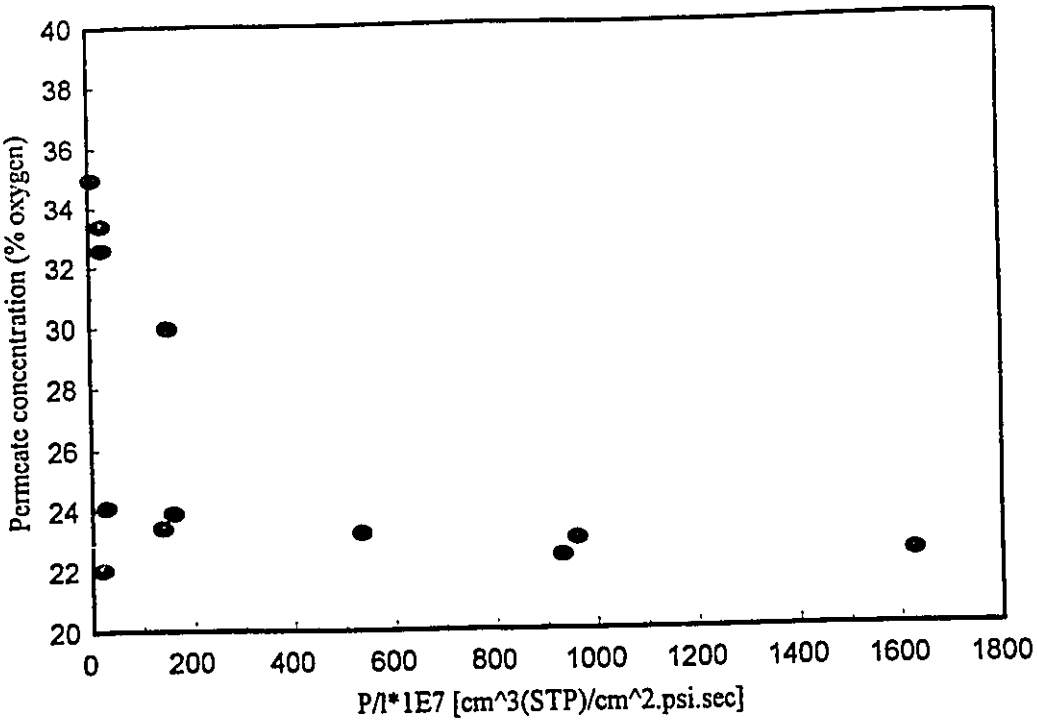

Figure 5.23: Composition of the permeate (mole % oxygen) vs. the air permeability for annealed membranes after silver nitrate impregnation and reduction at various EDTA conc. in the nonsolvent mixture.

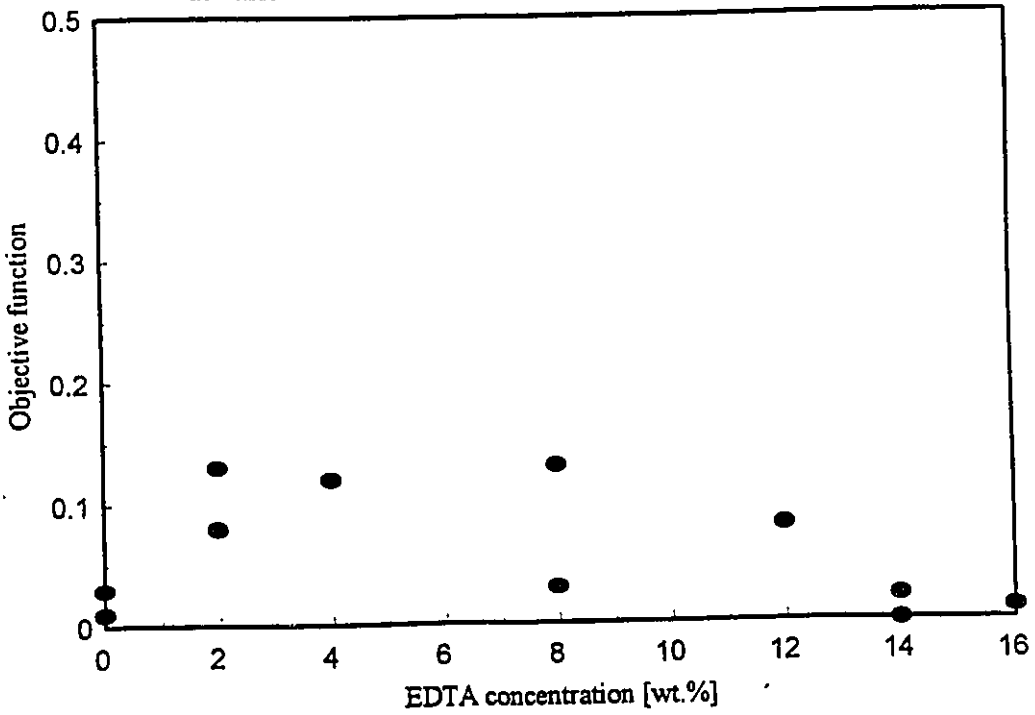

Figure 5.24: Objective function (θ) vs. the EDTA conc. in the nonsolvent mixture for annealed membranes after silver nitrate impregnation and reduction.

5.7 Membrane Characterization

The second part of this study was to characterize the porosity of the membranes using nitrogen adsorption-desorption experiments. As previously described, the membrane was scraped from the surface of the backing material and characterized using ASAP 2000. The surface area distribution of the pores within a membrane was determined for an entire 7x12 in (18x30 cm). Following gelation, the as-cast, non-annealed, cellulose acetate membrane with different addition levels of additive (EDTA) in the casting solution were subjected to post-treatment, solvent exchanged dried and tested.

Due to space limitations in this thesis and illustrative purposes, only casting solutions containing EDTA concentrations of 0, 2, 8 and 12 % were reported. The results of these pore area analyses are included in Figures 5.25 to 5.38 and all the numerical data for the pore area frequency used in generating these Figures have been included in Appendix B.

5.7.1 Effect of Annealing without EDTA

A pore area distribution of non-annealed and annealed membranes is shown in Figure 5.25. A large peak is present at a pore diameter of 35 Å with a tail decreasing to 80-100 Å. These membranes would typically be a reverse osmosis membranes having a pore diameter of 20 to 40 Å which is precisely the range in which the most pronounced peak in our distribution occurs. This supports the premise that the fine pores of the support layer are representative of the skin layer.

Shulz and Asnumaa (1970), reported that the skin had pores of average radius 23 Å, between CA crystallites of 188 Å size. The number of pores in the 30 to 40 Å diameter range is nearly double on annealing which indicates an increase in the number of crystallites present in the membrane.

5.7.2 Effect of Annealing with EDTA

For non-annealed membranes, Figures 5.25 to 5.28, the addition of EDTA up to a level of 2% appears to shift the pore size distribution to the right. This favors higher air permeability and low oxygen separation. Addition above 2% (Figures 5.27 and 5.28) greatly reduces membrane porosity which suggest a decrease in air permeability. This agrees with the air permeability observations shown in Figure 5.2.

The effect of annealing, Figures 5.25 to 5.28 appears to cause a shift towards a larger average pore size and a flattening of the pore size distribution curves. From Figure 5.26, at the 2% EDTA addition level, most of the pores appear to be located in the 50 to 70 Å diameter range which is a distinct shift to a larger average pore size. At higher addition levels of EDTA the tendency for the distribution to shift to the right and flatten is very evident, as can be seen in Figures 5.27 and 5.28.

The disappearance of both smaller and larger pores cause an increase in the ratio of larger to smaller pores leading to a less selective membrane. As seen in Figures 5.27 and 5.28, a greater number of large pores from 100 to 500 Å diameter range are present with the addition of EDTA.

5.7.3 Effect of Silver Nitrate Impregnation for Annealed Membranes

As seen in Figure 5.29, the addition of silver nitrate followed by heat treatment appears to increase the total small pore area and perhaps marginally the total pore area of the skin layer. The flattening of the pore size distribution curve of silver nitrate treated membranes is very pronounced up to 2% EDTA (Figures 5.29 and 5.30). At higher levels of EDTA addition the behavior after silver nitrate impregnation and annealing (Figures 5.31 and 5.32) to produce a pore size distribution similar to that of annealed membranes which indicates that at higher level of EDTA, the polymer network is highly populated with EDTA and the addition of silver causes a reduction in the porosity of the membrane.

The results also indicate a considerable uptake of silver even without EDTA as seen in Figure 5.29. However, in the presence of EDTA the ratio of the largest peaks in the 30-40 Å diameter range at 0% EDTA in Figure 5.29 is 3.76 while that of Figure 5.30 is 7.24 which indicates that a greater amount of silver uptake by the membranes at the 2% EDTA level.

5.7.4 Effect of Silver Nitrate Impregnation and Reduction to Silver Metal for Annealed Membranes

In the absence of EDTA, Figure 5.33, reduction to silver metal tends to increase the porosity in the 30-40 Å diameter range. In the absence of EDTA silver nitrate is loosely bound within the membrane and is released during the reduction process or the annealing step. The importance of EDTA in the casting solution to trap silver nitrate

within the membrane is easily seen in Figure 5.34 where larger pores (in the 30-40 Å range) are completely blocked on annealing.

As seen in Figures 5.34 to 5.36, increasing the amount of EDTA in the casting solution causes a dramatic decrease in the membrane porosity. Above 2% EDTA, the relative number of smaller pores <20 Å decrease with respect to the number of larger pores in the 30-40 Å diameter range leading to a less selective membrane as seen in Figure 5.21.

5.7.5 Effect of Silver Nitrate Impregnation and Reduction to Silver Metal for 2% EDTA, Non-annealed Membrane

Addition of silver nitrate to the membrane with 2% EDTA without annealing (Figure 5.37) appears to maintain the number of smaller pores <20 Å while decreasing pores in the 35 to 200 Å diameter range, thus creating a more selective membrane. Decreasing the ratio of larger pores to smaller pores appears to enhance the oxygen separation of these membranes. The same observation was obtained with the silver metal membrane (Figure 5.38).

5.8 Summary of Permeation, Oxygen Separation Tests and Porosity

The objective of this section is to relate the pore-area distribution with the oxygen separation and air permeability results. Several models exist in the literature to explain gas transport through a membrane. For an individual pore, Knudsen flow, slip flow or viscous flow may occur depending on the ratio of the pore radius r and the mean free path of the gas molecules λ. The mean free path λ is given by;

$$\lambda = \frac{3\eta}{2P}\left(\frac{\pi RT}{2M}\right)^{1/2} \qquad (17)$$

The mean free path for oxygen and nitrogen were calculated respectively as 714 and 650 Å. Knudsen flow occurs in the range of (r/λ) between 0 and 0.05, slip flow occurs in the range of (r/λ) = 0.05 to 50, viscous flow when (r/λ) is greater than 50.

Therefore, based on the pore area distributions in Figures 5.25 to 5.38, both Knudsen and slip flow are occurring within the pores of the membranes. Knudsen flow is not a good model to represent our results since it is based on the assumption that the separation is proportional to the inverse square root ratio of molecular weight of the two gases. This model predicts that nitrogen would permeate faster than oxygen which is the opposite of our results.

Slip flow occurs in the larger diameter pores which could be a good representation of the diffusion in the support layer. The free volume model (Stern, 1976) cannot be used directly in this work since it requires unknown free volume parameters as essential inputs.

The solution diffusion model is the most appropriate model to represent our results since it is based on both solubility and mobility factors. Diffusivity selectivity favors the smallest molecule while solubility selectivity favors the most condensable molecule. Basically adsorption phenomena originate from molecular interactions known as dispersion forces, electrostatic forces and hydrogen bonding. The dispersion forces are always present in adsorption. The interaction potential can be expressed by the Lennard-Jones potential as;

$$E_d = \sigma \left[(r/r_o)^{-12} - (r/r_o)^{-6} \right] \tag{18}$$

The two parameters σ and r_o are functions of the basic properties of the molecules such as polarizability, magnetic susceptibility and ionization potential. Since the interaction of a simple gas molecule with a polymer matrix tends to be rather small, the main factor governing the solubility is the ease of condensation of the gas. A linear relation ship exists between the critical temperature of the gas, T_c , the normal boiling point, T_b , and the Lennard Jones potential force constant, ε/k. The values of these parameters are listed below in Table 5.7.

Table 5.7: Intermolecular force parameters and critical properties.

Gases	Molecular weight M	Kinetic Diameter[a] (Å)	ε/k[b] (°K)	T_b[c] (°C)
O_2	32.00	3.46	113	-183
N_2	28.02	3.64	91.5	-195.8

[a]Breck, 1974 : [b]Hirschfelder et al., 1960 : [c]Kobe and Lynn, 1952

In general, the normal boiling point T_b , and the Lennard Jones potential force constant, ε/k, increases with molecular size and thus, solubilities increase with molecular size. Usually the increase in solubility with increasing size is much less than the decrease in diffusivity and the net result is that permeabilities decrease with the increasing size of diffusant by almost as much as the diffusion coefficient (Park, 1986). This explains why in our case, the selectivity (oxygen separation) for a particular component is greatly affected by the kinetic diameter.

More data on the interaction of oxygen with silver is needed to truly eliminate the role of solubility as a factor in the oxygen separation process. However, it is reasonable to estimate that the main role of silver in increasing oxygen separation at a given air permeability is due to the blockage within the polymer matrix. This yields a reduced effective thickness of the selective layer compared to the thickness of a non impregnated membrane of same porosity.

The membrane materials tested in the ASAP porosimeter contained a substantial amount of the support layer of the asymmetric membrane. It is assumed in this work that for pore diameters <100 Å the porosity of the support layer is similar to that of the skin layer. Two points favor this assumption in our work, since acetone is a very low boiling point solvent and is very miscible in water it is released very rapidly from the support layer of the membrane leaving a fine pore structure on the walls of the supporting structure which is similar to that of the skin layer. Also especially in the case of a cellulosic ester, the molecule is relatively rigid and would have a steric hinderance in packing of the molecular chains on precipitation.

In Figure 5.25, and in general, a considerable peak or number of pores exists between 30 and 70 Å pore diameter. The maximum in this peak is centered between 30 and 40 Å diameter. Ohya et al. (1974), measured pore area distributions by nitrogen adsorption for homogeneous ultrathin membranes, having a 1 μm thickness. Ohya's results indicate the same peak between 30 and 70 Å for non-annealed membranes and a more pronounced and narrower distribution of 20 to 50 Å for annealed membranes. The distributions obtained by these workers are in excellent agreement with those obtained in this study shown in Figure 5.25.

Gas transport through a membrane is mainly occurring through the thin selective layer of the membrane. Work on characterizing the structure of the skin layer of cellulose acetate membranes has revealed the absence of pores greater than 100 Å diameter and a skin thickness of 0.25 μm (Riley et al. 1964, 1966). As previously mentioned, Shultz and Asunmaa (1970) reported that the skin layer of Loeb-Sourirajan membrane have pores of average radius 23 Å, between cellulose acetate crystallites of 188 Å size.

The pore area distributions measured in this work are in such good agreement with those using ultrathin membranes and other independent observations that it is reasonable to consider that pore area distributions, below 100 Å diameter, obtained for the membrane scraped from the surface of the backing material are representative of the porosity of the skin layer of the membranes prepared in this work.

Generally, annealing the membrane may result in densification which can be advantageous or disadvantageous depending upon its extent. Excessive densification is commonly encountered with polar and hence hydrophilic polymers where polymer water

interactions are almost as strong as the surface tension of water. Some densification is desirable to seal defects in the skin layer. However, in the skin and substructure layers excessive densification may effect cell collapse to the extent that opposing cell walls make contact with one another and result in polymer-polymer interaction forces which can be bring about complete loss of porosity. In such cases, an integrally skinned bilayer is replaced by a dense monolayer with a catastrophic loss of air permeability (Kesting and Fritzsche, 1993). In the absence of EDTA, annealing increases the number of pores in the 30-50 Å diameter range, as seen in Figure 5.25. This indicates an increase in crystallinity which is in a good agreement with the above statements and the morphology proposed by Shulz and Asnumaa, (1970).

If an addition such as EDTA is completely soluble and mobile within the gelling membrane, it can escape leaving a fairly porous structure which has good air permeability. If too much EDTA remains in the membrane, lower air permeabilities and oxygen separations are noticed. As in Figures 5.26 to 5.28 the number of inter-crystallite pores in the 30-40 Å diameter range has decreased in the presence of EDTA which indicates the reduced crystallinity of the membrane. If the additive is entrapped within the membrane, the pore size reduction as described by Kesting and Fritzche, (1993), would be enhanced.

The sharp drop in porosity in good agreement with the limiting solubility of EDTA in water (Flaschka, 1964). The solubility limit explains why the air permeability at 2% is much greater than at other concentrations. Above the 2% limit, EDTA is present as a precipitate in the casting solution and cannot readily escape the membrane during the

gelation process. The EDTA would then be trapped during the gelation process reducing the porosity of the membrane.

The solubility limit of the EDTA additive defines the trade off between the need for a maximum amount of ligand in the casting solution to entrap the silver metal and the need for a highly porous network for good membrane air permeability. The addition of EDTA to its solubility limit of 2 wt % in water is optimal in order to improve the selectivity of the skin layer while maintaining reasonable air permeabilities.

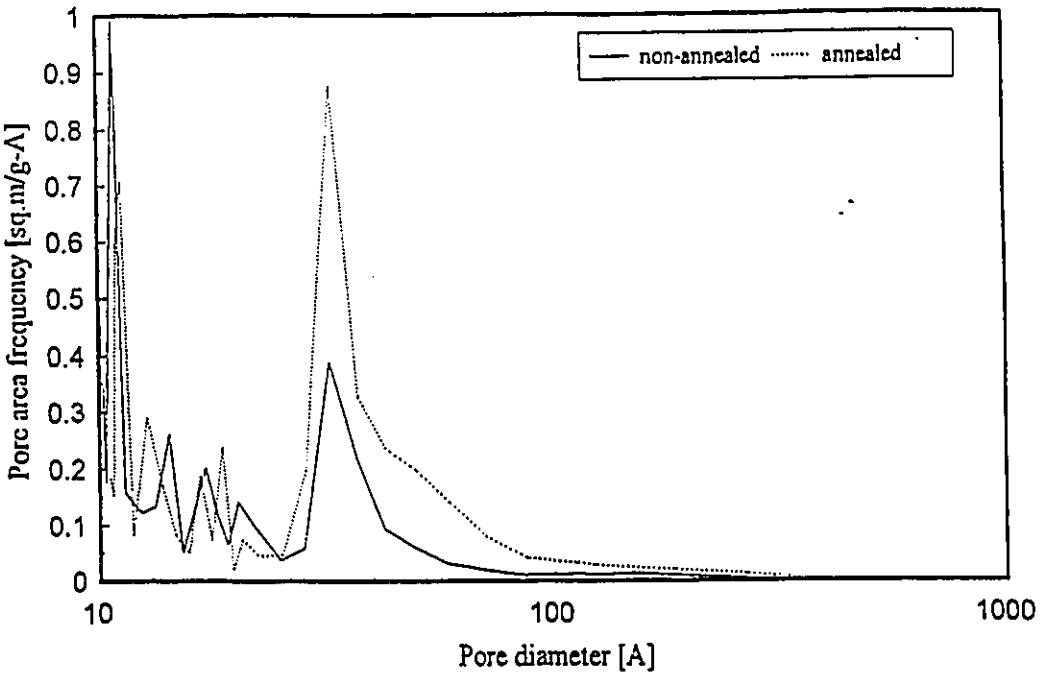

Figure 5.25: Effect of annealing on the pore area distributions for a concentration of 0% EDTA in the nonsolvent mixture.

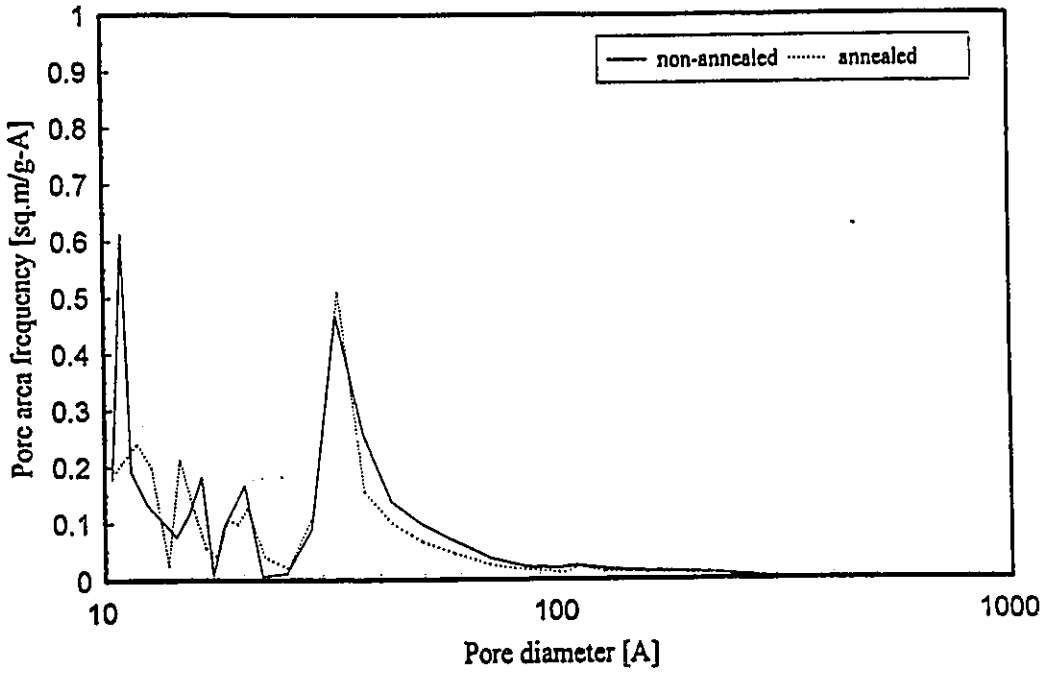

Figure 5.26: Effect of annealing on the pore area distributions for a concentration of 2% EDTA in the nonsolvent mixture.

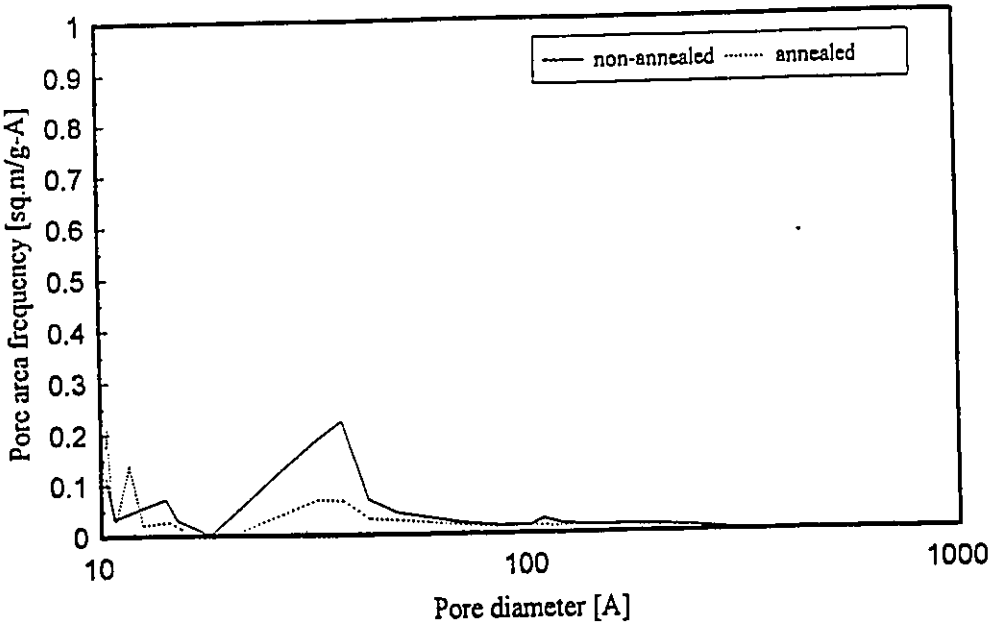

Figure 5.27: Effect of annealing on the pore area distributions for a concentration of 8% EDTA in the nonsolvent mixture.

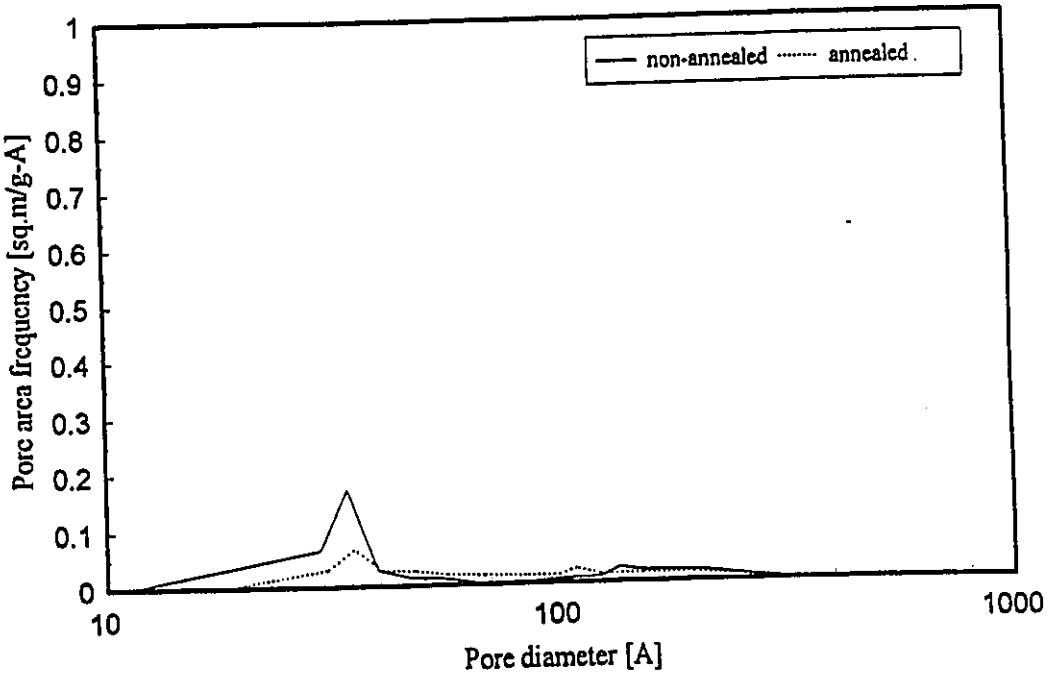

Figure 5.28: Effect of annealing on the pore area distributions for a concentration of 12% EDTA in the nonsolvent mixture.

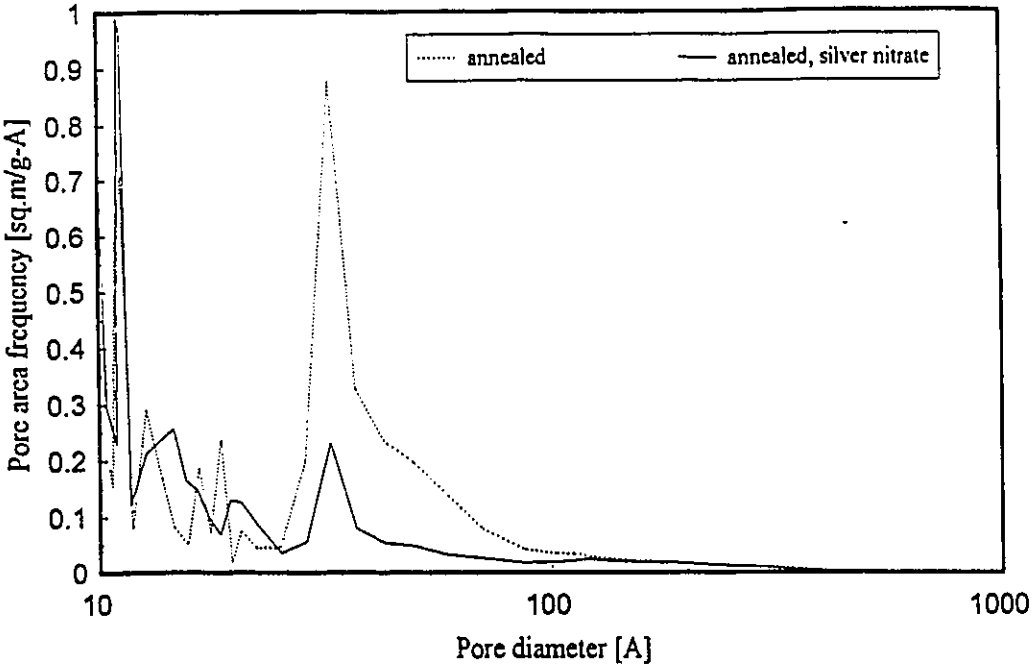

Figure 5.29: Effect of silver nitrate impregnation on the pore area distributions for annealed membranes at a concentration of 0% EDTA in the nonsolvent mixture.

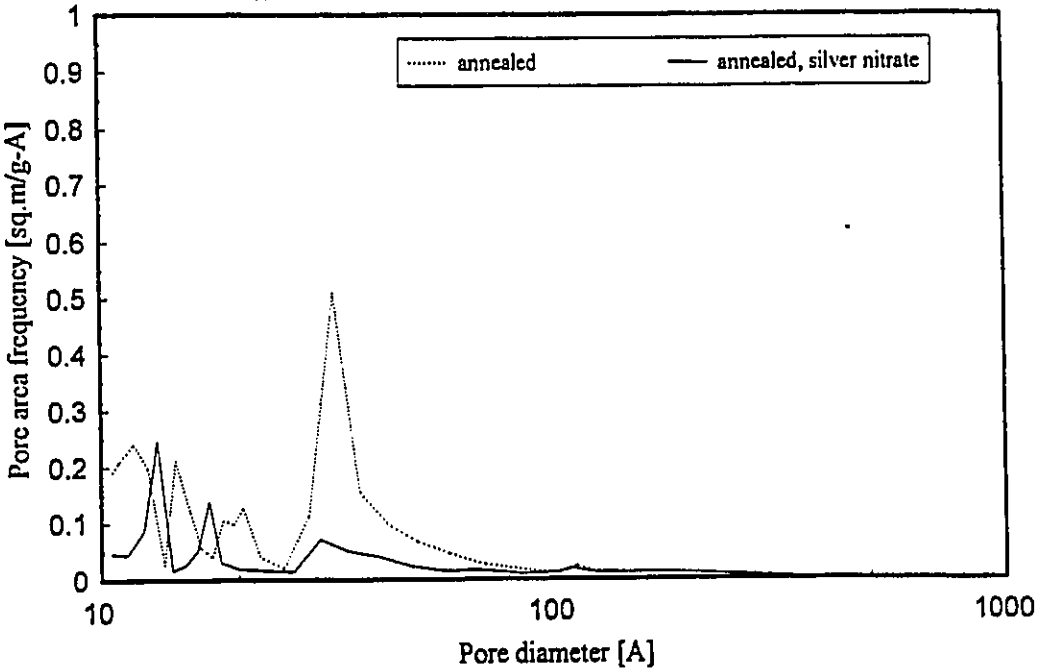

Figure 5.30: Effect of silver nitrate impregnation on the pore area distributions for annealed membranes at a concentration of 2% EDTA in the nonsolvent mixture.

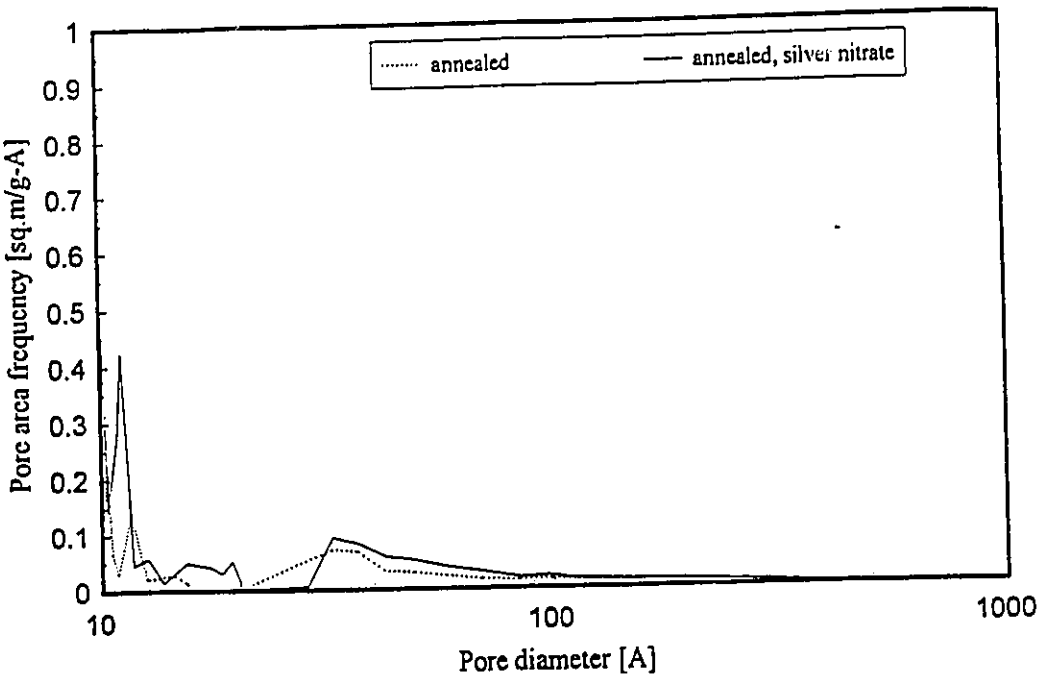

Figure 5.31: Effect of silver nitrate impregnation on the pore area distributions for annealed membranes at a concentration of 8% EDTA in the nonsolvent mixture.

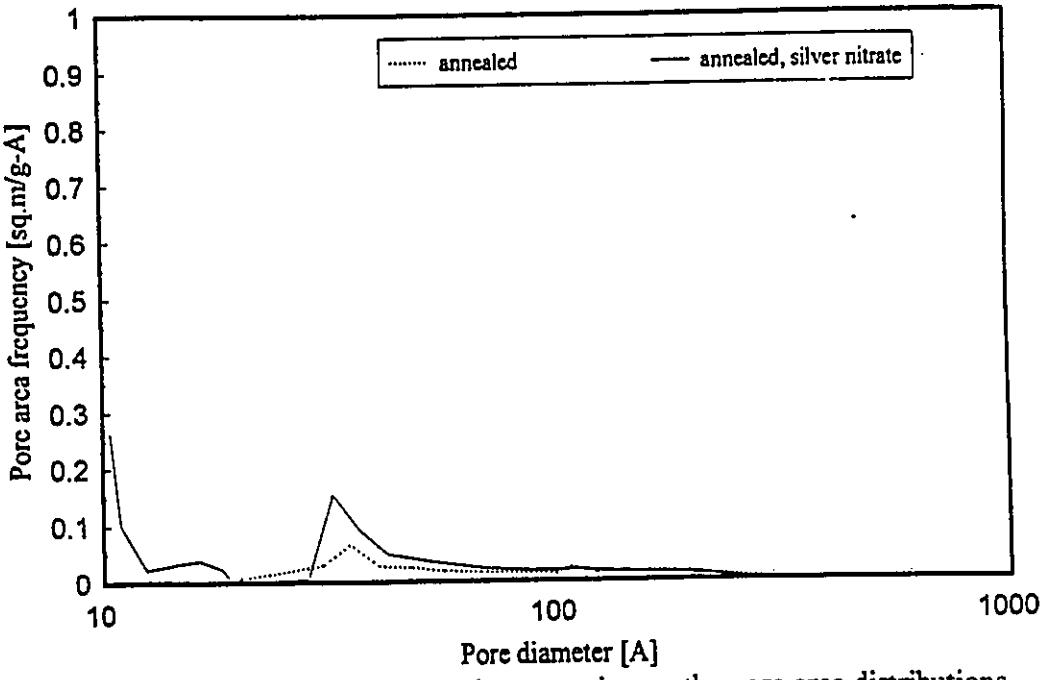

Figure 5.32: Effect of silver nitrate impregnation on the pore area distributions for annealed membranes at a concentration of 12% EDTA in the nonsolvent mixture.

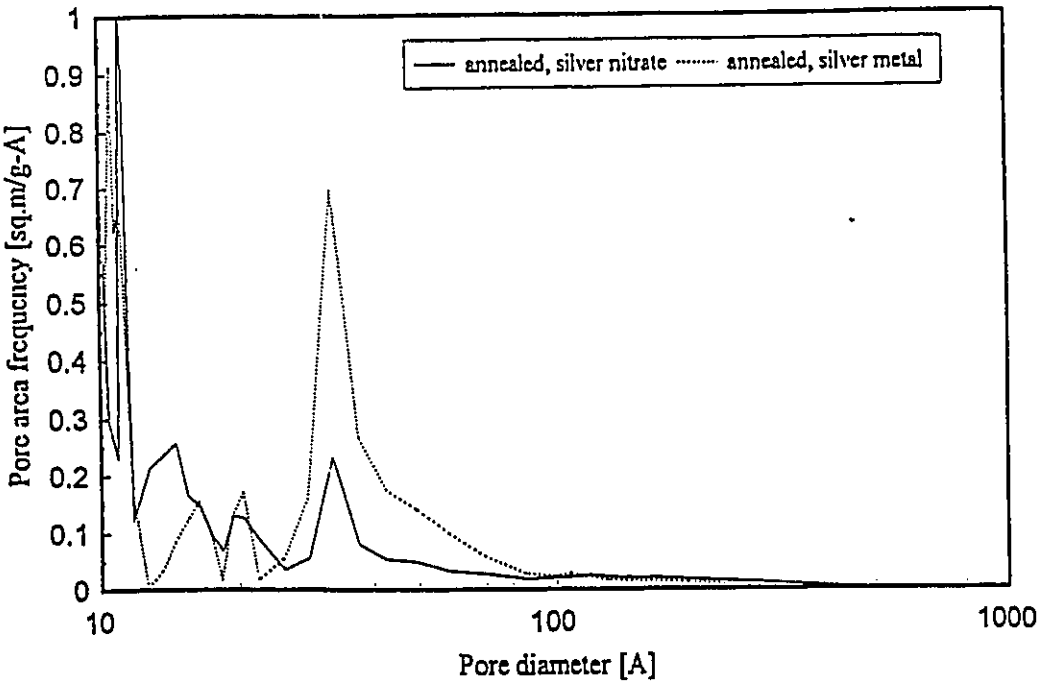

Figure 5.33: Effect of silver nitrate impregnation followed by reduction on the pore area distributions for annealed membranes at a concentration of 0% EDTA in the nonsolvent mixture.

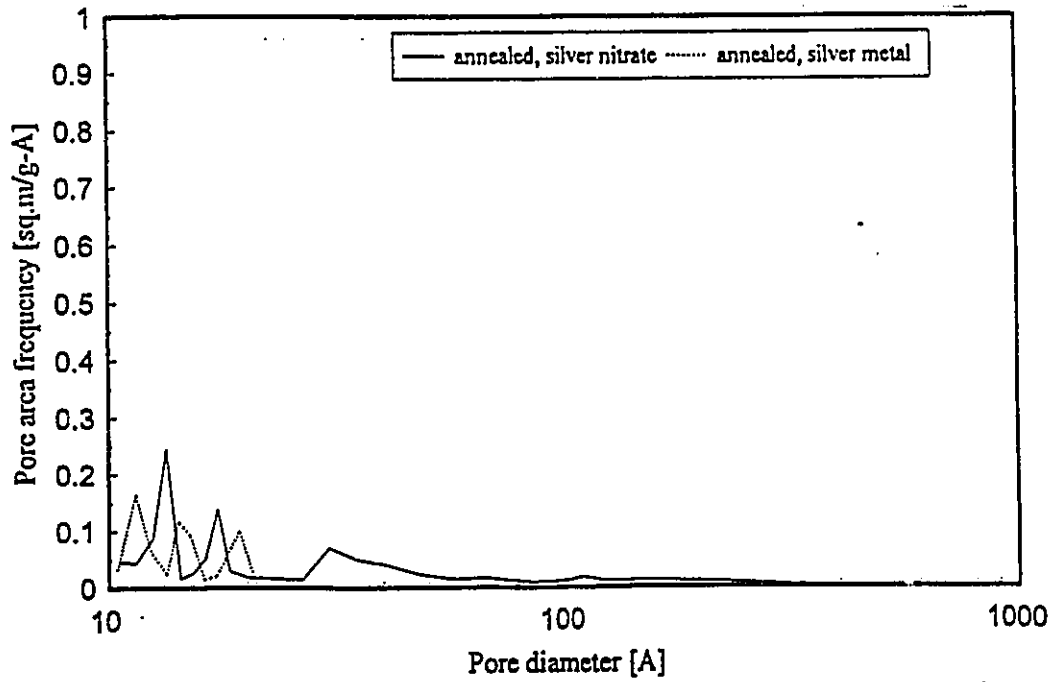

Figure 5.34: Effect of silver nitrate impregnation followed by reduction on the pore area distributions for annealed membranes at a concentration of 2% EDTA in the nonsolvent mixture.

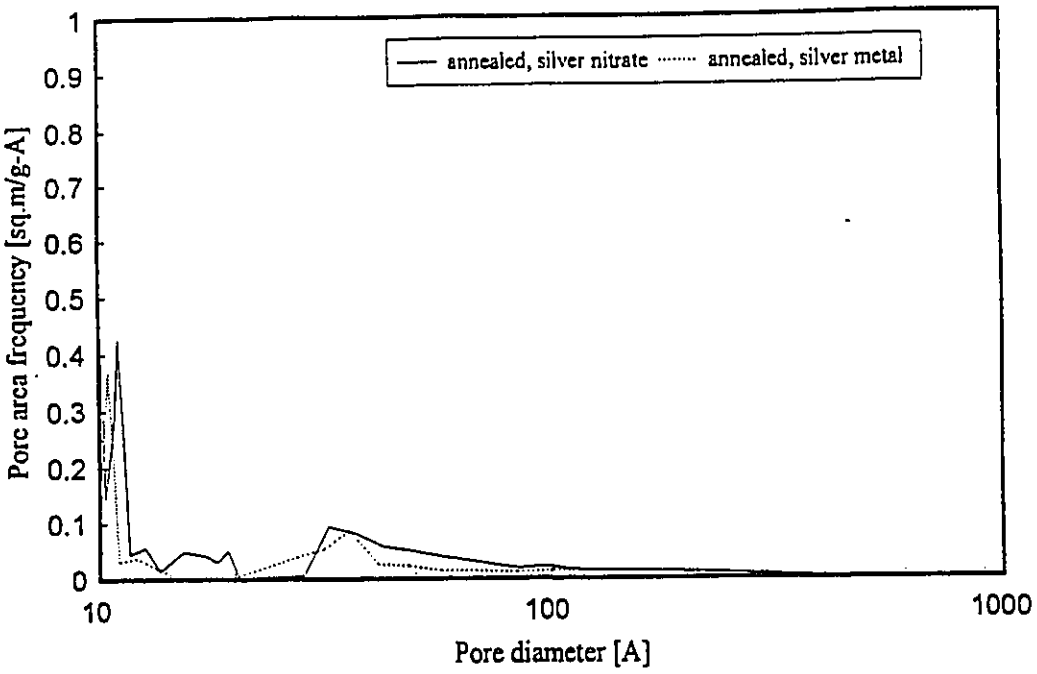

Figure 5.35: Effect of silver nitrate impregnation followed by reduction on the pore area distributions for annealed membranes at a concentration of 8% EDTA in the nonsolvent mixture.

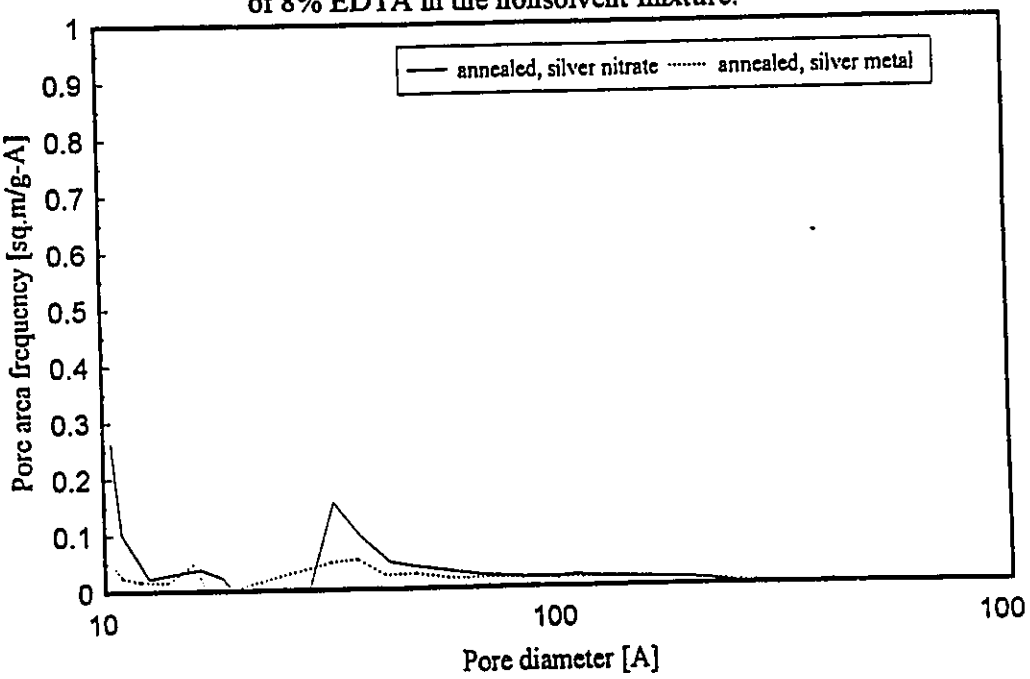

Figure 5.36: Effect of silver nitrate impregnation followed by reduction on the pore area distributions for annealed membranes at a concentration of 12% EDTA in the nonsolvent mixture.

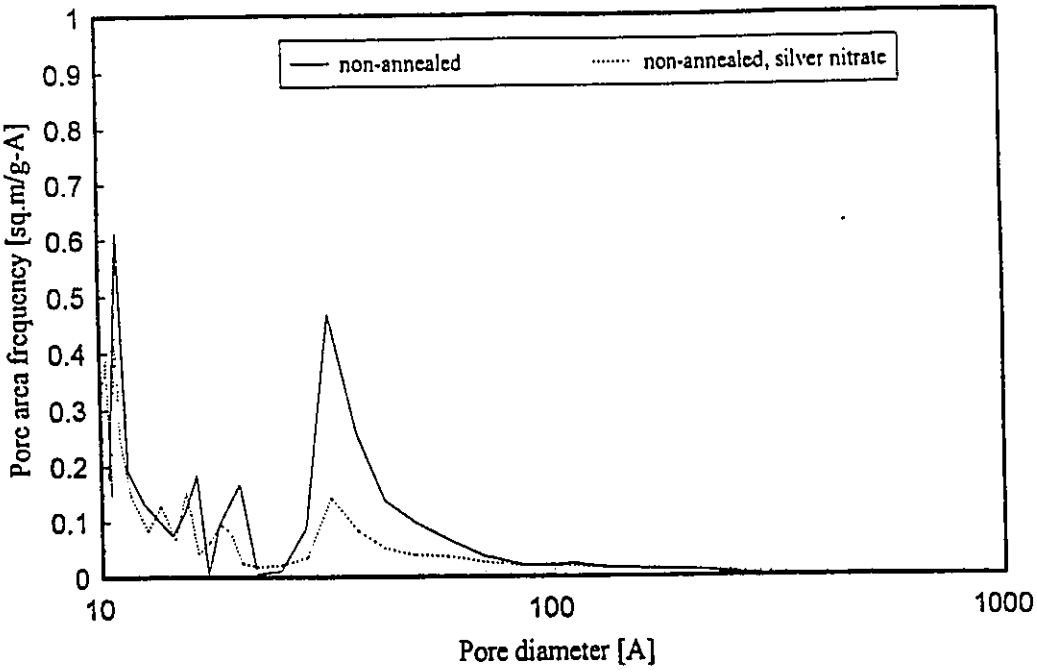

Figure 5.37: Effect of silver nitrate impregnation on the pore area distributions for non-annealed membranes at a concentration of 2% EDTA in the nonsolvent mixture.

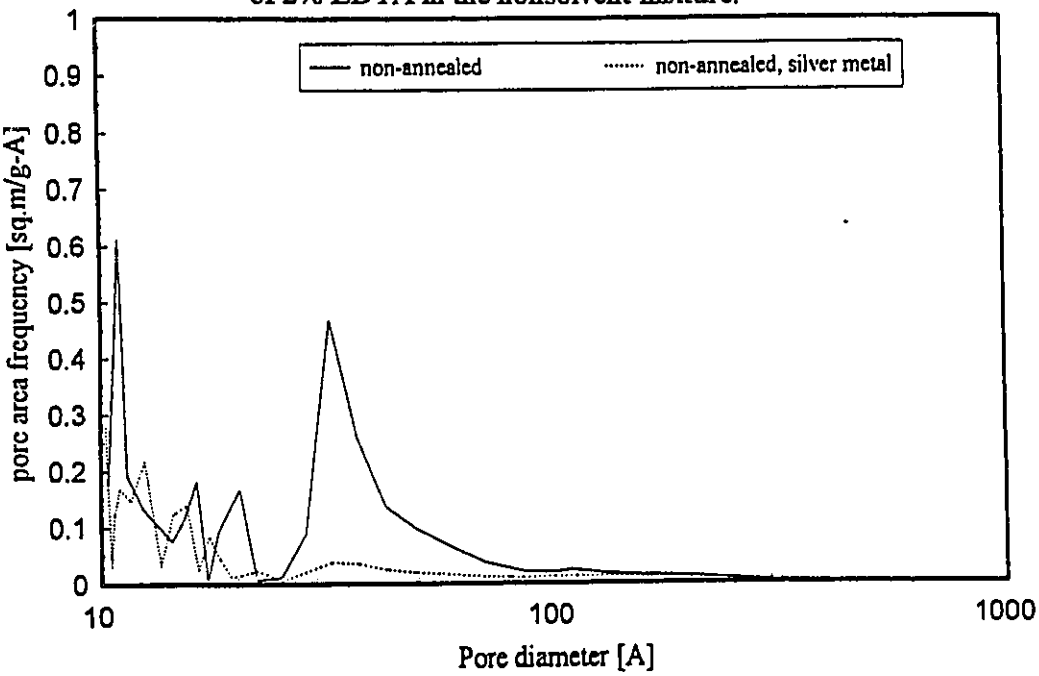

Figure 5.38: Effect of silver nitrate impregnation followed by reduction on the pore area distributions for non-annealed membranes at a concentration of 2% EDTA in the nonsolvent mixture.

Chapter 6

Conclusions

1. Cellulose acetate membranes having both higher air permeability and oxygen separation than conventional membranes can be produced by silver impregnation.
2. Gas sorption techniques are a valuable tool in membrane characterization. The porosity measurement made for the complete membrane (skin plus support layer), below 100 Å diameter were representative of the porosity of the skin layer. These porosity measurements are in good agreement with the trends observed for the air permeability and oxygen separation of various membranes.
3. For membranes cast without EDTA; lower air permeabilities and higher oxygen separations were obtained, and an increase in crystallinity with annealing was observed.
4. The presence of silver in the membrane causes the blockage of pores in 30-100 Å diameter range.
5. Optimal air permeability and oxygen separation were obtained for non-annealed silver impregnated membranes where the ligand additive EDTA was at its solubility limit of 2 wt % in water.
6. Greater amounts of EDTA in the casting solution, beyond the 2 wt % solubility limit in water, were found to decrease membrane porosity, reducing air permeability and oxygen separation.

7. For concentrations of EDTA at and below the solubility limit, annealing considerably increased membrane air permeability this was also in agreement with an increase in the frequency of pores in the 30-40 Å diameter range, observed in porosity measurements.

Recommendations

The following recommendations could be useful in future work:

1. Adapt or develop a transport model which includes membrane pore size and gas-membrane interactions to predict oxygen separation.
2. Study the effect of higher concentrations of silver nitrate in the impregnating solutions.
3. Perform a chemisorption oxygen analysis on the membranes impregnated with silver metal.
4. Estimate the amount of silver deposited on the membrane.
5. Produce silver impregnated membranes from other materials.
6. Study the mechanism of oxygen diffusion through the silver metal layer.
7. Reduce the silver ions in the membranes by passing hydrogen gas into the high pressure compartment of the test cell.

Bibliography

Agrawal, R. and Auvil, S., "Process for the Generation of Gaseous and/or Liquid Nitrogen", *US Patent 4,595,405*, 1986.

Anderson, M.A., Gieselmann, M.J. and Xu, Q., "Titania and Alumina Ceramic Membranes", *J. Membrane Sci.*, **39**, 243(1988).

Anonymous, "Facts and Figures for the Chemical Industry", *Chem. Eng. News*, **68**(25), 34(1990).

Asakawa, S., "Oxygen Permeable Membrane", *Kobunshi*, **34**, 902(1985).

Baker, R.W. and Blume, H., "Permeselective Membranes Separate Gases", *CHEMTECH*, **16**(4), 232(1986).

Balkus, K.J., Kortz, A. and Drago, R.S., "Carbon Monoxide Binding by Copper(I) Complexes supported on Polystyrene", *Inorg. Chem*, **27**, 2955(1988).

Barrett, E.P., Joyner, L.S. and Halenda, P.P., "The determination of Pore Volume and Area Distributions in Porous Substances. I. Computations from Nitrogen Isotherms", *J. Am. Chem. Soc.* **73**, 373(1951).

Beaver, E.R., Bhat, P.V. and Sarcia, D.S., "Integrations of Membranes with other Air Separation Technologies", *AIChE Symp. Ser.*, **84**(261), 113(1988).

Bhat, P.V. and Beaver, E.R., "Innovations in Nitrogen Inerting using Membrane Systems", *AIChE Symp. Ser.*, **84**(261), 124(1988).

Bouchilloux, J., Fabre, S. and Fauvre, A., "Anisotropic Organosilicon Polymer Membrane", *US Patent 3,754,375*, 1973.

Breck, D.W., "Zeolite Molecular Sieves", John Wiley & Sons., New York (1974).

Chapman, B.N. and Anderson, J., "Science and Technology of Surface Coating", Academic Press, New York (1974).

Cheng, K.L., "Increasing Selectivity of Analytical Masking", *Anal. Chem.*, **33**, 783(1963).

Crank, J., "The Mathematics of Diffusion", Clarendon Press, New York (1975).

Crank, J. and Park, G.S., "Diffusion in Polymers", Academic Press, New York (1968).

Dietz, W.A., "Response Factors For Gas Chromatographic Analyses", *J. of Gas Chrom.*, **5**, 68(1967).

Drago, R.S. and. Balkus, K.J., "Cobalt (II)-Facilitated Transport of Dioxygen in a Polystyrene Membrane", *Inorg. Chem.*, **25**, 716(1986).

Flaschka, H.A., "EDTA Titrations: An Introduction to Theory and Practice", Pergamon Press Ltd, New York (1964).

Fouda, A.E., Kutowy, O. and Capes, C.E., "Simulation of the Effect of Membrane Shrinkage on Separation Behavior", *J. Separ. Proc. Technol.*, **8**, 1(1987).

Gantzel, P.K. and Merten, U., "Gas Separation with High Flux Cellulose Acetate Membranes", *Ind. Eng. Chem. Process. Des. Dev.*, **9**, 331(1970).

Gardner, R.J., Crane, R.A. and Hannan, J.F., "Hollow Fiber Permeator for Separating Gases", *Chem. Eng. Prog.*, **73**, 76(1977).

General American Transportation Corp., "Oxygen Permeable Membranes", *US Patent 3,350,355*, 1970.

Gollan, A. and Kleper, M.H., "Membrane- Based Air separation", *AIChE Symp. Ser.*, **250**(82), 38(1989).

Gottschlich, D.E., Roberts, D.L. and Way, J.D., "A Theoretical Comparison of Facilitated Transport and Solution-Diffusion Membrane Modules for Gas Separation", *Gas Sep. and Purification*, **2**, 71(1988).

Govind, R., Atnoor, D. and Zhao, D., "Future Prospects and Applications for Metal Based Membranes", *Key Engineering Materials*, **61**, 319(1991).

Graham, T., "The Absorption and Dialytic Separation of Gases by Colloid Septa", **32**, 401(1866).

Gregor, H.P. and Gregor, C.D., "Synthetic-Membrane Technology", *Sci. Am.*, **239**, 112(1978).

Gryaznov, V.M., "Hydrogen Permeable Palladium Membrane Catalysts", *Platinum Metals Rev.*, **30**, 68(1986).

Haggin, J., "New Generation of Membranes Developed for Industrial Separations", *Chem. Eng. News*, **66**(23), 7(1988).

Harkins, W.D. and Jura, G., "An Adsorption Method for the Determination of the Area of a Solid without the Assumption of a Molecular Area and the Area Occupied by N_2 Molecules on the Surface of Solids", *J. Chem. Phys.*, **11**, 431(1943).

Helfferich, F.G., "Ion Exchange", McGraw-Hill Book Company, New York (1962).

Henis, J.M.S. and Tripodi, M.K., "A Novel Approach to Gas Separation using Composite Capillary Membranes", *Sep. Sci. Tech.*, **15**(4), 1059(1980).

Henis, J.M.S. and Tripodi, M.K., "Composite Hollow Fiber Membrane for Gas Separations: The Resistance Model Approach", *J. Membrane Sci.*, **8**, 233(1981).

Henis, J.M.S. and Tripodi, M.K., "The Developing Technology of Gas Separating Membranes", *Science*, **220**(4592), 11(1983).

Hirschfelder, J.O., Curtiss, C.F. and Bird, R.B., "Molecular Theory of Gases and Liquids", John Wiley & Sons., New York (1954).

Hsieh, H.P., "Inorganic Membrane Reactors- A Review", *AIChE Symp. Ser.*, **268**(85), 53(1988).

Hwang, S.T., Choi, C.K. and Kammermeyer, K., "Gaseous Transfer Coefficients in Membranes", *Sep. Sci.*, **9**(6), 461(1974).

Hwang, S.T. and Thorman, J.M., "The Continuous Membrane Column", *AIChE J.*, **26**, 558(1980).

Ilias, S. and Govind, R., "Development of High Temperatures Membranes for Membrane Reactor: An Overview", *AIChE Symp. Ser.*, **85**(268), 18(1989).

Johnson, F. M. G. and P. Larose, "The Diffusion of Oxygen through Silver", *J. Amer. Chem. Soc.*, **46**, 1377(1924).

Kawakami, Y., Aoki, T. and Yamashita, Y., "Enhanced Oxygen Permeation through Surface Modified Blend Films containing Polydimethylsiloxane Graft Copolymers", *Polym. J.*, **18**, 243(1986).

Kelvin, J., "The Equilibrium of Vapor at a Curved Surface of Liquid", *Phil. Mag.*, **42**, 448(1871).

Kesting, R.E., "Semipermeable Membranes of Cellulose Acetate for Desalination in the Process of Reverse Osmosis. I. Lyotropic Swelling of Secondary Cellulose Acetate", *J. Appl. Polym. Sci.*, **9**, 663(1965).

Kesting, R.E., "Synthetic Polymeric Membranes: A Structural Perspective", 2nd ed., McGraw-Hill Book Company, New York (1971).

Kesting, R.E., "Phase Inversion Membranes", in "Materials Science of Synthetic Membranes", D.R. Lloyd, Ed., ACS Publishers, Washington (1985), p.269.

Kesting, R.E. and Fritzsche, A.K., "Polymeric Gas Separation Membranes", John Wiley & Sons., New York (1993).

Kim, T. H., Koros, W.J., Husk, G.R. and O'Brien, K.C, "Relationship between Gas Separation Properties and Chemical Structure in a Series of Aromatic Polyimides", *J. Membrane Sci*, **37**, 45(1988).

Kimura, S. G., "Preparation of Asymmetric Polymer Membranes", *US Patent 3,709,774*, 1973.

Kobe, K.A. and Lynn, R.E., "The Critical Properties of Elements and Compounds", *J. Chem. Rev.*, **52**, 117(1952).

Kokan, N., "Hydrocarbon Vapor Recovery with Membrane Technology", Technical Bulletin, Nippon Kokan, Tokyo, Japan (1987).

Koros, W. J. and Chern, R.T., "Handbook of Separation Process Technology", John Wiley & Sons., New York (1987).

Koros, W.J. and Fleming, G.K., "Membrane-based Gas Separations", *J. Membrane Sci.*, **83**, 1(1993).

Koros, W.J., Fleming, G.K., Jordan, S.M., Kim, T.H. and Hoehn, H.H., "Polymeric Membrane Materials for Solution-diffusion based Permeation Separations", *Prog. Polym. Sci.*, **13**, 339(1988).

Laverty, B. W. and O'Hair, J.G., "Applications of Membrane Technology in the Gas Industry", in "Membranes in Gas Separation and Enrichment: The Proceedings of the Fourth BOC Priestley Conference", Royal Society of Chemistry Publishers, Leeds (1986), p.291.

Lewis, F.A, "The Palladium Hydrogen Systems", Academic Press, London (1967).

Lloyd, D.R., "Material Science of Synthetic Membranes", *AIChE*, **1**(18), 339(1985).

Lloyd, M.R., "Correlation of Separation Factor versus Permeability for Polymeric Membranes", *J. Membrane Sci.*, **62**, 165(1991).

Loeb, S. and Sourirajan, S., "Sea Water Demineralization by means of an Osmotic Membrane", *Adv. Chem. Ser.*, **38**, 117(1962).

Lonsdale, H.K., "Membrane Separation Technology in the 1980s", in "Membrane and Ultrafiltration Technology: Development since 1981", S. Torrey, Ed., Noyes Data Co. Publishers, Park Ridge (1984), p.419.

MacDonald, W. and Pan, C., "Method of Drying Water-Wet Membrane", *US Patent 4,080,743*, 1978.

MacLean, D. L., Prince, C.E. and Chae, Y.C., "Energy-Saving Modifications in Ammonia Plants", *Chem. Eng. Prog.*, **76**, 98(1980).

MacLean, D. L., "The Structure of Gas Separation Technology", in "Membranes in Gas Separation and Enrichment: The Proceedings of the Fourth BOC Priestley Conference", Royal Society of Chemistry Publishers, Leeds (1986), p.382.

Manjikian, S., "Desalination Membranes from Organic Casting Solutions", *Ind. Eng. Chem. Prod. Res. Dev.*, **6**, 23(1967).

Manos, P., "Gas Separation Membrane Drying with Water Replacement Liquid", *US Patent 4,080,744*, 1978.

Mazur, W. H. and Chan, M.C., "Membranes for Natural Gas Sweeting and Carbon Dioxide Enrichment", *Chem. Eng. Prog.*, **78**, 38(1982).

Meares, P., "Diffusion in Polymers", Academic Press, London (1968).

Mercea, P., Muresan, L. and Mecea, V., "Permeation of Gases through Metallized Polymer Membranes", *J. Membrane Sci.*, **24**, 297(1985).

Micromeritics, ASAP 2000 "Accelerated Surface Area and Porosimetry System", Operator's Manual, Part No. 200-42800-01, Norcross (1992).

Minhas, B.S., Matsuura, T. and Sourirajan, S., "Solvent-Exchange Drying of Cellulose Acetate Membranes for the Separation of Hydrogen-Methane Gas Mixtures", *ACS. Symp. Ser.*, **281,** 451(1984).

Minhas, B.S., Wang, S.P. and Sherwin, M.B., "Effect of Process Variables on Cellulose Acetate Membranes Performance for Separation of Carbon Dioxide-Methane Mixtures", in "Proceedings of the International Membrane Conference on the 25th Anniversary of Membrane Research in Canada", Malaiyandi, M., Kutowy, O. and Talbot, F., Eds., National Research Council of Canada, Ottawa (1986), p.213.

Mulder, M, "Basic Principles of Membrane Technology", Kluwer Academic Publishers, Boston, MA (1991).

Murphy, M. K., Beaver, E.R. and Rice, A.W., "Post Treatment of Asymmetric Membranes for Gas Applications", *AIChE Symp. Ser.*, **85**(272), 34(1989).

Nishide, N., Ohyanagi, M., Okada, O. and Tsuchida, E., "Highly Selective Transport of Molecular Oxygen in a Polymer containing a Cobalt Prophyrin Complex as a Fixed Carrier", *Macromolecules*, **19**, 494(1986).

Ohno, M., Ozaki, O. and Sato, H. "Radioactive Rare Gas Separation Using a Separation Cell with Two Kinds of Membrane Differing in Gas Permeability Tendency", *J. of Nuclear Sci. and Tech.*, **14**(8), 589(1977).

Ohya, H., Imura, Y., Moriyama, T. and Kitaoka, M., "A Study on Pore Size Distribution of Modified Ultrathin Membranes", *J. Appl. Polym. Sci.*, **18**, 1855(1974).

Pan, C. Y. and Habgood, H.W., "Gas Separations by Permeators- Part 1: Calculation Methods and Parametric Analysis", *Can. J. Chem. Eng.*, **56**, 197(1978a).

Pan, C.Y. and Habgood, H.W., "Gas Separations by Permeators - Part 2: Effect of Permeate Pressure Drop and Choice of Permeate Pressure", *Can. J. Chem. Eng.*, **56**, 210(1978b).

Park, K.M. and Shim, I.W., "Preparation of Rh-Containing Cellulose Acetate Films and the Chemistry of Rh in Cellulose Acetate", *J. Appl. Polym. Sci.*, **42**, 1361(1991).

Park, G.S., "Transport Principles-Solution, Diffusion and Permeation in Polymer Membranes", in "Synthetic Membranes, science, Engineering and Applications", Bungay, P.M., Lonsdale, H.K. and de Pinho, M.N., Eds., D.Reidel Publishers, Boston (1986), p.57.

Perrin, J.E. and Stern, S.A., "Modeling of Permeators with two Different Types of Polymers Membranes", *AIChE J.*, **31**, 1167(1985).

Pinnau, I. and Koros, W.J., "Defect-Free Ultrahigh Flux Asymmetric Membranes", *US Patent 4,902,422*, 1990.

Riley, R.L, Gardner, J.O. and Merten, U., "Cellulose Acetate Membranes: Electron Microscopy of Structure", *Science*, **143**, 801(1964).

Riley, R.L, Gardner, J.O. and Merten, U., "Replication Electron Microscopy of Cellulose Acetate Osmotic Membranes", *Desalination*, **1**, 30(1966).

Ruf, A. and Egli, S., "Application of Gas Separation shown through the Purification of Landfill Gas", *Gas Sep. and Purification.*, **2,** 90(1988).

Ruthven, D.M., "Diffusion Controlled Gas Separations", in "Gas Separations Technology: The Proceedings of the International Symposium on Gas Separations Technology", Vansant, E.F. and Dewolfs. R., Eds., Elsevier Applied Science Publishers, Belgium (1989), p.1.

Sakai, T., Takenaka, H., Wakabayashi, N., Kawami, Y. and Torikai, E., "Preparation of Nafion-Metal Fine Particles Composite Membrane", *Bull. Gov. Ind. Res. Inst.*, Osaka, **36**(1), 10(1985).

Schell, W. J., "Separations of Coal Hydrogasification of Gases by Permeselective Membrane", *ACS. Div. Fuel. Chem. Reprints*, **20,** 253(1975).

Schendel, R. L., "Separation of Acid Gas and Hydrocarbons", in "Membranes in Gas Separation and Enrichment: The Proceedings of the Fourth BOC Priestley Conference", Royal Society of Chemistry Publishers, Leeds (1986), p.311

Schwarzenbach, G. *Die Komplexometrische Titration.* F. Encke, Stuttgart, 2nd edition (1956). English translation (H.Irving): Complexometric Titration. Methuen, London (1957).

Shim, I.W. and Risen, W., "Spectral and Thermal Studies of Transition Metal PSSA Ionomers", *Bull. Korean Chem. Soc.*, **9**, 368(1988).

Schultz, R. and Asunmaa, S., "Ordered Water and the Ultrastructure of the Cellular Plasma Membrane", *Rec. Prog. Surface Sci.*, **3**, 291(1970).

Shumilova, N.A. and Zhutaeva, G.V., "Silver", in "Encyclopedia of Electrochemistry of the Elements", Vol. VIII, Marcel Dekker, A.J. Bard, Ed., New York (1978), p.1.

Sirkar, K.K., "Asymmetric Permeators-Conceptual Study", *Sep. Sci. Tech.*, **15**, 1091(1980).

Skoog, D. and West, D.M., "Analytical Chemistry : An Introduction", Holt, Rinehart and Winston Inc., New York (1974).

Spillman, R.W., "Economics of Gas Separation Membranes", *Chem. Eng. Prog.*, **85**, 41(1989).

Springer, J. and Brite, H., "Permeabilitate Galvanisch Beschicheter Polymerfolien", *J. Appl. Polym. Sci.*, **24**, 329(1979).

Stanley, M., "Thomas Graham and Gaseous Diffusion", in "Membranes in Gas Separation and Enrichment: The Proceedings of the Fourth BOC Priestley Conference", Royal Society of Chemistry Publishers, Leeds (1986), p.161.

Stannet, V.T., Koros, W.J., Paul, D.R., Lonsdale, H.K and Baker, R.W., "Recent Advances in Membrane Science and Technology", *Adv. Polym. Sci.*, **32**, 69(1979).

Stern, S.A., Sen, S.K. and Rao, A,K., "The Permeation of Gases through Symmetric and Asymmetric (Loeb-Type) Cellulose Acetate Membranes", *J. Macromol. Sci. Phy*, **10**, 507 (1974).

Stern, S.A., "The Separation of Gases by Selective Permeation", in "Membrane Separation Processes", P. Meares, Ed., Elsevier Applied Science Publishers, New York (1976), p.295.

Stern, S.A., "New Developments in Membrane Processes for Gas Separations", in "Synthethic Membranes", M.B. Chenoweth, Ed., Midland Macromolecular Institute Press by Harwood Academic Publishers, New York (1986), p.1.

Stern, S.A., "Polymers for Gas Separations: The Next Decade", *J. Membrane Sci.*, **94**, 1(1994).

Stoever, H., "Space Technology Utilization-The Role of ESA and National Organizations", *ESA Bull.*, **48**, 18(1986).

Strathmann, H., "Membrane Separation Processes", *J. Membrane Sci.*, **9**, 121(1981).

Strathmann, H., "Production of Microporous Media by Phase Inversion Processes", in "Materials Science of Synthetic Membranes", D.R. Lloyd, Ed., ACS Publishers, Washington (1985), p.165.

Strathmann, H., "Synthetic Membranes and their Preparations", in "Synthetic Membranes Science, Engineering and Applications", Bungay, P.M., Lonsdale, H.K. and de Pinho, M.N., Eds., D.Reidel Publishers, Boston (1986).

Strathmann, H., Bell, C.M.and Kimmerle, K., "Development of Synthetic Membranes for Gas and Vapor Separation", *Pure & Appl. Chem.*, **58**(12), 1663(1986).

Union Carbide Corp., "Oxygen Permeable Membranes", *US Patent 3,359,705*, 1967.

Vinit, J., Noel, J.C. and Monnerie, L., "Physicochemical Processes occurring during the Formation of Cellulose diacetate Membranes, Research of Criteria for Optimizing Membrane Performance. II- Influence of Cellulose diacetate Chain Hydration on the Effect of Heat Treatment", *Desalination*, **15**, 267(1974).

Vos, K. D. and Burris, F.O., Jr., "Drying Cellulose Acetate Reverse Osmosis Membranes", *Ind. Eng. Chem. Prod. Res. Dev.*, **8**, 84(1969).

Ward, J.W., Browall, W.R. and Salemme, R.H., "Ultrathin Silicone/Polycarbonate Membranes for Gas Separation Processes", *J. Membrane Sci.*, **1**, 99(1976).

Werner, U., "Some Technical and Economical Aspects of Gas Separations by means of Membranes", in "Membranes Gas separations and Enrichment: The Proceedings of the Fourth BOC Priestley Conference", Leeds (1986), p.43.

Welcher, F.J., "The Analytical Use of EDTA", Van Nostrand, Princeton (1958).

Wijmans, J.G. and Smolders, C.A., "Preparation of Asymmetric Membranes by the Phase Inversion Process", in "Synthetic Membranes: Science, Engineering and Applications", Bungay, P.M., Lonsdale, H.K. and de Pinho, M.N., Eds., D.Reidel Publishers, Boston (1986), p.39.

Yong, C., Fouda, A.E. and Matsuura, T., "Effect of Drying Conditions on the Performance and Quality of Synthetic Membranes used for Gas Separations", *AIChE Symp. Ser.*, **85**(272), 18(1989).

Zhang, W.Z., Nodera, A., Satoh, M., Komiyama, J., "Effects of Nonvolatile Additives on Permeabilities of O_2 and N_2 through Water-Swollen Poly(Vinyl Alcohol) Membranes", *J. Membrane Sci.*, **35**, 311(1968).

Zhu, C. L. and Liu, M.E., "Handbook of Membrane Processes", Chemical Industry Press, Beijing (1988).

Appendix A

Raw Experimental Data

Table A1: Air Flow Rate *(V)* for various EDTA concentrations in the nonsolvent, for non-annealed membranes.

Membrane Ident.	EDTA [wt %]	Test 1 V [cm^3/sec]	Test 2 V [cm^3/sec]	Test 3 V [cm^3/sec]
NA0-1	0	0.0014	0.0011	0.0015
NA0-2	0	0.0010	0.0011	0.0010
NA0-3	0	0.0089	0.0098	0.0097
NA1-1	1	0.0069	0.0070	0.0070
NA2-1	2	0.1400	0.1370	0.1300
NA2-2	2	0.1625	0.1460	0.1560
NA3-1	3	0.0456	0.0455	0.0455
NA4-1	4	0.0125	0.0143	0.0152
NA4-2	4	0.0096	0.0093	0.0092
NA8-1	8	0.0057	0.0070	0.008
NA8-2	8	0.0106	0.0110	0.0110
NA12-1	12	0.0330	0.0290	0.0270
NA12-2	12	0.0038	0.0033	0.0033
NA14-1	14	0.0100	0.0104	0.0104
NA14-2	14	0.0250	0.0240	0.025
NA16-1	16	0.0065	0.0071	0.0068

Table A2: Air Flow Rate *(V)* for various EDTA concentrations in the nonsolvent, for annealed membranes.

Membrane Ident.	EDTA [wt %]	Test 1 V [cm^3/sec]	Test 2 V [cm^3/sec]	Test 3 V [cm^3/sec]
A0-1	0	0.0018	0.0018	0.0018
A0-2	0	0.0015	0.0012	0.0014
A0-3	0	0.0107	0.0107	0.0107
A1-1	1	0.0109	0.0106	0.0108
A2-1	2	0.7140	0.6660	0.7250
A2-2	2	0.7090	0.7000	0.7510
A3-1	3	0.0029	0.0029	0.0029
A4-1	4	0.0315	0.0250	0.0313
A4-2	4	0.0215	0.0235	0.0222
A8-1	8	0.0077	0.0083	0.0083
A8-2	8	0.0084	0.0073	0.0073
A12-1	12	0.0051	0.0051	0.0046
A12-2	12	0.0145	0.0147	0.0147
A14-1	14	0.0100	0.0104	0.0104
A14-2	14	0.0250	0.0263	0.0258
A16-1	16	0.0503	0.0510	0.0500

Table A3: Air Flow Rate *(V)* for various EDTA concentrations in the nonsolvent, for non-annealed membranes impregnated with silver nitrate.

Membrane Ident.	EDTA [wt %]	Test 1 V [cm^3/sec]	Test 2 V [cm^3/sec]	Test 3 V [cm^3/sec]
NA0SN-1	0	0.0002	0.0002	0.0002
NA1SN-1	1	0.0200	0.0200	0.0207
NA1SN-2	1	0.0133	0.0137	0.0133
NA2SN-1	2	0.0304	0.0280	0.0290
NA2SN-2	2	0.0453	0.0440	0.0444
NA2SN-3	2	0.0352	0.0344	0.0367
NA3SN-1	3	0.0702	0.0689	0.0706
NA3SN-2	3	0.0213	0.0211	0.0209
NA4SN-1	4	0.0071	0.0072	0.0072
NA8SN-1	8	0.0130	0.0133	0.0133
NA12SN-1	12	0.0093	0.0091	0.0091
NA14SN-1	14	0.0260	0.0276	0.0283
NA16SN-1	16	0.0022	0.0022	0.0023

Table A4: Air Flow Rate *(V)* for various EDTA concentrations in the nonsolvent, for non-annealed membranes impregnated with silver nitrate, reduced to silver metal.

Membrane Ident.	EDTA [wt %]	Test 1 V [cm^3/sec]	Test 2 V [cm^3/sec]	Test 3 V [cm^3/sec]
NA0SM-1	0	0.0050	0.0050	0.0050
NA1SM-1	1	0.0132	0.0128	0.0128
NA1SM-2	1	0.0097	0.0097	0.0098
NA2SM-1	2	0.0375	0.0360	0.0354
NA2SM-2	2	0.0440	0.0430	0.0420
NA2SM-3	2	0.0407	0.0406	0.0403
NA3SM-1	3	0.0092	0.0091	0.0091
NA3SM-2	3	0.0093	0.0093	0.0093
NA4SM-1	4	0.0133	0.0133	0.0133
NA8SM-1	8	0.0100	0.0100	0.0100
NA12SM-1	12	0.0089	0.0087	0.0085
NA14SM-1	14	0.0053	0.0056	0.0055
NA16SM-1	16	0.0035	0.0032	0.0029

Table A5: Air Flow Rate *(V)* for various EDTA concentrations in the nonsolvent, for annealed membranes impregnated with silver nitrate.

Membrane Ident.	EDTA [wt %]	Test 1 V [cm^3/sec]	Test 2 V [cm^3/sec]	Test 3 V [cm^3/sec]
A0SN-1	0	0.0130	0.0120	0.0014
A0SN-2	0	0.0012	0.0014	0.0014
A0SN-3	0	0.0040	0.0033	0.0032
A2SN-1	2	0.0168	0.0168	0.0175
A2SN-2	2	0.0416	0.0405	0.0436
A4SN-1	4	0.0023	0.0023	0.0022
A4SN-2	4	0.0166	0.0153	0.0158
A8SN-1	8	0.0050	0.0053	0.0058
A8SN-2	8	0.0084	0.0078	0.0084
A12SN-1	12	0.0263	0.0268	0.0268
A12SN-2	12	0.0026	0.0027	0.0028
A14SN-1	14	0.0050	0.0046	0.0045
A14SN-2	14	0.0025	0.0025	0.0025
A16SN-1	16	0.0033	0.0032	0.0320

Table A6: Air Flow Rate *(V)* for various EDTA concentrations in the nonsolvent, for annealed membranes impregnated with silver nitrate, reduced to silver metal.

Membrane Ident.	EDTA [wt %]	Test 1 V [cm^3/sec]	Test 2 V [cm^3/sec]	Test 3 V [cm^3/sec]
A0SM-1	0	0.0023	0.0024	0.0023
A0SM-2	0	0.0004	0.0008	0.0008
A0SM-3	0	0.0011	0.0027	0.0028
A2SM-1	2	0.0492	0.0434	0.0506
A2SM-2	2	0.0866	0.0833	0.0867
A4SM-1	4	0.0020	0.0194	0.0196
A8SM-1	8	0.1440	0.1450	0.1450
A8SM-2	8	0.0146	0.0143	0.0143
A12SM-1	12	0.0830	0.0833	0.0833
A14SM-1	14	0.0020	0.0018	0.0020
A14SM-2	14	0.0125	0.0125	0.0124
A16SM-1	16	0.0026	0.0026	0.0026

Table A7: Concentration of oxygen in the permeate for various EDTA concentrations in the nonsolvent, for non-annealed membranes.

Membrane Ident.	EDTA [wt %]	Inject1 *	Inject2 *	Inject3 *	Inject4 *	Average (GC peak area ratio)	% O_2 Average Corrected
NA0-1	0	33.98	34.22	34.06	34.21	34.12	35.2
NA0-2	0	38.10	38.33	38.73	38.95	38.48	39.6
NA0-3	0	28.71	28.78	28.83	28.89	28.80	29.8
NA1-1	1	24.83	24.88	25.19	25.21	25.03	25.9
NA2-1	2	22.25	22.06	22.23	22.19	22.18	23.0
NA2-2	2	21.24	21.95	21.28	21.48	21.49	22.1
NA3-1	3	22.60	22.34	22.64	22.36	22.49	23.3
NA4-1	4	26.05	26.02	25.95	25.96	25.99	26.9
NA4-2	4	26.72	26.76	26.76	26.75	26.75	27.7
NA8-1	8	25.07	24.99	24.99	25.10	25.04	25.9
NA8-2	8	25.58	25.24	25.56	25.22	25.40	26.3
NA12-1	12	23.08	22.99	22.98	23.13	23.04	23.9
NA12-2	12	29.59	29.43	29.57	29.77	29.59	30.6
NA14-1	14	23.08	22.99	22.98	23.13	23.04	23.9
NA14-2	14	22.37	22.35	22.28	22.22	22.30	23.1
NA16-1	16	22.61	23.38	23.42	23.32	23.18	24.1

* GC peak area ratio: % O_2 corrected using thermal response value (Dietz, 1967).

Table A8: Air permeability (*P/l*) for various EDTA concentrations in the nonsolvent, for non-annealed membranes.

Membrane Ident.	EDTA [wt %]	Test 1 *P/l* [cm^3(STP)/ cm^2.psi.sec]	Test 2 *P/l* [cm^3(STP)/ cm^2.psi.sec]	Test 3 *P/l* [cm^3(STP)/ cm^2.psi.sec]	Average *P/l* [cm^3(STP)/ cm^2.psi.sec]
NA0-1	0	1.57E-06	1.2E-06	1.69E-06	1.52E-06
NA0-2	0	1.12E-06	1.2E-06	1.12E-06	1.16E-06
NA0-3	0	1.00E-05	1.1E-05	1.09E-05	1.06E-05
NA1-1	1	7.75E-06	7.9E-06	7.86E-06	7.85E-06
NA2-1	2	1.57E-04	0.00015	1.46E-04	1.52E-4
NA2-2	2	1.83E-04	0.00016	1.75E-05	1.74E-4
NA3-1	3	5.12E-05	5.1E-05	5.11E-05	5.1E-05
NA4-1	4	1.39E-05	1.6E-05	1.71E-05	1.6E-05
NA4-2	4	1.08E-05	1E-05	1.03E-05	1.1E-05
NA8-1	8	6.38E-06	7.9E-06	9.04E-06	7.8E-06
NA8-2	8	1.20E-05	1.2E-05	1.24E-05	1.2E-05
NA12-1	12	3.70E-05	3.3E-05	3.04E-05	3.28E-05
NA12-2	12	4.27E-06	3.7E-06	3.70E-06	3.87E-06
NA14-1	14	1.12E-05	1.2E-05	1.17E-05	1.14E-05
NA14-2	14	2.80E-05	2.7E-05	2.80E-05	2.81E-05
NA16-1	16	7.30E-06	8E-06	7.64E-06	7.64E-06

Table A9: Concentration of oxygen in the permeate for various EDTA concentrations in the nonsolvent, for annealed membranes.

Membrane Ident.	EDTA [wt %]	Inject1 *	Inject2 *	Inject3 *	Inject4 *	Average (GC peak area ratio)	% O_2 Average Corrected
A0-1	0	34.18	34.33	34.18	34.32	34.25	35.3
A0-2	0	37.57	36.68	37.67	37.67	37.39	38.5
A0-3	0	24.09	23.93	23.62	24.00	23.91	24.8
A1-1	1	24.39	24.36	24.36	24.22	24.33	25.2
A2-1	2	21.85	21.85	21.88	21.97	21.89	22.7
A2-2	2	21.36	21.64	21.38	21.42	21.45	22.3
A3-1	3	22.87	22.89	22.73	22.06	22.64	23.5
A4-1	4	25.24	25.14	25.06	25.10	25.13	26.1
A4-2	4	24.02	24.01	24.05	24.05	24.03	24.9
A8-1	8	27.83	27.68	27.84	27.82	27.79	28.9
A8-2	8	24.06	24.11	24.18	24.10	24.11	25.0
A12-1	12	24.53	24.52	24.53	24.35	24.48	25.4
A12-2	12	22.96	22.84	22.96	22.83	22.90	23.8
A14-1	14	22.32	22.29	22.29	22.06	22.24	23.1
A14-2	14	21.58	21.61	21.70	21.68	21.64	22.5
A16-1	16	22.99	22.94	22.99	23.04	22.99	23.9

* GC peak area ratio: % O_2 corrected using thermal response value (Dietz, 1967).

Table A10: Air permeability (P/l) for various EDTA concentrations in the nonsolvent, for annealed membranes.

Membrane Ident.	EDTA [wt %]	Test 1 P/l [cm^3(STP)/ cm^2.psi.sec]	Test 2 P/l [cm^3(STP)/ cm^2.psi.sec]	Test 3 P/l [cm^3(STP)/ cm^2.psi.sec]	Average P/l [cm^3(STP)/ cm^2.psi.sec]
A0-1	0	2E-06	2E-06	2.02E-06	2.01E-06
A0-2	0	1.7E-06	1.3E-06	1.57E-06	1.54E-06
A0-3	0	1.2E-05	1.2E-05	1.21E-05	1.21E-05
A1-1	1	1.2E-05	1.2E-05	1.21E-05	1.21E-05
A2-1	2	0.00802	0.000748	8.14E-04	7.88E-04
A2-2	2	0.000796	0.000786	8.44E-04	8.09E-04
A3-1	3	3.3E-06	3.3E-06	3.26E-06	3.26E-06
A4-1	4	3.5E-05	2.8E-05	3.52E-05	3.29E-05
A4-2	4	2.4E-05	2.6E-05	3.52E-05	2.86E-05
A8-1	8	8.6E-06	9.3E-06	9.32E-06	9.09E-06
A8-2	8	9.4E-06	8.2E-06	8.19E-06	8.61E-06
A12-1	12	5.7E-06	5.7E-06	5.17E-06	5.54E-06
A12-2	12	1.6E-05	1.7E-05	1.65E-05	1.64E-05
A14-1	14	2.8E-05	3E-05	2.89E-05	2.88E-05
A14-2	14	5.6E-05	5.7E-05	5.61E-05	5.66E-05
A16-1	16	9.1E-06	9.6E-06	9.49E-06	9.41E-06

Table A11: Concentration of oxygen in the permeate for various EDTA concentrations in the nonsolvent, for non-annealed membranes impregnated with silver nitrate.

Membrane Ident.	EDTA [wt %]	Inject1 *	Inject2 *	Inject3 *	Inject4 *	Average (GC peak area ratio)	% O_2 Average Corrected
NA0SN-1	0	29.26	28.96	29.15	28.86	29.06	30.1
NA1SN-1	1	24.56	24.63	24.61	24.61	24.60	25.5
NA1SN-1	1	23.64	23.78	23.60	23.83	23.71	24.6
NA2SN-1	2	32.02	31.75	31.71	31.94	31.85	32.9
NA2SN-2	2	29.74	29.75	29.75	29.61	29.71	30.7
NA2SN-3	2	31.82	31.80	31.80	31.75	31.80	32.9
NA3SN-1	3	22.48	22.41	22.35	22.28	22.38	23.2
NA3SN-2	3	22.95	23.01	22.98	22.98	22.98	23.8
NA4SN-1	4	24.31	24.26	24.32	24.67	24.39	25.3
NA8SN-1	8	23.03	22.97	22.98	22.57	22.89	23.8
NA12SN-1	12	23.17	23.46	23.01	23.44	23.27	24.1
NA14SN-1	14	22.33	22.37	22.43	22.09	22.30	23.2
NA16SN-1	16	25.97	25.90	25.88	25.69	25.86	26.8

* GC peak area ratio: % O_2 corrected using thermal response value (Dietz, 1967).

Table A12: Air permeability (*P/l*) for various EDTA concentrations in the nonsolvent, for non-annealed membranes impregnated with silver nitrate.

Membrane Ident.	EDTA [wt %]	Test 1 *P/l* [cm^3(STP)/ cm^2.psi.sec]	Test 2 *P/l* [cm^3(STP)/ cm^2.psi.sec]	Test 3 *P/l* [cm^3(STP)/ cm^2.psi.sec]	Average *P/l* [cm^3(STP)/ cm^2.psi.sec]
NA0SN-1	0	2.24E-07	2.24E-07	2.24E-07	2.24E-07
NA1SN-1	1	2.24E-05	2.24E-05	2.34E-05	2.27E-05
NA1SN-1	1	1.49E-05	1.54E-05	1.49E-05	1.50E-05
NA2SN-1	2	3.41E-05	3.14E-05	3.28E-05	3.28E-05
NA2SN-2	2	5.09E-05	4.93E-05	4.99E-05	5.00E-05
NA2SN-3	2	3.95E-05	3.86E-05	4.13E-05	3.98E-05
NA3SN-1	3	2.39E-05	2.37E-05	2.34E-05	2.37E-05
NA3SN-2	3	2.38E-05	2.34E-05	2.33E-05	2.35E-05
NA4SN-1	4	7.97E-06	8.09E-06	8.09E-06	8.05E-06
NA8SN-1	8	1.46E-05	1.49E-05	1.52E-05	1.49E-05
NA12SN-1	12	1.04E-05	1.02E-05	1.02E-05	1.03E-05
NA14SN-1	14	2.92E-05	3.09E-05	3.18E-05	3.06E-05
NA16SN-1	16	2.47E-06	2.47E-06	2.58E-06	2.51E-06

Table A13: Concentration of oxygen in the permeate for various EDTA concentrations in the nonsolvent, for non-annealed membranes impregnated with silver nitrate, reduced to silver metal.

Membrane Ident.	EDTA [wt %]	Inject1 *	Inject2 *	Inject3 *	Inject4 *	Average (GC peak area ratio)	% O_2 Average Corrected
NA0SM-1	0	27.15	27.22	27.05	27.16	27.15	28.1
NA1SM-1	1	23.77	23.57	23.72	24.65	23.93	24.8
NA2SM-1	2	29.84	29.85	29.80	30.05	29.88	30.9
NA2SM-2	2	29.10	28.30	29.23	29.22	28.96	29.9
NA2SM-3	2	28.90	28.13	28.11	28.20	28.33	29.3
NA3SM-1	3	23.71	23.69	23.86	23.68	23.73	24.6
NA3SM-2	3	23.65	23.53	23.64	24.52	23.83	24.7
NA4SM-1	4	23.65	24.60	24.00	24.45	24.17	25.1
NA8SM-1	8	23.31	23.21	23.35	23.16	23.26	24.1
NA12SM-1	12	23.31	23.17	22.92	23.22	23.16	24.0
NA14SM-1	14	24.84	24.76	24.88	24.47	24.74	25.6
NA16SM-1	16	22.94	23.93	23.10	24.00	23.49	24.4

* GC peak area ratio: % O_2 corrected using thermal response value (Dietz, 1967).

Table A14: Air permeability (*P/l*) for various EDTA concentrations in the nonsolvent, for non-annealed membranes impregnated with silver nitrate, reduced to silver metal.

Membrane Ident.	EDTA [wt %]	Test 1 *P/l* [cm^3(STP)/ cm^2.psi.sec]	Test 2 *P/l* [cm^3(STP)/ cm^2.psi.sec]	Test 3 *P/l* [cm^3(STP)/ cm^2.psi.sec	Average *P/l* [cm^3(STP)/ cm^2.psi.sec]
NA0SM-1	0	5.6E-07	5.6E-07	5.61E-07	5.61E-07
NA1SM-1	1	1.5E-05	1.4E-05	1.44E-05	1.45E-05
NA2SM-1	2	4.2E-05	4E-05	3.97E-05	4.07E-05
NA2SM-2	2	4.9E-05	4.8E-05	4.71E-05	4.83E-05
NA2SM-3	2	4.6E-05	4.6E-05	4.52E-05	4.55E-05
NA3SM-1	3	1E-05	1E-05	1.02E-05	1.03E-05
NA3SM-2	3	1E-05	1E05	1.04E-05	1.04E-05
NA4SM-1	4	1.5E-05	1.5E-05	1.49E-05	1.49E-05
NA8SM-1	8	1.1E-05	1.2E-05	1.12E-05	1.12E-05
NA12SM-1	12	1E-05	9.8E-06	9.55E-06	9.77E-06
NA14SM-1	14	6E-06	6.3E-06	6.18E-06	6.14E-06
NA16SM-1	16	3.9E-06	3.6E-06	3.26E-06	3.59E-06

Table A15: Concentration of oxygen in the permeate for various EDTA concentrations in the nonsolvent, for annealed membranes impregnated with silver nitrate.

Membrane Ident.	EDTA [wt %]	Inject1 *	Inject2 *	Inject3 *	Inject4 *	Average (GC peak area ratio)	% O_2 Average Corrected
A0SN-1	0	34.65	35.07	34.97	35.16	34.96	36.1
A0SN-2	0	32.70	32.07	32.09	32.90	32.44	33.5
A0SN-3	0	28.51	28.34	28.49	28.44	28.44	29.4
A2SN-1	2	21.41	21.53	21.29	21.57	21.45	22.3
A2SN-2	2	21.32	21.49	21.33	21.63	21.44	22.3
A4SN-1	4	25.43	25.49	25.34	25.03	25.32	26.3
A4SN-2	4	24.27	24.36	24.41	24.26	24.32	25.2
A8SN-1	8	27.53	27.44	27.39	26.91	27.32	28.3
A8SN-2	8	24.88	24.88	24.89	24.76	24.85	25.7
A12SN-1	12	22.20	22.13	22.08	22.01	22.11	22.9
A12SN-2	12	27.59	27.58	27.61	27.55	27.58	28.6
A14SN-1	14	24.31	24.11	24.20	24.20	24.21	25.1
A14SN-2	14	22.28	22.18	22.13	22.11	22.17	23.0
A16SN-1	16	23.89	23.85	23.48	23.53	23.69	24.6

* GC peak area ratio: % O_2 corrected using thermal response value (Dietz, 1967).

Table A16: Air permeability (*P/l*) for various EDTA concentrations in the nonsolvent, for annealed membranes impregnated with silver nitrate.

Membrane Ident.	EDTA [wt %]	Test 1 *P/l* [cm^3(STP)/ cm^2.psi.sec]	Test 2 *P/l* [cm^3(STP)/ cm^2.psi.sec]	Test 3 *P/l* [cm^3(STP)/ cm^2.psi.sec]	Average *P/l* [cm^3(STP)/ cm^2.psi.sec]
A0SN-1	0	1.5E-06	1.3E-06	1.57E-06	1.46E-06
A0SN-2	0	1.3E-06	1.6E-06	1.57E-06	1.50E-06
A0SN-3	0	4.5E-06	3.7E-06	3.60E-06	3.93E-06
A2SN-1	2	0.000189	0.000189	1.97E-04	1.91E-04
A2SN-2	2	4.7E-05	4.5E-05	4.9E-05	4.70E-05
A4SN-1	4	2.6E-06	2.6E-06	2.47E-06	2.54E-06
A4SN-2	4	1.9E-05	1.7E-05	1.77E-05	1.78E-05
A8SN-1	8	5.6E-06	6E-06	6.52E-06	6.03E-06
A8SN-2	8	9.4E-06	8.8E-06	9.43E-06	9.21E-06
A12SN-1	12	3E-05	3E-05	3.01E-05	2.99E-05
A12SN-2	12	2.9E-06	3E-06	3.14E-06	3.03E-06
A14SN-1	14	5.6E-05	5.2E-05	5.05E-05	5.28E-06
A14SN-2	14	2.80E-05	2.80E-05	2.80E-05	2.80E-05
A16SN-1	16	3.7E-06	3.6E-06	3.6E-06	3.63E-06

Table A17: Concentration of oxygen in the permeate for various EDTA concentrations in the nonsolvent, for annealed membranes impregnated with silver nitrate, reduced to silver metal.

Membrane Ident.	EDTA [wt %]	Inject1 *	Inject2 *	Inject3 *	Inject4 *	Average (GC peak area ratio)	% O_2 Average Corrected
A0SM-1	0	31.57	31.54	31.52	31.46	31.52	32.6
A0SM-2	0	33.96	33.50	33.97	33.99	33.85	34.9
A0SM-3	0	32.56	32.40	32.22	32.13	32.33	33.4
A2SM-1	2	22.34	22.37	22.35	22.35	22.35	23.2
A2SM-2	2	22.22	22.11	22.01	22.16	22.13	22.9
A4SM-1	4	29.01	28.91	28.94	28.98	28.96	29.9
A8SM-1	8	21.62	21.59	21.57	21.52	21.57	22.4
A8SM-2	8	23.03	22.99	23.04	22.92	22.99	23.9
A12SM-1	12	21.72	21.64	21.48	21.50	21.58	22.4
A14SM-1	14	27.24	27.45	27.49	27.60	27.44	28.4
A14SM-2	14	22.54	22.55	22.52	22.51	22.53	23.4
A16SM-1	16	23.47	23.00	22.96	23.36	23.20	24.1

* GC peak area ratio: % O_2 corrected using thermal response value (Dietz, 1967).

Table A18: Air permeability (P/l) for various EDTA concentrations in the nonsolvent, for annealed membranes impregnated with silver nitrate, reduced to silver metal.

Membrane Ident.	EDTA [wt %]	Test 1 P/l [cm^3(STP)/ cm^2.psi.sec]	Test 2 P/l [cm^3(STP)/ cm^2.psi.sec]	Test 3 P/l [cm^3(STP)/ cm^2.psi.sec]	Average P/l [cm^3(STP)/ cm^2.psi.sec]
A0SM-1	0	2.6E-06	2.7E-06	2.59E-06	2.62E-06
A0SM-2	0	4.5E-07	9E-07	8.99E-07	7.49E-07
A0SM-3	0	1.2E-06	3E-06	3.14E-06	2.46E-06
A2SM-1	2	5.5E-05	4.9E-05	5.68E-05	5.36E-05
A2SM-2	2	9.8E-05	9.4E-05	9.74E-05	9.62E-05
A4SM-1	4	2.2E-06	2.2E-05	2.2E-05	1.54E-05
A8SM-1	8	1.62E-04	1.63E-04	1.63E-04	1.63E-04
A8SM-2	8	1.6E-05	1.6E-05	1.61E-05	1.61E-05
A12SM-1	12	9.3E-05	9.4E-05	9.35E-05	9.34E-05
A14SM-1	14	2.3E-06	2E-06	2.25E-06	2.17E-06
A14SM-2	14	1.4E-05	1.4E-05	1.39E-05	1.40E-05
A16SM-1	16	2.9E-06	2.9E-06	2.92E-06	2.92E-06

Appendix B

BJH Pore Area Distributions Results

Table B1: Pore area distributions for 0% EDTA membrane, non-annealed.

Pore diameter [Å]	Pore area [sq.m/g-Å]
1015	3.1368E-05
333.9	0.002821
196.2	0.0097266
153	0.01319
127.9	0.011726
113.2	0.013596
103	0.011338
85.9	0.011459
69.7	0.020676
57.9	0.03164
49.1	0.059735
42.3	0.092919
36.8	0.22111
32.2	0.38963
28.3	0.058367
24.8	0.037987
21.9	0.095525
20.1	0.14249
19	0.065084
18	0.11797
17	0.20301
15.1	0.050274
14.2	0.26202
13.2	0.13274
12.3	0.12211
11.3	0.15974
10.8	1.0066
10.3	0.17677
10	0.62133

Sample Weight = 0.1855 g

Table B2: Pore area distributions for 2% EDTA membrane, non-annealed.

Pore diameter [Å]	Pore area [sq.m/g-Å]
1623.3	2.3135E-05
328.7	0.0022564
199.3	0.012671
132.2	0.016694
109.4	0.024512
100.6	0.01987
86.2	0.020966
70	0.038107
58.1	0.067666
49.3	0.098629
42.4	0.13729
36.9	0.25938
32.3	0.46897
28.4	0.088999
24.9	0.010812
22	0.0066976
20.2	0.16792
18.1	0.093571
17.1	0.0058858
16.2	0.18336
15.2	0.11651
14.3	0.075659
12.4	0.13111
11.4	0.19127
10.9	0.61278
10.4	0.17729

Sample Weight = 0.1570 g

Table B3: Pore area distributions for 4% EDTA membrane, non-annealed.

Pore diameter [Å]	Pore area [sq.m/g-Å]
1294.5	4.4402E-05
439.5	0.0019384
281.1	0.01033
183.1	0.01493
135.4	0.016145
109.4	0.016262
97.8	0.021352
84.1	0.014369
68.7	0.0147
57.1	0.018878
48.4	0.016385
41.6	0.011482
36.1	0.017057
31.5	0.010167
12.5	0.0015321
11.5	0.10394
10.9	0.17978
10.7	0.52093
10.2	0.13225

Sample Weight = 0.2870 g

Table B4: Pore area distributions for 8% EDTA membrane, non-annealed.

Pore diameter [Å]	Pore area [sq.m/g-Å]
1321.6	1.522E-05
340.9	0.0017709
207.3	0.014277
152	0.015167
121	0.017848
108.2	0.029028
101	0.016912
85.4	0.016162
69.4	0.022869
57.6	0.033778
48.8	0.043425
42	0.07038
36.5	0.22368
31.9	0.18673
17.9	0.0024429
15	0.031362
14.1	0.071952
10.7	0.034514
10.2	0.11921

Sample Weight = 0.2700 g

Table B5: Pore area distributions for 12% EDTA membrane, non-annealed.

Pore diameter [Å]	Pore area [sq.m/g-Å]
760.5	6.1041E-05
313.6	0.0034619
196.1	0.018708
152.7	0.020189
134.3	0.026334
123.5	0.0097559
112.2	0.0085384
100.7	0.0068951
83.3	0.0035722
66.9	0.00344
55.2	0.011701
46.4	0.014875
39.6	0.029493
34.1	0.17227
29.5	0.065146
11.4	0.0018673

Sample Weight = 0.1330 g

Table B6: Pore area distributions for 14% EDTA membrane, non-annealed.

Pore diameter [Å]	Pore area [sq.m/g-Å]
851.1	2.4037E-05
302.7	0.0013953
195.6	0.0072533
154.5	0.0087845
138	0.01076
127.2	0.0087257
115.2	0.0082546
103.2	0.0093309
85.7	0.010689
69.3	0.016008
57.5	0.025302
48.7	0.039358
41.9	0.052517
36.5	0.22479
31.8	0.24131
27.8	0.03591
19.8	0.0026291
14.9	0.00065515
12.2	0.012099
11.2	0.001705
10.6	0.095165
10.4	0.069916
10.1	0.28326

Sample Weight = 0.3152 g

Table B7: Pore area distributions for 0% EDTA membrane, annealed.

Pore diameter [Å]	Pore area [sq.m/g-Å]
1091	2.3849E-05
400.9	0.0030893
264.6	0.012909
182.6	0.020312
141.4	0.025094
121.9	0.030377
111.5	0.03497
102.7	0.035308
86.6	0.042081
70.2	0.081073
58.3	0.14092
49.5	0.19769
42.6	0.23505
37.1	0.32797
32.7	0.87744
28.6	0.19896
25.1	0.046645
22.2	0.045201
20.5	0.074781
19.5	0.020207
18.5	0.23824
17.5	0.073215
16.5	0.18881
15.6	0.051271
14.6	0.082532
13.7	0.16956
12.7	0.29115
11.8	0.081068
11.2	0.70785
10.9	0.59212
10.7	0.15415
10.5	0.18824

Sample Weight = 0.2120 g

Table B8: Pore area distributions for 2% EDTA membrane, annealed.

Pore diameter [Å]	Pore-area [sq.m/g-Å]
1212.6	1.6923E-05
369.3	0.0017147
207.3	0.0097857
155.9	0.012421
125.5	0.013308
111.9	0.023887
103	0.012426
86.3	0.016236
70.2	0.026517
58.3	0.046073
49.6	0.067005
42.7	0.097542
37.2	0.15565
32.7	0.51096
28.7	0.11278
25.2	0.020529
22.3	0.039965
20.5	0.12682
19.5	0.097636
18.5	0.10539
17.5	0.040577
16.5	0.055511
15.6	0.12162
14.6	0.21394
13.7	0.025106
12.7	0.19767
11.8	0.24218
10.9	0.20798
10.5	0.18799

Sample Weight = 0.2756 g

Table B9: Pore area distributions for 4% EDTA membrane, annealed.

Pore diameter [Å]	Pore-area [sq.m/g-Å]
1032.8	2.5841E-05
388.5	0.0029338
210.7	0.016121
154.3	0.019119
120.3	0.020007
101.7	0.023975
84.5	0.019332
69.1	0.022265
57.6	0.023107
48.9	0.038061
42.1	0.043558
36.6	0.090394
32	0.18657
16.2	0.0067634
14.3	0.026109
12.5	0.051106
11.5	0.086714
10.9	0.10277
10.7	0.33087
10.4	0.24001
10.2	0.62676

Sample Weight = 0.2104 g

Table B10: Pore area distributions for 8% EDTA membrane, annealed.

Pore diameter [Å]	Pore-area [sq.m/g-Å]
1353.9	3.5397E-05
384.5	0.0012405
222	0.011564
154.6	0.01396
116.7	0.014418
98.9	0.016633
83.7	0.01468
69.1	0.017592
57.8	0.023521
49.1	0.029177
42.3	0.032202
36.8	0.067955
32.2	0.070777
20.3	0.0037535
18.2	0.0014608
16.3	0.0029074
15.3	0.013834
14.4	0.027736
12.5	0.021541
11.6	0.13848
10.8	0.0305
10.5	0.065907
10.3	0.21066
10	0.095453

Sample Weight = 0.3920 g

Table B11: Pore area distributions for 12% EDTA membrane, annealed.

Pore diameter [Å]	Pore area [sq.m/g-Å]
1051.2	0.00020488
312.1	0.0022328
196.2	0.014954
151.3	0.015568
122.3	0.015108
108.5	0.025302
100.1	0.014013
84.1	0.014326
68	0.016717
56.2	0.01938
47.5	0.025152
40.7	0.028229
35.2	0.067009
30.6	0.030666
18.9	0.0033923
10.4	0.0042588

Sample Weight = 0.2485 g

Table B12: Pore area distributions for 14% EDTA membrane, annealed.

Pore diameter [Å]	Pore area [sq.m/g-Å]
812.8	3.4173E-05
296.2	0.0019322
192	0.0090361
153.2	0.010687
137.8	0.011181
127.2	0.0094217
115.3	0.0092756
103.3	0.0086989
85.7	0.012067
69.2	0.014927
57.5	0.018311
48.7	0.0285
41.9	0.040172
36.4	0.092593
31.8	0.11254
27.9	0.0051699
21.5	0.005977
19.7	0.062963
17.7	0.0069901
15.8	0.00018472
14.8	0.13004
13	0.043176
11.1	0.008332
10.5	0.47798
10.1	0.1097

Sample Weight = 0.2514 g

Table B13: Pore area distributions for 0% EDTA membrane, annealed after impregnation wih silver nitrate.

Pore diameter [Å]	Pore area [sq.m/g-Å]
835.3	2.8118E-05
433.8	0.0042254
275.5	0.012746
184.1	0.019378
139.3	0.020654
120	0.025198
110.8	0.022821
102.6	0.020694
86.4	0.019441
70.1	0.028784
58.2	0.033716
49.5	0.049199
42.6	0.054568
37.1	0.081484
32.6	0.23302
28.7	0.056696
25.2	0.035736
22.3	0.086251
20.5	0.12648
19.4	0.13054
18.4	0.068655
17.4	0.09933
16.4	0.1492
15.5	0.16559
14.6	0.25786
12.7	0.21358
11.7	0.12124
11.1	1.1274
10.9	0.23007
10.4	0.29541
10.1	0.67541

Sample Weight = 0.2120 g

Table B14: Pore area distributions for 2% EDTA, annealed after impregnation with silver nitrate

Pore diameter [Å]	Pore area [sq.m/g-Å]
1038.3	2.5266E-05
382.8	0.002705
201.6	0.011151
152.3	0.012123
122.8	0.011838
109.6	0.019143
101	0.011444
84	0.010474
67.8	0.016773
56.1	0.015659
47.3	0.024779
40.5	0.041699
35	0.050675
30.4	0.070244
26.5	0.014313
20.1	0.018403
18.3	0.030876
17.2	0.13957
16.2	0.052627
15.2	0.026187
14.3	0.015844
13.3	0.24529
12.4	0.087374
11.4	0.043845
10.5	0.047636

Sample Weight = 0.2204 g

Table B15: Pore area distributions for 4% EDTA membrane, annealed after impregnation with silver nitrate.

Pore diameter [Å]	Pore area [sq.m/g-Å]
1219.6	1.6878E-05
434.2	0.0023174
279.6	0.011698
183.2	0.018607
137.4	0.020492
118.1	0.024386
109.5	0.025823
102.1	0.020481
86.1	0.022058
69.6	0.026744
57.8	0.037068
49	0.044886
42.3	0.066115
36.8	0.12088
32.2	0.10514
28.3	0.0077655
24.9	0.016168
20.1	9.3135E-05
19.1	0.12504
18	0.077775
17	0.018768
16.1	0.070305
15.1	0.11504
14.2	0.066125
13.3	0.067049
12.3	0.045713
11.4	0.067615
10.8	0.3792
10.5	0.46503
10.3	0.347
10	0.25785

Sample Weight = 0.2403 g

Table B16: Pore area distributions for 8% EDTA, annealed after impregnation with silver nitrate.

Pore diameter [Å]	Pore area [sq.m/g-Å]
1456.2	3.5161E-05
464.7	0.0014034
288.5	0.0076981
185.7	0.011708
136.4	0.014633
110.6	0.017018
98.9	0.022179
85.1	0.019129
69.7	0.029788
58	0.039161
49.3	0.051444
42.5	0.05817
37	0.081661
32.4	0.093546
28.5	0.0065305
20.4	0.0030178
19.3	0.052377
18.3	0.029747
17.3	0.041884
15.4	0.049574
13.6	0.014181
12.6	0.057159
11.7	0.044754
11.1	0.42525
10.8	0.27401
10.3	0.14587
10.1	0.45194

Sample Weight = 0.3549 g

Table B17: Pore area distributions for 12% EDTA, annealed after impregnation with silver nitrate.

Pore diameter [Å]	Pore area [sq.m/g-Å]
1090.3	7.3255E-05
291.8	0.0012745
198.2	0.011869
155.2	0.015799
126.2	0.017679
110.9	0.021945
101.2	0.019342
85.6	0.019592
69.6	0.023358
57.7	0.031812
49	0.040123
42.3	0.04964
36.8	0.094114
32.2	0.15469
28.3	0.0057266
19.1	0.00091913
18.1	0.024816
16.2	0.03949
12.4	0.023333
10.9	0.10134
10.4	0.26451

Sample Weight = 0.3855 g

Table B18: Pore area distributions for 14% EDTA membrane, after impregnation with silver nitrate.

Pore diameter [Å]	Pore area [sq.m/g-Å]
1141	7.3258E-05
252.2	0.0010655
154.8	0.0076502
120	0.010895
108.5	0.011751
101.5	0.010686
85.9	0.0087366
69.4	0.014388
57.5	0.019376
48.6	0.027872
41.7	0.038407
36.2	0.083461
31.6	0.14625
27.7	0.0060536
19.6	0.015754
18.5	0.022595
17.5	0.061157
14.6	0.032866
12.8	0.04351
11.9	0.046134
10.9	0.082379
10.3	0.19461

Sample Weight = 0.2505 g

Table B19: Pore area distributions for 0% EDTA membrane, annealed after impregnation with silver nitrate and reduction.

Pore diameter [Å]	Pore area [sq.m/g-Å]
1228.5	2.6219E-05
339.9	0.0028879
193.7	0.011578
130	0.016757
107.9	0.029403
99.4	0.02287
85.6	0.029624
70	0.058975
58.2	0.098362
49.4	0.14077
42.6	0.17355
37.1	0.26772
32.6	0.69867
28.5	0.16112
25.1	0.057765
22.1	0.017733
20.4	0.17222
19.3	0.12899
18.3	0.018183
17.4	0.096619
16.4	0.15642
14.5	0.085329
13.6	0.034539
12.6	0.0045295
11.7	0.16921
11.1	0.66531
10.8	0.62309
10.6	0.91522
10.3	0.50075

Sample Weight = 0.1780 g

Table B20: Pore area distributions for 2% EDTA membrane, annealed after impregnation with silver nitrate and reduction.

Pore diameter [Å]	Pore area [sq.m/g-Å]
1715.7	1.5985E-05
392.9	0.0017553
197.8	0.0089221
128.7	0.004363
105	0.003741
21	0.00055998
19.2	0.10032
17.1	0.021889
16.1	0.014158
15.1	0.0909
14.2	0.11772
13.3	0.024342
12.3	0.064113
11.4	0.16415
10.4	0.029263

Sample Weight = 0.2058 g

Table B21: Pore area distributions for 4% EDTA membrane, annealed after impregnation with silver nitrate and reduction.

Pore diameter [Å]	Pore area [sq.m/g-Å]
1494	7.5012E-05
429	0.0011415
287.7	0.0077104
188.3	0.010699
137.5	0.0095507
109.6	0.0089503
98.2	0.010677
84.9	0.0062278
69.6	0.0068233
58.1	0.0061393
49.3	0.0090648
42.5	0.0078041
37	0.012346
32.4	0.030581
28.5	0.01563
25.1	0.014253
22.1	0.013471
20.3	0.030384
19.2	0.076536
18.2	0.019967
17.2	0.073693
16.3	0.096613
15.3	0.11987
14.4	0.074022
13.5	0.095946
12.5	0.14424
11.5	0.16494
11	0.01778
10.7	0.24934
10.2	0.126

Sample Weight = 0.4215 g

Table B22: Pore area distributions for 8% EDTA membrane, annealed after impregnation with silver nitrate and reduction.

Pore diameter [Å]	Pore area [sq.m/g-Å]
921.5	4.5421E-05
359.9	0.0027838
202.5	0.01322
151.1	0.013404
119.4	0.01371
101.4	0.015222
84.2	0.012917
68.6	0.014577
57.2	0.014473
48.5	0.024487
41.7	0.025737
36.2	0.086063
31.6	0.053913
19.7	0.0024288
14.8	0.0037689
12.1	0.038261
11.1	0.031806
10.5	0.36736
10	0.14335

Sample Weight = 0.2798 g

Table B23: Pore area distributions for 12% EDTA membrane, annealed after impregnation with silver nitrate and reduction.

Pore diameter [Å]	Pore area [sq.m/g-Å]
915.8	9.3091E-05
360.6	0.0020447
204.7	0.011671
153.3	0.016413
120.1	0.016155
101	0.017194
83.7	0.016402
68.5	0.019599
57.1	0.019695
48.4	0.028433
41.6	0.025469
36.2	0.054362
31.6	0.048837
18.6	0.0014538
16.6	0.0021065
15.6	0.049466
13.7	0.01691
11.9	0.018595
10.9	0.025728
10.4	0.047991

Sample Weight = 0.3422 g

Table B24: Pore area distributions for 14% EDTA membrane, annealed after impregnation with silver nitrate and reduction.

Pore diameter [Å]	Pore area [sq.m/g-Å]
1261.8	0.00013297
366.1	0.0014225
198.7	0.0086124
152.3	0.016127
121.7	0.013623
108	0.020703
100.5	0.010597
85.2	0.012762
69.3	0.017432
57.5	0.025694
48.8	0.033246
41.9	0.044917
36.5	0.10595
31.9	0.15136
17.9	0.00079443
17	0.0035154
11.3	0.0032485
10.7	0.10553
10.5	0.28679

Sample Weight = 0.3845 g

Tble B25: Pore area distributions for 2% EDTA membrane, non-annealed after impregnation with silver nitrate.

Pore diameter [Å]	Pore area [sq.m/g-Å]
1011.3	2.6798E-4
480.6	0.002351
293.8	0.0082432
220.7	0.010965
183.6	0.014278
161.8	0.015791
144.9	0.016078
129.7	0.018227
115.7	0.019681
103.4	0.021736
86.2	0.022082
69.8	0.026968
58.1	0.032909
49.4	0.039086
42.7	0.040566
37.2	0.062187
32.7	0.076718
28.8	0.013526
22.4	0.012639
20.6	0.032927
19.5	0.068086
18.5	0.071276
17.6	0.075230
16.6	0.072191
15.6	0.13445
14.7	0.13408
13.8	0.037153
12.8	0.15028
11.9	0.097638
11.3	0.11493
11.0	0.15550
10.8	0.52745
10.3	0.21666
10.0	0.12269

Sample Weight = 0.4134 g

Table B26: Pore area distributions for 2% EDTA membrane, non-annealed after impregnation with silver nitrate and reduction.

Pore diameter [Å]	Pore area [sq.m/g-Å]
1180.5	0.0002406
476.9	0.0025204
271.8	0.0075968
177.3	0.010895
134.6	0.011908
112	0.011672
100.5	0.012391
85.5	0.010152
69.8	0.011911
58.1	0.016437
49.3	0.020556
42.5	0.026014
37	0.035877
32.4	0.038242
25.1	0.005918
22.1	0.023953
20.3	0.015397
19.3	0.012275
18.3	0.043651
17.3	0.084402
16.3	0.025129
15.4	0.13884
14.4	0.12432
13.5	0.032527
12.5	0.21906
11.6	0.14702
11	0.16877
10.7	0.12286
10.5	0.031377
10.2	0.3059

Sample Weight = 0.2981 g

Appendix C

Sample Calculation for Air Permeability (*P/l*)

Permeability of air is expressed as *P/l* and calculated using Equation (10);

$$\frac{P}{l} = \frac{V}{A}\frac{1}{\Delta p_A}\left(\frac{273.15}{273.15+T_R}\right) \qquad (10)$$

Where;

V Air flow rate measured using the bubble flow meter, cm^3/s,

A Membrane area, 9.62 cm^2,

Δp_A Total pressure difference across the membrane, 100 -14.67 = 85.33 psi,

T_R Room temperature, 23°C.

For example, for 0% EDTA membrane (Coupons NA0-1)(non annealed, 0% EDTA, coupons #1)(Table A1):

The flow rate of air for 0% EDTA (Test1) is equal to 0.0014 cm^3/s (Table A1, Appendix A)

Therefore;

P/l = 1.57E-6 cm^3(STP)/cm^2.psi.sec (Table A8)